ABSTRACT

HICKS, JULIE ANN. Characterization of Interactions between Porcine Reproductive and Respiratory Syndrome Virus and its Intracellular Environment. (Under the direction of Dr. Sunny Liu.)

Porcine reproductive and respiratory syndrome (PRRS) has a major impact on the swine industry. PRRS is characterized by abortions in pregnant sows and respiratory disease, particularly in young pigs. The causative agent is porcine reproductive and respiratory syndrome virus (PRRSV), a member of the arterivirus family. GP5 and M are the major envelope proteins encoded by PRRSV. Here we demonstrate by means of a yeast two-hybrid system that the cellular Snap-Associated Protein (Snapin) specifically interacts with GP5 and M. GP5 and M proteins are known to form a heterodimeric complex which is important for viral structural and infectivity. Snapin has recently been found to interact with many proteins involved in membrane fusion via its interaction with the SNARE complex. Through the use of siRNA-mediated knock-down of snapin expression in PRRSV infected MARC-145 cells we demonstrate that the GP5/M/snapin interaction is an important aspect of PRRSV pathogenesis. Reduced snapin expression results in reduced PRRSV replication as evidenced by reduced viral titers and reduced nucleocapsid (N protein) mRNA and protein levels. Based on snapin's involvement in mediating membrane fusion events, it is likely that the interaction between GP5 and M with snapin is involved in intracellular trafficking events during PRRSV infections. To further assess the interactions between PRRSV with its intracellular environment we determined changes in cellular microRNA (miRNA) expression during the course of an *in vitro* PRRSV infection in swine alveolar macrophages (SAMs). We have shown that expression of ~40 cellular miRNAs is altered within the first 48 hours of PRRSV infection in SAMs. Analysis of the potential genes and pathways regulated by these

differentially expressed miRNAs suggests that they are involved in regulating multiple cellular pathways including the immune related and intracellular trafficking pathways. Interestingly we found that one of the differentially expressed miRNAs, *miR-147*, which was significantly down regulated in PRRSV infected cells at 24hpi, likely regulates snapin expression. A decrease in *miR-147* expression in PRRSV infected macrophages should result in a reciprocal increase in Snapin. The studies presented here were undertaken to further the current understanding of the interaction between PRRSV and its intracellular environment. As these studies are continued a more complete picture of the complexity of interactions between PRRSV and its intracellular environment will be revealed.

Characterization of Interactions between Porcine Reproductive and Respiratory Syndrome Virus and its Intracellular Environment

by
Julie Hicks

A dissertation submitted to the Graduate Faculty of
North Carolina State University
in partial fulfillment of the
requirements for the degree of
Doctor of Philosophy

Animal Science & Poultry Science

Raleigh, North Carolina

2012

APPROVED BY:

_____	_____
Dr Sunny Liu Committee Chair	Dr Bob Petters
_____	_____
Dr Chad Stahl	Dr Matt Koci

BIOGRAPHY

Julie Hicks was born and raised in Boone, NC located in the Appalachian Mountains. After graduating from Watauga High School in 2000, she moved to Charlotte, NC to attend the University of North Carolina at Charlotte. At the University of North Carolina at Charlotte Julie obtained a B.S. in Biology with a minor in Spanish in May, 2004. That summer she moved to Raleigh, NC so she could further pursue her education by entering graduate school at North Carolina State University in the Animal Science Department. She obtained her master's degree in 2007 under the direction of Dr Sunny Liu. She then continued her studies in persuit of a doctorate also under the direction of Dr Sunny Liu.

ACKNOWLEDGEMENTS

I would like to thank my committee members, Dr Bob Petters, Dr Matthew Koci, and Dr Chad Stahl for taking time out of their schedules to help me. I would also like to extend my gratitude to all the members of the Liu Lab past and present for all of their help and friendship through the years. I would also like to thank my mentor Dr. Sunny Liu for her guidance throughout my graduate career. I appreciate her efforts to teach me that there is more to being a scientist than pipetting and for always giving her students opportunities to learn and grow. Last, but certainly not least I would like to thank my family for their constant and unwavering support. In particular, I would like to thank my parents Kenneth and Nancy, without their support and guidance I would not be where I am today.

TABLE OF CONTENTS

LIST OF TABLES

LIST OF FIGURES

Chapter One: Literature Review

Virology History

After the discovery of bacteria by Louis Pasteur in 1860, it was thought that all microorganism diseases were caused by bacterial infections. In the late 1800s, a German microbiologist, Martinus Beijerinck, often considered a founding father of the virology field, was trying to identify the causative agent, suspected of being a bacterium, of tobacco mosaic disease (Calisher and Harzinek 1999). In what was considered standard practice at the time to identify a bacterium, Beijerinck passed the sap from infected plants through increasing smaller porcelain filters. For all previously discovered bacteria, passing infected cultures through filters would trap the bacteria in the filter and the cultures would not pass the disease when put into a susceptible host. To Beijerinck's surprise, even sap passed through the smallest of filters was still able to cause the disease when put into healthy plants. After repeating the experiment and getting the same results, along with the fact that he was unable to see a "bacterium" using a microscope, he concluded that tobacco mosaic disease was not caused by a bacterium but rather by what he termed a "contagium vivum fluidum." He and his contemporaries thought that the "contagium vivum fluidum" was enzymatic in nature and somehow originated in the infected organism, and was not an independent pathogenic organism. In fact the term "virus" to describe the causative agent of tobacco mosaic disease and other virally-induced diseases was not coined until 1903 (Calisher and Harzinek 1999). In late 1930's images of the tobacco mosaic virus particles were obtained by electron microscopy. As microscopy techniques improved in the coming years, more and more

viruses were discovered. Today virology is a thriving area of research that incorporates all aspects of molecular biology techniques to identify, characterize and combat the thousands of known and continually discovered viruses.

Intracellular transport and virus trafficking

Intracellular transport pathways

Endocytosis and intracellular transport pathways are essential for cell survival and homeostasis. There are several endocytic pathways that mediate the transport of various molecules, including nutrients, signaling factors, and receptor-ligand complexes, throughout the cell (Andersson 2012). The first major endocytic process identified was that of clathrin-dependent trafficking. During clathrin-dependent endocytosis, adaptor protein complexes, AP-1 or AP-2, form in the membrane at molecule uptake sites (Rodemer and Haucke 2008). Then clathrin bind to these adaptor complexes and forms lattices in the plasma membrane. Clathrin-coated vesicles (sometimes called pits), containing the molecule(s) that are to be transported, are formed by invagination of the clathrin lattices. Energy is required for this process and is thought to be provided by GTPases, such as dynamin. A major homeostatic function of clathrin endocytosis is the recycling and degradation of receptor/ligand complexes, including low density lipoproteins and trasnferrin (Grant and Donaldson 2009). Many external signals received by a cell are initiated by reorganization of a ligand by a receptor present in the cell membrane, which then induces an internal signaling cascade. After initiating this signaling, the receptor/ligand complexes are taken up by clathrin-coated vesicles. The clathrin-coated vesicles then transport the complexes to early endosomes, in

which the receptor and the ligand are separated. The ligand is then transported to lysosomes for degradation. Meanwhile the receptor is transported back to the plasma membrane by recycling vesicles. Receptors may be recycled and reused up to 10 times per hour (Grant and Donaldson 2009).

Cells also have clathrin-independent endocytic pathways. One such pathway is mediated by the protein caveolin (Kiss and Botos 2009). Caveolin molecules gather at specific membranes, most often in the intracellular organelles. Caveolin-coated vesicles then bud off of the membrane, forming what are called calveolae. Smaller molecules, such as solutes and some types of nutrients are more likely to be transported via caveolin-mediated transport than via clathrin-mediated trafficking. Clathrin-dependent and caveolin-mediated endocytosis are universal transport mechanisms shared by many different cell types.

There is also a more specialized endocytic pathway used by a small set of immune cells, termed phagocytosis. Phagocytosis is mainly used by macrophages and neutrophils. The two major functions of phagocytosis by these cells are first, the degradation of bacteria and second, the processing and presentation of antigens to T-cells for the initiation of the humoral immune response (Verschoor et al. 2012). Phagocytosis is initiated by the recognition of large particles, such as a bacterium, by receptors on the cell surface of phagocytic cells. These receptors include the Fc receptor, which recognize antibody-coated particles. Activation of the receptors then induces changes in the actin structure of the cell to create a pseudopod on the cell membrane. The pseudopod then surrounds the particle, which is then taken into the cell, in what is called a phagosome. The phagosome transports the

particle to endosomes and lysozomes, where it is enzymatically-degraded. Antigenic peptides are then presented via MHC presentation to T-cells.

Virus trafficking

A major factor affecting virus productivity is the efficient intracellular transport of the virus and its components. As obligate intracellular parasites viruses are dependent on the host cells for survival. Therefore it is not surprising that viruses have been shown to manipulate many aspects of the host's cell transport machinery to facilitate trafficking of virus particles and/or viral components to sites of release, replication, and assembly.

Entry of enveloped viruses into host cells requires membrane fusion between the virus particle and the cell at one or more sites, including the cell surface and/or intracellular vesicles or organelles. It is thought that the coronavirus mouse hepatitis virus (MHV) has two possible modes of entry into its host cell (Zhu et al. 2009). The entry mode is strain dependent. In strains where the major envelope protein, the spike (S) protein, is proteolytically cleaved there is direct fusion between the virus and the plasma membrane of the host cell. In MHV strains in which S is not cleaved the virus enters the cell via receptor-mediated endocytosis. Canine parvovirus (CPV) initially interacts with transferrin receptors on the host cell and then is taken up via a clathrin-mediated pathway (Suikkanen et al. 2003). The virus is then transported to endosomes, where a drop in pH activates the phospholipase A2 domain of the capsid protein VP1, mediating membrane penetration and the release of the viral genome.

Entry of enveloped viruses relies on some form of membrane fusion between the virus and the host cell, however for non-enveloped viruses penetration of a host cell membrane must be achieved by other means (Tasi 2007). In general, the release of non-enveloped viruses into target cells consists of approximately four steps. First the virus needs to be transported to the appropriate site within the cell. Next, interaction between viral and host factors at this site induces conformational changes of viral proteins leading to disruption of the membrane's lipid bilayer which ultimately results in the release of the virus particle or the viral genome. Adenoviruses are non-enveloped DNA viruses that enter target cells using receptor-mediated endocytosis (Leopold and Crystal 2007). A drop in pH within the endosome leads to conformation changes in the viral capsid, which disrupts the membrane and allows virus particle to enter into the cytoplasm. The virus particle is then transported via microtubules to the nucleus, where the viral genome is released. African Swine Fever Virus (ASFV) is a dsDNA virus which is the only member of Asfaviridae virus family that enters target cells via clathrin-mediated endocytosis. This mode of entry was recently found to be dependent on host dynamin GTPase activity (Hernaez and Alonso 2010). Recent advances in microscopic imaging technology has allowed for the labeling and tracking of individual particles within living cells. Single-particle tracking of Dengue flavivirus particles revealed that the virus particles engage cell surface receptors, diffuse across the plasma membrane and traffic to clathrin-coated pits (van der Schaar et al. 2007). The virus particles are taken to endosomes where a pH drop triggers a conformation change in the viral glycoprotein E, which then facilitates membrane fusion. Kaposi's sacrcoma-associated

herpesvirus (KSHV) is known to infect endothelial cells via clathrin-mediated endocytosis (Akula et al. 2003). When actin function of endothelial cells was disrupted, KSHV entry and trafficking was inhibited (Green and Gao 2009), suggesting that the actin cytoskeleton can be involved in viral transport.

Viral induced phosphorylation of host cell kinases was recently found to be important in the transport of herpes simplex virus (HSV) to the nucleus (Cheshenko et al. 2005). When focal adhesion kinase 1 (FAK1), a kinase involved in the regulation of cell migration, adhesion, actin reorganization and focal adhesion development, is knocked-down there is a significant decrease in the trafficking of HSV to the nuclear pore and infectivity was reduced by 90%. Knock-out of the Rab11 family interacting protein 2 (FIP2), a protein associated with the apical recycling endosome of polarized epithelial cells, results in a large decrease in the amount of respiratory syncytial virus, a paramyxovirus, released into the culture supernatant (Utley et al. 2008). However there is a significant increase in cell-associated virus, suggesting that RSV utilizes FIP2 and the apical endosome for virion budding. The functional endosomal sorting complex required for transport or ESCRT consists of three protein complexes termed ESCRT I, II, and III, which are essential for endosome transport and recycling (Carlton and Martin-Serrano 2009). The gag proteins of retroviruses interact with and recruit members of ESCRT to facilitate their transport and release within the infected host cell. Hepatitis C virus (HCV), a flavivirus, utilizes the ESCRT machinery, in particular ESCRT III, in order to escape endosomes (Lai et al. 2010). Treatment of infected cells with chemicals that disrupt ESCRT function and therefore endosomal trafficking, such

as nocodazole, which disrupts microtubule polymerization, greatly reduce the amount of HCV genomic RNA.

The baculovirus protein Exo0 is involved in the trafficking of newly synthesized virus particles from the nucleus (Fang et al. 2009). Exo0 was found to localize with microtubules and blockage of microtubule formation inhibited the egress of viral progeny. This indicates the baculoviruses facilitate virion transport via microtubules. Paramyxoviruses also make use of microtubules for virion transport (Chambers and Takimoto 2010). The components of paramyxovirus particles are trafficked to the plasma membrane where they are assembled prior to the budding of viral progeny via microtubule transport as determined using fluorescently labeled viral molecules. Viruses possessing the ability to infect multiple cell types may use cell-type specific transport mechanisms (Lambotin et al. 2010). HCV is able to infect both myeloid and plasmacytoid dendritic cells. Co-localization studies with organelle-specific markers suggests that in myeloid dendritic cells HCV associates with lysosomes, while in plasmacytoid dendritic cells it associates with late endosomes.

There are many different mechanisms by which viruses manipulate host trafficking pathways for transport of both virus particles and individual viral components. As viruses are dependent on host cells for completion of their life cycles, host transport machinery is an essential element for their survival. Thus disruption of the interaction of viruses with the host transport machinery provides an interesting avenue for viral treatment and prevention.

Porcine Reproductive and Respiratory Syndrome Virus

Genome Organization

In the late 1980's and early 1990's an unknown swine illness appeared in both North America and Europe (Keffaber 1989). Called the mysterious swine disease or blue ear syndrome, this disease was characterized by symptoms including late term abortions or stillbirths in sows and respiratory disease and high mortality in young pigs. The illness was later determined to be caused by an arterivirus, subsequently named Porcine Reproductive and Respiratory syndrome virus (PRRSV) (Wensvoort et al. 1991). PRRSV has a substantial impact on the swine industry worldwide. PRRSV-infected herds display poor reproductive health, increased mortality, and reductions in growth rates. In 2005 these effects were predicted to result in a loss of more than 560 million dollars a year in the US swine industry alone (Neumann et al. 2005) and today due to increased feed costs and a general increase in production costs it has an even greater industry impact (Osorio 2010).

PRRSV consists of a 15kb genome with nine opening reading frames (ORFs) (Figure 1.1). The first two ORFs encode the non-structural proteins (NSPs), while the remaining seven ORFs encode the structural proteins. Together, the first two ORFs, ORF1a and ORF1b, encode for a total of 14 non-structural proteins. Both ORF1a and ORF1b are initially translated as polyproteins. The polyprotein produced from ORF1 is termed pp1a. A frameshift in the viral genomes results in the production of the second polyprotein called pp1ab (Dokland 2010). PRRSV has four viral proteases, NSP1α, NSP1β, NSP2, and NSP4, which are responsible for the cleavage of the polyproteins into individual mature proteins.

NSP9 is the RNA-dependent RNA polymerase, while NSP10 and NSP11, are a helicase and an endonuclease, respectively. NSP9 and NSP10 associate with each other in cytoplasmic double-membrane vesicles that serve as the site of viral genome replication in infected cells (Fang and Snijder 2010). Epitopes present in the NSP9 and NSP10 proteins are recognized by T-cells, and this recognition is linked to an IFNγ response to PRRSV infection (Parida et al. 2012). NSP1β interacts with the host cellular poly(c) binding proteins 1 and 2 (PCBP1 and PCBP2) at cytoplasmic viral replication sites (Beura et al. 2011). PCBP1 and PCBP2 are nucleic acid binding proteins that bind to the 5′UTR of the PRRSV genome. Small interfering RNAs (siRNAs) targeting both PCBP1 and PCBP2 reduce PRRSV genomic RNA replication. In addition to their roles in the production of virus progeny, NSP1α, NSP1β, NSP2 and NSP7 have been show to modulate the production of cytokines during the immune response to PRRSV. For example, both nsp1α and nsp1β block the activity of the TNFα promoter by inhibiting the activity of transcription factors that bind to and activate the promoter (Subramaniam et al. 2010). The seven structural proteins are translated from subgenomic RNAs (sgRNAs) transcribed from the ORFs located in the 3' end of the PRRSV genome (Figure 1.2). The transcription of the sgRNAs is initiated at the 3' terminus of the genome, and discontinuous extension during (-)RNA strand synthesis results in a group of (-)RNA strands of varying lengths (Fang and Snijder 2010). A common leader transcription regulating sequence (TRS) is located in the 5' end of the ORF 2 in the genomic RNA and a body TRS is found preceding each of the structural proteins. As the RdRp begins (-) RNA strand synthesis base pairing occurs between the newly synthesized sgRNA body TRS and

the common leader TRS, which translocates the (-) RNA strand to the 5' end of the genome template. Subsequently synthesis resumes adding the complement of the leader sequence. Discontinuous extension of the nascent minus strand RNAs then yields subgenomic length (-) RNA strands for the production of the sg mRNAs for protein synthesis. ORF2-4 encode minor envelope proteins, while ORF5 and ORF6 encode the major envelope proteins, and ORF7 encodes the nucleocapsid protein. ORF2a encodes glycoprotein 2 (GP2). ORF2b, which is entirely located within ORF2b, encodes E protein, which is thought to function as an ion channel. ORF 3 encodes glycoprotein 3 (GP3) and ORF4 encodes GP4. GP2, GP3, and GP4 form a heterotrimer within the viral envelope. ORF5 encodes the major glycoprotein of PRRSV, called GP5 and ORF6 encodes the membrane or M protein. GP5 and M form a heterodimer (Figure 1.3) within the PRRSV envelope and are thought to be the key players in receptor recognition on the host cell.

PRRSV entry

Though some details of PRRSV entry into susceptible cells are known, the exact mechanism of PRRSV intracellular transport is unclear. Initial studies into the cellular tropism of PRRSV found that most tested cell lines are unable to bind the virus (Kreutz 1998). Vero cells bind and internalize PRRSV but do not support virion production. Currently it is thought that PRRSV enters cells using receptor-mediated endocytosis (Nauwynck et al. 1999). PRRSV was found to co-localize with clathrin and in macrophage cultures treated with chloroquine, which is commonly used in the treatment of malaria and affects vacuole pH levels, and treated cells are resistant to PRRSV uptake (Nauwynck 1999).

Treatment of infected cells with weak bases prevents the release of virions from endosomes, which suggests that a low pH is also required for the release of the virus. Several cellular receptors have been identified for PRRSV susceptibility though more likely remain to be identified. A macrophage-specific cell surface molecule CD163 mediates PRRSV entry in macrophages (Calvert et al. 2007). CD163 was also recently found to be expressed on the surface of MARC-145 cells, derived from African Green Monkey kidney cells, a PRRSV-permissive cell line. CD163 is up-regulated in activated macrophages. Tranfection of various mammalian encoded CD163s into cells non-permissive to PRRSV results in PRRSV uptake in these cells (Delrue et al. 2010). CD163 consists of 9 scavenger receptor cysteine rich (SRCR) domains (exposed to the cell surface), a transmembrane domain and a cytoplasmic domain. Proteins containing SRCR domains are often expressed on immune cells and are associated with ligand recognition. In addition to CD163, PRRSV M is known to interact with heparan sulfate proteoglycans present on the cell surface (Welch and Calvert 2010). PRRSV is also known to interact with CD169 (sialoadhesin) (Vanderheijden et al. 2003). Additional evidence suggests that PRRSV also binds to vimentin to facilitate an interaction with CD151 and DC-SIGN, members of the cytoskeleton (Kim et al. 2006).

GP5 and M

As discussed above, GP5 protein is considered to be the major glycoprotein of PRRSV. GP5 is a ~25kDa protein containing a variable number of glycosylation sites between heterologous PRRSV strains (Figure 1.3A). North American strains have three putative glycosylation sites (N34, N44, and N51) located near the N-terminus of the protein, while

GP5 of European strains is predicted to possess only two glycosylation sites (N46 and N53) (Wissink 2004). The glycosylation sites of GP5 lie near the neutralizing epitope (aa27-41), suggesting that glycosylation of these sites may function to mask the antigenic site from neutralizing epitopes, a common form of antigenic masking of viral glycoproteins. Glycosylation epitope shielding of GP3 is also an important for PRRSV immune evasion (Vu et al. 2011). In an attempt to identify the glycosylation pattern of potential glycosylation sites of GP5, Ansari et al. (2006) created full length PRRSV infectious cDNA clones in which the GP5 glycosylation sites were either individually mutated or in which multiple glycosylation sites were altered. It was discovered that mutation of either the N34 or the N51 sites or both sites together still produce infectious virus, albeit at lower levels than wtPRRSV. However, mutation of the N44 glycosylation site completely abrogates the production of virus progeny, suggesting that the N44 glycosylation is essential for PRRSV infectivity.

Though there is a large degree of variation in the genomic sequence of GP5 among different PRRSV strains, the overall organization and structure of GP5 is similar among all PRRSV isolates. The first 31 amino acids of GP5 likely constitute a signal peptide. GP5 has three membrane spanning regions, an N-terminal ectodomain and a C-terminal endodomain (Figure 1.3A). In addition to its involvement in virus assembly and transport, GP5 has been also linked to the induction of apoptosis in PRRSV infected cells. It was found that exogenous expression of the GP5 protein induces apoptosis in either COS-1 or BSC40 cells (Fernández et al. 2002). Mutagenesis of GP5 revealed that the region likely responsible for the induction of apoptosis in PRRSV infected cells lies within the first 118aa of GP5.

ORF6 of PRRSV encodes the non-glycosylated 19kDa protein, termed M protein (Figure 1.3B). Along with GP5, M protein is considered a major structural envelope protein and a class III integral membrane protein. Sequence analysis of M protein suggests that it contains three hydrophobic regions that likely form several membrane-spanning domains (Dokland 2010). In addition only a short region, the first 16 amino acids at the amino terminus, of M is exposed to the virion surface. M protein does not contain any predicted signal peptide sequences and is likely brought to the virion surface via association with GP5. Along with the formation of GP5/M heterodimers, M protein homodimers have also been observed in PRRSV infected cells, however these M homodimers are not incorporated into the virion and it is unknown what if any function they serve (Dea et al. 2000). As with GP5, a major function of M protein during PRRSV infections is likely virus assembly and budding. To elucidate possible functions of the M protein, chimeric PPRS viruses in which the ectodomain of M was substituted with the ectodomains of M proteins encoded by other Arteriviruses including murine lactate dehydrogenase-elevating virus (LDV) and equine arteritis virus (EAV) were generated (Verheije et al. 2002). Analysis of the infectivity of these viruses revealed that M protein is needed for virion assembly but is not involved in viral tropism as these chimeric PRRSV viruses were unable to infect cells that are permissive to LDV or EAV.

The GP5 and M heterodimer is formed by the covalent linkage of cysteine at the ninth position of M and the cysteine at position 44 of GP5. This heterodimer is thought to function in virion assembly and budding and possibly in entry of the virus and is required for viral

particle formation (Dokland 2010). It is thought that the GP5/M heterodimer is formed in the endoplasmic reticulum during virus particle assembly and serves as the basic protein matrix of the virion envelope (Snijder et al. 2003). However, little else is known about the functional roles that GP5 and M and their heterodimer have in PRRSV pathogenesis, particularly their specific involvement in the entry and transport of the PRRS virus.

Immunological Response to PRRSV infection

During the acute phase of infection only weak innate and adaptive immune responses are generated against PRRSV infection (Murtaugh et al. 2002). In the earliest stages of infection there is little if any production of innate interferons or cytokines. A delayed adaptive immune response is eventually mounted which eases PRRSV symptoms, but does not clear the virus as PRRSV-infected pigs often maintain persistent infections and may shed virus up to 200 days post infection. It is well known that young pigs infected with PRRSV have an increased susceptibility to secondary respiratory infections (Thanawongnuwech et al. 2000). There are several explanations for this phenomenon. One of which is, alveolar macrophages, the cellular tropism of PRRSV, serve to both protect from bacterial infections and also in antigen presentation and cytokine production for an effective immune response (Karp and Murray 2012). *In vitro* PRRSV infection of porcine alveolar macrophages induces apoptosis in these cells (Drew 2000). Therefore, a reduction in the number and function of macrophages in the lung of PRRSV infected pigs likely contributes to their increased susceptibility to secondary bacterial infections. *In vivo* infection of young pigs with PRRSV results in a large number of apoptotic cells in both the lungs and lymphoid tissues (Sur et al.

1998). Also, many of these cells do not necessarily co-localize with PRRSV infected cells, suggesting that PRRSV infection is a potent inducer of apoptosis in both susceptible macrophages as well as in other cell types. *In vivo* analysis of a highly virulent strain of PRRSV revealed that widespread pathological damage occurs in the lungs of infected pigs (Xiao et al. 2010). In addition to direct damage caused by PRRSV, an intense and sustained aberrant inflammatory response also contributes to the tissue damage in infected pigs. Analysis of the cell-mediated immune response to PRRSV infection found that T-cell proliferation is undetectable until 4 weeks post infection, peaks a couple of weeks later, and then declines after 11 weeks (Bautista and Molitor 1997). This delay in the cell-mediated immune response is another contributing factor to PRRSV pathogenesis and the increased susceptibility to secondary infections. Interestingly, it was also found that not only do antibodies generated against PRRSV antigens fail to block infection of macrophages, but they actually enhance infection both *in vitro* and *in vivo*. Characterization of immune cell populations in the broncho-alveolar lavage of PRRSV infected pigs demonstrated there is a large migration of both cytotoxic T-cells as well as natural killer cells into the lungs within a few weeks of infection (Samsom et al. 2000). Several studies have reported an increase of Toll-like receptor 3 (TLR3) expression in alveolar macrophages of PRRSV infected pigs (Sang et al. 2008; Miller et al. 2009). TLR3 is a component of the innate immune system, which recognizes double-stranded viral RNA and induces the expression of type I interferons (Yu and Levine 2011). *In vitro* studies in which type 1 interferons were added to PAM cultures infected with PRRSV, revealed that the virus is susceptible to the antiviral properties

of interferons (Buddaret et al. 1998). However, as discussed previously there is only a weak induction of type 1 interferons during PRRSV infection, suggesting that the virus is actively regulating interferon production. This was demonstrated in an *in vitro* study using Marc-145 cells. In PRRSV-infected Marc-145 cells, not only is interferon expression inhibited, but its production can even not be induced even by the addition of dsRNA (Miller et al. 2004). Several PRRSV NSPs have been shown to interfere with various regulators of IFN production. For example, NSP1α prevents IFN regulatory factor 3 (IRF3) from binding to IFNβ promoter, while NSP1β prohibits STAT1 from entering the nucleus, which prevents the induction of interferons by the JAK-STAT pathway (Sagong and Lee 2011). NSP1α also blocks IFNβ production by inhibiting NFκB activation via the RIG-1 signaling pathway (Luo et al. 2008). Closer analysis revealed that NSP1α prevents the nuclear translocation of NFκB by inhibiting the phosphorylation of IκB (Song et al. 2010).

PRRSV Vaccines

Several strategies have been undertaken to develop more potent PRRSV vaccines. One strategy currently being studied is the addition of adjuvants to increase the immunogenicity of the vaccine. One adjuvant that has been tested with PRRSV vaccines consists of oligonucleotides containing CpG motifs (Zhang et al. 2007; Guo et al. 2011). Intranasal delivery of the CpG adjuvant in addition to a killed virus vaccine appeared to increase the immune response in vaccinated pigs (Zhang et al. 2007). Animals vaccinated with the adjuvant containing vaccine exhibit increased T-helper type 1 and type 2 responses compared to controls. However, large amounts of the adjuvant must be included in order for

the animals to produce an effective immune response to the vaccine. The response to the vaccine is also delayed with strong immune responses not being detected until ~4-5 weeks post vaccination. Another strategy that has been employed to develop a PRRSV vaccine is DNA immunization using recombinant plasmids containing PRRSV proteins. Most often the PRRSV protein of choice is the major glycoprotein GP5 as this protein has been determined to contain the major epitopes of the virus. In one approach using this strategy a plasmid vaccination expressing either the PRRSV GP5 or N protein in conjunction with either IL-2 or IFN-γ (both of which are up regulated during a PRRSV infection) was developed (Xue et al. 2004). The vaccine expressing GP5 in conjunction with IFN-γ appeared to be the most effective vaccine with 2 out of 3 vaccinated pigs lacking clinical symptoms, including lung lesions, after viral challenge. The vaccines expressing either GP5 and IL-2 or N protein and IL-2 each protected one pig from developing clinical symptoms in the study. However, PRRSV replication was detected in all pigs though it was reduced in vaccinated animals. This suggests that the addition of cytokines (especially IFNγ) at the time of vaccination may aid in developing a better immune response and therefore offer better protection against a PRRSV infection. However, it appears this will still not be effective in some animals and does not completely prevent the virus from replicating. Another study tested the efficacy of a PRRSV plasmid vaccine expressing a recombinant protein consisting of the GP5 protein and the swine ubiquitin protein (Hou et al. 2008). Proteins that are fused with ubiquitin are degraded by the proteosome and presented by MHCI, so the concept behind this vaccine is that fusion of the antigen of interest to ubiquitin will increase presentation of the antigen and

will therefore induce a stronger immune response. This could be particularly useful in the development of a PRRSV vaccine since PRRSV down regulates the expression of MHCI. It is likely the virus is sensitive to this aspect of the immune system and so could be a good target for vaccine development. Another plasmid expressing GP5 alone produced a high level of antibodies as expected, however the recombinant GP5-ubiqitin protein did not produce any detectable antibody response, though this vaccine did increase the cell-mediated Th1 response and protected 4 of 6 pigs from developing clinical symptoms. These vaccinated pigs also had decreased viral titers and virema, suggesting vaccines that increase the Th1 response, which is known to be weak in a PRRSV infection, may increase protection against this virus. Another vaccine approach that has been attempted to combat PRRSV is the development of replication-defective vaccines (Welch et al. 2004). In this approach two modified viruses were created, lacking either ORF2 (encodes GP2a and b) or ORF4 (encodes GP4). These mutations are lethal to the virus *in vitro*; therefore supplying the missing proteins in *trans* produces replication-defective viruses. These viruses were used to immunize pigs and ~ 1 month post-immunization the animals were challenged with a homologous virus strain. A small group of the vaccinated pigs did display decreased viral titers compared to non-vaccinated controls, however there was no significant difference in clinical disease between vaccinated and non-vaccinated animals suggesting that neither virus vaccine is effective in protecting against PRRSV infection. Overall, many different approaches have been undertaken to develop PRRSV vaccines, however, currently no single vaccine exists that protects the majority of vaccinated animals, that induces a rapid immune

response, and that can protect against a broad range of PRRSV strains. All of these issues will need to be resolved in order to develop a highly efficacious PRRSV vaccine.

Small Regulatory RNAs

In the decade since their discovery, small RNAs have been established as a major branch of the gene regulatory network. The biogenesis of small RNAs is well known and has been extensively covered (e.g. Okamura 2012; Janga and Vallabhaneni 2011), and so will only be briefly mentioned here. Instead, the goal of this review is to summarize our current knowledge of the involvement of small RNAs in eukaryotic immunity and in pathogenic counter-defense.

Small RNA biogenesis

There are several classes of small RNA families, and of these, short-interfering RNAs (siRNAs) and microRNAs (miRNAs) are the major small RNA groups associated with eukaryotic immunity. Biogenesis pathways of siRNAs and miRNAs are well conserved and greatly overlap (for an in depth review see Okamura 2012). In the generation of both groups a precursor molecule is processed into a short dsRNA duplex by a member of the Dicer family of endonucleases. However, in animals, primary miRNA transcripts, which can contain multiple miRNAs, are initially processed into single precursor miRNAs by the endonuclease Drosha. For siRNAs, the precursor molecule for dicer processing is a longer dsRNA, while the miRNA precursor is an RNA hairpin. Currently, mammals are thought to have only a single dicer, flies and worms encode two dicers, while plants can have up to four dicer-like endonucleases (DCLs), depending upon the species. In addition to its

endonuclease activity, dicer also functions as a helicase and separates duplex RNA into two single-stranded small RNA molecules. One strand, often termed the guide strand, interacts with members of the Argonaute protein family to form the RNA-induced silencing complex or RISC, while the other strand, called the passenger or star strand is usually degraded. RISC then facilitates the interaction of the small RNA with its target sequence, resulting in silencing or suppression of gene expression, by one of several mechanisms, which will be briefly reviewed below.

Plant small RNA-an overview

Plants produce a variety of small RNA species, which possess three main functions: (1) regulation of transposon activity, (2) pathogenic defense, and (3) regulation of intrinsic pathways such as, development and the response to environmental stresses (Hohn and Vazquez 2011). Unlike animals, plants produce endogenous siRNAs. In general, plants encode four DCLs, each of which processes distinct small RNA (sRNA) classes, but also share some overlapping or redundant functions (Figure 1.4a). DCL1 is involved in the generation of 21-22nt sRNAs. DCL1 preferentially associates with hairpin precursor RNAs (Hohn and Vazquez 2011). RNA processing by DCL2 results in small 22nt siRNAs. DCL3 generates sRNAs of 24nt, while DCL4 is involved in the generation of 21nt sRNAs from precursors consisting of long perfect complementary dsRNA precursors (Hohn and Vazquez 2011). DCL1 is mainly involved in miRNA processing and possesses functions analogous to both Dicer and Drosha in animals (Jaskiewicz and Filipowicz 2008), while DCL2 and DCL4 are the major siRNA processors (Martínez de Alba et al. 20011). DCL2 siRNAs mainly

function in host defense against viruses, though in the absence of DCL2, DCL4 can also produce antiviral siRNAs (Earley et al. 2010). DCL3 siRNAs mainly regulate transposon activity and chromatin modification (Jaskiewicz and Filipowicz 2008). DCL4 processing is mainly reserved for trans-acting siRNAs (tasiRNAs). DCL4 tasiRNAs are mainly induced by and regulate the response to environmental stresses, such as drought. Plants encode approximately ten different argonaute proteins (Agos), and similar to DCLs, these Agos have both distinct and overlapping functions (reviewed by Czech and Hannon 2011). AGO1 is the major ago protein in miRNA RISCs. AGO2 interacts with tasiRNA generated from DCL4, while AGO4 is the main ago mediator of DCL3 processed siRNA function.

Animal small RNA- An overview

Animals also produce several distinct small RNAs, though not as many as the wide range found in plants. The major endogenous class of small RNAs involved in regulating the immune response and immune system development in animals is miRNAs. The other types of endogenous small RNAs are mainly involved in regulation of development, particularly in embryos. In animals miRNA genes are mainly located in either the introns of protein-coding genes, termed mirtrons or are located in intergenic regions. Intergenic miRNAs are under the control of their own promoters, while mirtrons most often are under the control of their host gene, though some mirtrons have been found to have their own promoter. Though single miRNAs exist, miRNAs are often found in clusters in animal genomes. Many miRNAs are initially expressed as a single primary transcript, consisting of multiple pre-miRNA hairpins. These hairpins are individually released by Drosha. After Drosha processing the miRNA

hairpins are transported from the nucleus to the cytoplasm by an exportin protein. Once in the cytoplasm the hairpin is further processed by Dicer and the mature miRNA guide sequence is then loaded onto the RISC (for review see Janga and Vallabhaneni 2011) (Figure 1.4b).

Plant immunity and small RNA

In contrast to animals, a major plant antiviral defense mechanism involves RNA silencing. Upon infection, viral dsRNA is recognized by DCLs and is cleaved into viral siRNA (vsiRNA) that are 21-24nt in length (Llave 2010). These vsiRNAs are then amplified by host RNA-dependent RNA polymerases. The secondary population of siRNAs is then transported throughout the plant as part the antiviral response. Of the four plant DCLs, DCL2 appears to be the major DCL associated siRNA-mediated viral defense, though DCL4 may also contribute.

Plant PRRs (pathogen recognition receptors) are evolutionarily related to Toll-like receptors in animals (Coll et al. 2011). They are typically receptor-like kinases. The resistance proteins involved in effector-triggered immunity are structurally analogous to Nod-like receptors in mammals. Unlike PRRs, these resistance genes are intracellular molecules that function to survey the cytosol for pathogen-derived molecules. In plants, the chloroplast is also important in the immune defense. This defense is also involved in the production of oxidative species that are associated with the hyper sensitive cell death response. The PAMPs (pathogen-associated molecular patterns) recognized by plant immune proteins are not necessarily pathogenic and are often structural (Bittel and Robatzek

2007). For example, in *A. thaliana* the PRR, FLAGELLIN SENSING 2, is a well known receptor-like kinase involved in the detection of bacterial flagellin (Bittel and Robatzek 2007). In addition to PRRs/PAMPs triggered immunity, another major defense mechanism in plants is effector-triggered immunity (ETI). In ETI a family of proteins termed resistance or R proteins recognizes bacterial and viral antigens, which then trigger an immune response (Xiao et al. 2011). PRRs/PAMPs triggered immunity and ETI are both regulated by and regulate small RNAs (Jin 2008). For example, bacterial infections can alter miRNA expression, including *miR-393*, *miR-167*, *miR-160*, and *miR-825* (Fahlgren et al. 2007). These miRNAs regulate the expression auxin signaling genes as well as biotic stress related genes that are associated with PAMP signaling. Also important in ETI are host-encoded resistance genes termed nucleotide binding site and leucine-rich repeat resistance proteins or NBS-LRR proteins. In healthy plants the expression of NBS-LRR proteins is regulated by *miR-482* (Shivaprasad et al. 2012). However, when a plant becomes infected with either a virus or bacterium, *miR-482* expression is down-regulated, which then allows for increased expression of NBS-LRR proteins and induction of ETI. Melons express a member of the NBS-LRR protein family, Vat, which participates in resistance to aphids (Sattar et al. 2012). MiRNA profiling during aphid infestations of resistant and susceptible plants revealed that in general, miRNAs are up-regulated in the resistant plants and down-regulated in susceptible plants (Sattar et al. 2012). Many of the miRNAs up-regulated in resistant plants regulate biotic and abiotic stress response genes. This data suggests that miRNA regulation is likely associated with disease resistance in plants. SiRNAs, such as *nat-siRNAATGB2*, and *Atl-*

siRNA-1, are induced upon pathogenic infection and regulate the expression of several resistance genes (Katiyar-Agarwal et al. 2007). In plants, siRNAs also play a role in the silencing of transposition by facilitating the methylation of transposable elements (Earley et al. 2010). However, this mechanism requires the cooperation of histone deacetylase 6 (HDA6). In *HDA6* mutant plants siRNAs accumulate and induce de novo methylation, but this methylation does not result in the suppression of gene expression (Earley et al. 2010). In the plant germline there exists a special class of siRNA which is termed epigenetically activated 21nt siRNAs or easiRNAs (Calarco and Martienssen 2011). EasiRNAs are involved in the regulation of numerous host defense genes via epigenetic mechanisms.

Animal immunity and small RNA

The involvement of miRNAs in the regulation of immunity and the immune response is well characterized in animals. Analysis of miRNA expression and regulation in lymphocytic progenitors and in differentiated lymphocytes found that on average each of these cell types expresses ~100 different miRNA (Kuchen et al. 2010). CHIP-seq analysis further revealed that in lymphocytic progenitor cells that lymphocyte-specific miRNAs are under epigenetic expression regulation and are only fully expressed upon differentiation. In all ~50 miRNAs are up-regulated upon lymphocyte maturation. MiRNA expression profiling of human primary macrophages found 119 expressed miRNAs and several of the highest expressed miRNAs, such as *miR-146a* and *miR-212* are known to have immune-related functions (Luers et al. 2010). Treatment of the acute myeloid leukemia cell line THP-1 cells with phorbol myristate acetate (PMA) to induce differentiation was found to cause the

expression of 23 PMA-regulated miRNAs (Forrest et al. 2010). Further analysis revealed that four miRNAs, *miR-155, miR-222, miR-424,* and *miR-503* work in concert to induce cell-cycle arrest and induce differentiation of myeloid progenitor cells.

Several immune miRNAs have been well characterized; among these is *miR-155*. There are currently over 100 studies published on *miR-155*, the majority of which reveal its involvement in modulating the immune response and in immune cell proliferation. *MiR-155* expression is induced in murine macrophages following treatment with either polyriboinosinic:polyribocytidylic acid or IFN-β, suggesting a role for *miR-155* in the inflammatory response (O'Connell et al. 2007). This increase in *miR-155* expression was found to be facilitated by TLR signaling. *MiR-155* was identified as part of an IFN signaling feedback system that is MyD88 and NF-κB dependent (Wang et al. 2010). Two other TLR-regulated miRNAs have also been identified, *miR-21* and *miR-146a* (Quinn and O'Neill 2011). *MiR-155* expression can be induced by TLR2, TLR3, TLR4 or TLR9, *miR-146a* is responsive to TLR2-TLR5, and *miR-21* is induced by TLR4 (O'Neill et al. 2011). TLR signaling in turn can be regulated by miRNAs. *TLR3* and *TLR4* contain *miR-223* binding sites (O'Neill et al. 2011). TLR4 is also a target of *let-7i* and *let-7c*, while *TLR2* is regulated by *miR-105*.

Multiple studies have revealed a reciprocal relationship between NFκB and miRNAs, i.e. NFκB signaling regulates the expression of multiple miRNAs and in turn miRNAs regulate the expression of multiple members of NFκB signaling. NFκB signaling up-regulates the expression of the pro-inflammatory cytokine IL-6 by reducing *let-7* expression,

an *IL6* regulator (Li et al. 2011). Conversely, NFκB up-regulates the expression of both *miR-146* isoforms, which in turn reduce the expression of IRAK1/TRAF6, which then decreases NF-κB activity (Vaz et al. 2011).

Pathogenic manipulation of small RNA pathways

The majority of currently known viral miRNAs are encoded by herpesviruses, encoding between 3 (Herpes B virus) and 68 (Rhesus lymphocryptovirus) mature miRNA (miRBase v18; www.mirbase.org). Several studies have suggested that these herpesviral miRNAs are key regulators of viral latency. Herpes simplex virus 1 (HSV1) *LAT* (latency associated transcript) encodes 4 miRNAs (Umbach et al. 2008). One of these miRNAs, *miR-H2-3p*, is likely involved in latency regulation by targeting the viral gene *ICP0*, an immediate-early gene that is associated viral replication and reactivation (Umbach et al. 2008). Twelve miRNAs located in the latency associated region (LAR) of Kaposi's sarcoma-associated herpesvirus (KSHV) are expressed during viral latency (Malterer et al. 2011). These miRNAs have also been linked to viral latency and reactivation. A host gene involved in the epigenetic regulation of KSHV, *RBL2*, as well as the viral gene *RTA*, a reactivation regulator, are targets of KSHV miRNAs (Malterer et al. 2011). MicroRNA sequence analysis of KSHV tumors revealed that some KSHV-encoded miRNAs are more susceptible to mutations than others (Qin et al. 2012). The KSHV encoded miRNAs, *miR-K12- 1, 3, 8, 10, 11*, and *12* display a high degree of sequence conservation between patients, while *miR-K12- 2, 4, 5, 6, 7,* and *9* display much more inter-patient sequence variability. As miRNAs typically only share partial complementarity with their target sites, alterations in miRNA

sequences could affect target gene regulation. Human cytomegalovirus (HCMV), which encodes 17 mature miRNAs, expresses a miRNA termed *miR-UL112-1* during the late stages of infection that targets the host restriction factor *BclAf1* (Lee et al. 2012). This miRNA targeting and subsequent reduction in BclAf1 expression enhances viral gene expression and replication. BclAf1 has been shown to target the viral protein IE1 as part of the host anti-viral response to HCMV (Saffert and Kalejta 2006). These results suggest that HCMV *miR-UL112-1* is involved in viral evasion of the host immune response. Multiple miRNAs have been identified in the genome of Marek's Disease Virus (MDV), a well known herpesvirus of poultry. Oncogenic MDV strains, classified as MDV serotype 1 (MDV-1), encode 14 precursor miRNAs, which produce 26 mature miRNAs (miRBase v18). Expression studies found that MDV-1 miRNAs are differentially expressed during infections with strains of varying virulence (Morgan et al. 2008). It was shown that miRNAs located near *MEQ*, a known MDV oncogene, are expressed at higher levels during infections with highly virulent strains compared to less virulent strains. This differential expression has been linked to a polymorphism within the promoter of these viral miRNAs. Several herpesviruses encode an ortholog to a host miRNA, *miR-155*, including KSHV, and MDV. Currently, *miR-155* is one of the most studied miRNAs, in part, because it has been linked to lymphocyte development and is often up-regulated in lymphomas and other cancers (Lu et al. 2008). Recently, *miR-155* has been linked to EBV latency regulation, as treatment of latent EBV infected cells with a *miR-155* inhibitor reduces viral EBNA1 expression, which in turn, reduces EBV copy number (Lu et al. 2008). In KSHV infected lymphocytes, sustained expression of the KSHV

miR-155 ortholog, *miR-k12-11*, likely contributes to the increased proliferation seen in these cells (Skalsky et al. 2007). A miRNA located in the *MEQ* cluster of MDV-1, *mdv1-miR-M4*, is a *miR-155* ortholog (Morgan et al. 2008). Deletion or seed region mutagenesis of *miR-M4* prevents lymphoma induction in infected birds (Zhao et al. 2011), suggesting a role for *miR-M4* in MDV oncogenesis. However, insertion of miR-M4 into a related, but non-oncogenic virus, herpesvirus of turkeys (HVT), does not result in tumor formation in infected birds (Burnside and Morgan 2011), suggesting that other factors are needed for viral transformation. In addition to the *miR-155* ortholog, EBV encodes miRNAs sharing seed sequences with host *miR-29a/b/c*, *miR-18a/b*, *miR-520d-5p* and *miR-524-5p* (Riley et al. 2012). Target gene analysis using an AGO pull-down assay revealed that these homologous viral/host miRNAs share many of the same targets. These conserved targets are involved in regulating apoptosis, the cell cycle, and Wnt signaling.

Several host miRNAs have also been linked to herpesvirus infections. The EBV encoded protein LMP1 (latent membrane protein 1) induces the expression of host *miR-34a* upon EBV infection of human B-cells (Forte et al. 2012). *MiR-34a* is also highly expressed in several EBV-transformed cell lines. Interestingly, *miR-34a* is considered to be a tumor suppressor miRNA whose expression is directly regulated by p53 (Chang et al. 2007), however, increased *miR-34a* levels are associated with enhanced growth in EBV infected cells (Forte et al. 2012). Two additional host miRNAs have been linked to EBV infections. The miRNAs *miR-200b* and *miR-429* were recently shown to be involved in the EBV lytic/latent switch (Ellis-Connell et al. 2010). Exogenous expression of *miR-200b* and *miR-*

429 in EBV positive cells results in increased expression of EBV lytic genes. *MiR-200b* and *miR-429*, both members of the *miR-200* miRNA family, regulate the expression of *ZEB1* and *ZEB2*, whose gene products are transcriptional repressors involved in IL2 regulation and previously shown to regulate EBV latency (Ellis et al. 2010). In addition, EBV infection of blood-derived human B-cells results in the decreased expression of *miR-200b* (Ellis-Connell et al. 2010). In human CD34+ hematopoietic progenitor cells latently infected with HCMV, the host miRNA *miR-92a* is down-regulated (Poole et al. 2011). Decreased *miR-92a* expression results in an increase in its target gene expression, GATA-2. This increase in GATA-2 results in increased IL-10 expression, suggesting that IL-10 may be involved in HCMV latency. Knock-down of *miR-101* in HeLa cells increases HSV-1 production (Zheng et al. 2011). *MiR-101* targets the host gene *ATP5B*, an ATP synthase, and siRNA knock-down of ATP5B expression in HeLa cells greatly reduces HSV-1 production. Analysis of host miRNA expression in porcine dendritic cells upon infection of psuedorabies virus, an alpha herpesvirus, revealed multiple differentially expressed host miRNAs (Anselmo et al. 2011). These miRNAs regulate genes and pathways with shared functions. In an MDV-transformed T-cell line, MSB1, two related host miRNAs, *miR-221* and *miR-222*, are significantly up-regulated relative to splenocytes or CD4+ T-cells (Lambeth et al. 2009). Additionally, conserved binding sites for these miRNAs were identified in the 3'UTR of $p27^{kip1}$, a known *miR-221/222* target in mammals. However, the over-expression of *miR-221/222* is not found in other MDV-transformed cell lines, suggesting these miRNAs may not play a general role in MDV transformation. Overall, both viral and cellular miRNAs are

important regulators during herpesvirus infections, particularly during the lytic/latent switch and transformation,

Polyomaviruses have also been found to encode miRNAs, though much fewer in number and variation than with herpesvirus miRNAs. Currently, all examined polyomaviruses encode a single miRNA precursor, which produces one or two mature miRNAs (miRBase v. 18). The majority of polyomavirus encoded miRNAs are located antisense to the large T antigen (Tag) and function in a siRNA-like manner in the regulation of Tag expression (Lee et al. 2011; Bauman et al. 2011; Sullivan et al. 2009; Sullivan et al. 2005). Unlike herpesviruses, many polyomavirus miRNAs share sequence homology. The miRNA precursors encoded by the related polyomaviruses Bandicoot Papillomatosis Carcinomatosis Virus type 1 and 2 are located outside of the Tag gene, and regulate Tag expression by binding to a complementary site in its 3'UTR (Chen et al. 2011). SV40 miRNA Tag targeting reduces the cytotoxic T-lymphocyte (CTL) response (Bauman et al. 2011). Little is known about potential host gene targets of polyomavirus miRNAs. However, recently the host gene *ULBP3*, a stress-induced ligand, was identified as a target of JCV and BKV miRNAs (Bauman et al. 2011). This targeting was suggested to be involved in immune evasion, as it is associated with reduced NK cell killing of virally infected cells. No noticeable differences between a mutant murine polyomavirus lacking the miRNA precursor and wild type virus have been observed *in vitro* (Sullivan et al. 2009).

Though few viruses, other than herpesviruses and polyomaviruses, have been found to encode miRNAs, most of these viruses have been found to manipulate host miRNA

expression. Several host miRNAs, *miR-28*, *miR-125b*, *miR-150*, *miR-223* and *miR-382*, are found at much higher levels in resting CD4+ T-cells compared to activated cells (Huang et al. 2007). The 3'UTRs of several HIV mRNAs contain multiple binding sites for these particular miRNAs, suggesting that host miRNAs maybe involved in the maintenance of HIV latency in resting CD4+ T-cells (Huang et al. 2007). Furthermore, these miRNA binding sites are conserved between HIV strains. One symptom of hepatitis B virus induced hepatic cirrhosis is splenomegaly. Expression analysis revealed that 99 miRNAs were differentially expressed between normal spleens and spleens exhibiting HBV-induced hypersplenism (Li et al. 2008), suggesting host miRNAs are associated with HBV pathogenesis. A comparison of host miRNA expression differences during the infection of three influenza strains, H5N1 (also known as bird flu), a reconstructed 1918 H1N1 strain (r1918), and a seasonal H1N1 virus, suggests that miRNAs are involved in influenza pathogenesis (Li et al. 2011). The two highly pathogenetic strains, H5N1 and r1918 alter the expression of 23 host miRNAs that are not altered by the milder seasonal H1N1 (Li et al. 2011). A similar study comparing cellular miRNA expression differences between r1918 and a seasonal strain (A/Texas/36/91) in mice found over a hundred miRNAs are affected differently between the two strains (Li et al. 2010). Among these miRNAs are *miR-200a* and *miR-223*, whose target mRNAs are involved in the immune response and cell death pathways associated with the severe immune response found in r1918 infected lungs (Li et al. 2010). Microarray analysis of miRNA expression of cells infected with three influenza strains of varying pathogencity found that during early infection, *in vitro*, relatively few host miRNAs are up-regulated, with only 9%

of differentially expressed miRNAs being up-regulated at 24hpi (Loveday et al. 2012). However, at 48hpi and 72hpi the number of up-regulated miRNAs is greatly increased, with over 90% of the differentially miRNAs being up-regulated. Vaccinia virus (VACV), historically used in vaccinating against smallpox, was recently shown to induce a general down regulation of host miRNA expression in infected cells (Grinberg et al. 2012). This down-regulation of miRNA expression is observed within 24 hours of infection and is linked to a decrease in Dicer, a miRNA processing enzyme, expressed in VACV-infected cells.

One of the most well characterized examples of pathogen manipulation of host miRNAs is that of hepatitis C virus (HCV) and its use of the host liver-specific miRNA, *miR-122* (Jopling et al. 2005). Numerous profiling studies have shown that *miR-122* is highly expressed in the liver and functions in the regulation of lipid and cholesterol metabolism (Lewis and Jopling 2010). HCV has limited tropism *in vitro,* with very few permissive cell lines available. It was shown that a cell line permissive to HCV infection expresses high levels of *miR-122,* while non-permissive cell lines do not express *miR-122* (Jopling et al. 2005). When *miR-122* function was inhibited in the permissive cell line HCV replication was greatly reduced. Ectopic expression of *miR-122* in non-permissive cell lines did support viral replication; however no HCV infectious particles were produced (Fukuhara et al. 2012). *In silico* analysis predicted a *miR-122* binding site within the 5'UTR of the HCV genome and mutational analysis confirmed that the binding of *miR-122* to this site enhanced HCV replication (Jopling et al. 2005). It was recently shown that this enhanced viral replication was not due to a direct effect of *miR-122* on HCV RNA synthesis, as cells transfected with a

miR-122 inhibitor had lower levels of HCV RNA, but did not have reduced HCV RNA synthesis (Norman et al. 2010). Instead, the interaction between *miR-122* and the HCV genome is likely important in stabilizing viral RNA (Shimakami et al. 2012).

Though not as well studied as viral infections, bacterial infections have also been found induce changes in host miRNA expression. Virulent, but not avirulent, mycobacterium was found to inhibit TNF production by inducing the expression of host *miR-125b*, which subsequently reduces the expression of *TNF*, one of its target genes (Rajaram et al. 2011). *In vitro* infection of epithelial cells with listeria altered the expression of five host miRNAs, *miR-146b*, *miR-16*, l*et-7a*, *miR-145*, and *miR-155* (Izar et al. 2012). Several of these miRNAs are known to regulate immune genes. Furthermore, the expression changes of these miRNAs varied between wild-type bacteria and less pathogenic mutant strains (Izar et al. 2012). Taken together, these studies suggest that host miRNAs are also involved bacterial pathogenesis.

In response to siRNA-mediated antiviral response in plants, viruses have developed counter mechanisms. Many plant viruses encode proteins termed viral suppressors of RNA silencing or VSRs (Burgýan and Havelda 2011). Recently, the non-structural proteins (NSs) of tospoviruses were shown to bind with dsRNAs, including both siRNA duplexes and miRNA/miRNA* molecules (Pantaleo et al. 2010). The interaction between tomato spotted wilt virus (TSWV) NSs and dsRNA was shown to block Dicer-mediated cleavage. In addition, the binding of NSs to mature siRNA, after Dicer processing, also blocks this form of antiviral response. The 2b protein of cucumber mosaic virus (CMV), a cucumovirus,

possesses the ability to bind to and inhibit AGO1, thus blocking RISC function (González et al. 2010). Furthermore, similar to tospovirus NSs, 2b can also directly interact with small RNAs, suggesting that 2b employs multiple mechanisms to block antiviral RNA silencing. The helper component protease of tobacco etch virus (TEV) is able to interact with ds-siRNA and prevent strand separation (Kataya et al. 2009). The p19 protein of tomato bushy stunt virus (TBSV) blocks RISC loading by binding small dsRNA duplexes (Umbach and Cullen 2009). In addition to altering siRNA generation, plant VSRs can also alter host miRNA expression. Rice gall dwarf virus (RGDV), a phytoreovirus, encodes a VSR termed *Pns11* (Shen et al. 2012). When Pns11 is individually expressed in rice, the plants display phenotypic characteristics reminiscent of RGDV-infected plants. Transgenic Pns11-expressing plants exhibit altered levels of four host miRNAs, *miR-160, miR-162, miR-167,* and *miR-168*. The altered expression of these miRNAs, in particular the increased expression of *miR-167* correlates with the disease phenotype. It was suggested that alterations in the host gene targets of these differentially expressed miRNAs contribute to RGDV pathogenesis. For example, the expression of a *miR-167* target gene *ARF8* is altered in the Pns11 transgenic plants. Recently it has been demonstrated that co-infections of plant viruses can result in more severe alterations in miRNA expression (Pacheco et al. 2012). Tobacco plants co-infected with potato virus X (PVX) and either potato virus Y (PVY) or plum pox virus (PPV), show up to a 14-fold difference in host miRNA expression than do mock or singularly infected plants. These differentially expressed miRNAs target genes are

involved in stress responses, among others, suggesting that the more dramatic alterations in host miRNA expression may be linked the increased symptom severity of co-infected plants.

Viroids are a class of short non-coding circular ssRNA, which infect plants and can cause disease symptoms including growth retardation and necrosis (Ding 2010). Viroids rely entirely on host machinery for replication. As with viral infections plants often employ siRNA-mediated immunity in response to viroid infection (Navarro et al. 2009; St-Pierre et al. 2009). Multiple viroid derived sRNAs of 21nt, 22nt and 24nt are found in viroid infected grapevine tissues (Navarro et al. 2009). These varying lengths of sRNA suggest that multiple DCLs and therefore RNA silencing mechanisms are involved in the host defense against viroids. For example 60 distinct siRNA species generated from the peach latent mosaic viroid (PLMVd) ranging in size from 20nt to 26nt have been identified and are equally distributed between (+) and (-) polarities (St-Pierre et al. 2009). Rutgers tomato plants infected with the potato spindle tuber viroid (PSTVd) strain AS1 show disease symptoms, including necrosis and dwarfism (Diermann et al. 2010). Analysis of host small RNA expression patterns revealed that several host miRNAs, *miR-159, miR-396, miR-319,* and *miR-403*, are down-regulated in PSTVd infected plants (Diermann et al. 2010). These miRNAs are known to regulate transcription factors involved in plant morphology and development, suggesting that changes in host miRNA expression and function are associated with viroid pathogenesis.

Conclusion

Though often through different mechanisms, small RNAs are major players in host defense and pathogen manipulation in both plants and animals (Table 1.1). The fact that small RNAs can alter the expression of their target genes in varying degrees makes them ideal modulators of immunity. If an immune response is too robust it can be detrimental for the host, on the other hand, if the response is not potent enough, then the pathogen cannot be properly suppressed. Small RNAs therefore, provide eukaryotes with the ability to fine tune the immune system to obtain the optimal response. Pathogens, in turn, have evolved numerous ways in which to commandeer the small RNA mediated regulatory system. Small RNAs provide pathogens an ideal method in which to manipulate host gene expression, without triggering an anti-pathogenic response.

Figure 1.1. Organization of the PRRSV genome.

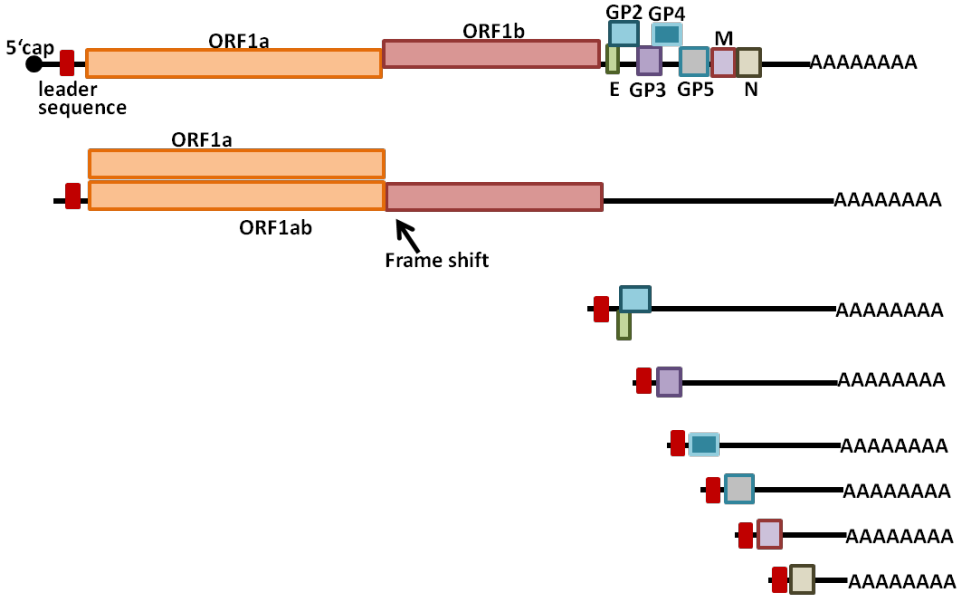

Figure 1.2. PRRSV subgenomic RNAs.

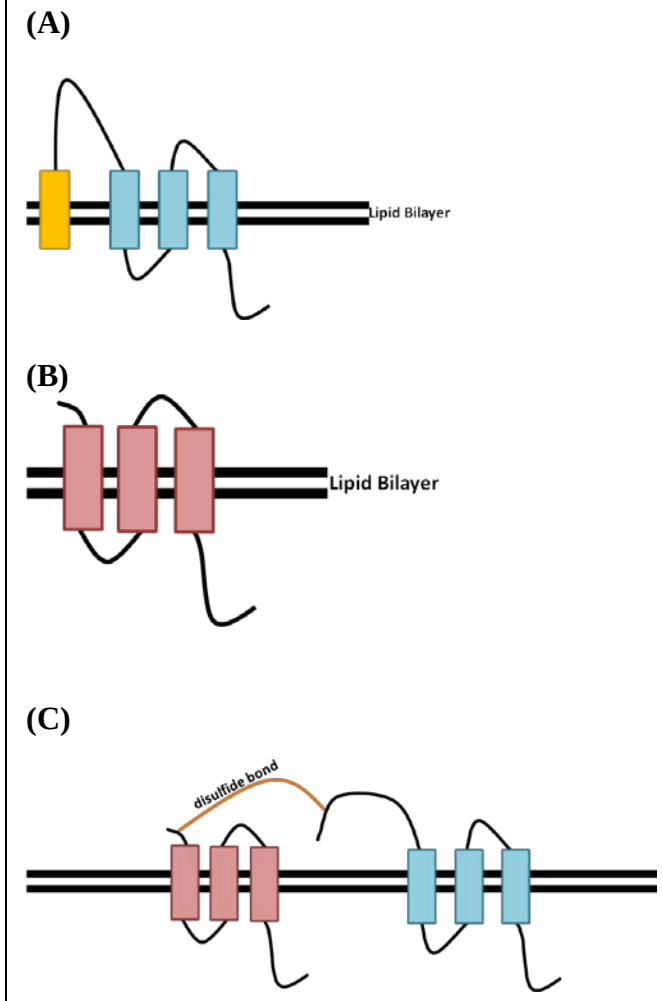

Figure 1.3. PRRSV GP5 and M protein topology
(A) GP5 topology. The signal peptide is shown as a yellow rectangle and transmembrane domains are shown as a blue rectangle.
(B) M topology. Transmembrane domains are shown in pink.
(C) The GP5 and M heterodimer. Note the signal peptide of GP5 is cleaved in the mature virion.

Figure 1.4.
Endogenous small RNA pathways involved in host defense and viral pathogenesis in animals and plants. (A) Small RNA biogenesis pathways mediated by the 4 dicer-like endonucleases (DCLs) in plant cells. 1. DCL3 generates siRNAs from transcripts produced via RNA Pol IV-dependent transcription. These siRNAs then form a RISC with AGO4, which mediates chromatin modifications at complementary genomic DNA sites. 2. Plant pri-miRNA transcribed by RNA Pol II are processed into a miRNA/miRNA* duplex by DCL1. The duplex is then transported to the cytoplasm by Hasty, a homolog of animal exportin-5, where the mature miRNA associates with AGO1 to from a miRISC. MiRISC facilitates the degradation of targeted mRNAs. 3. RDR6 produces dsRNAs from miRNA-mediated cleavage products of *TAS* gene transcripts. These dsRNAs are then processed into tasiRNAs by DCL4. Mature tasiRNAs form a RISC with AGO2 to mediate mRNA suppression. 4. Viral RNAs are utilized by RDR6 to produce dsRNAs, which are then processed into siRNAs by DCL2. These viral siRNAs undergo a second round of RDR6 amplification and are transported to peripheral sites where they form RISCs with either AGO1 or AGO2. These RISCs then degrade viral RNA as part of the anti-viral response. (B) MicroRNA biogenesis pathway of animal cells. Primary-miRNA transcripts (pri-miRNAs transcribed from either cellular DNA or viral DNA via an RNA Pol II mechanism, are processed into precursor hairpin molecules (pre-miRNA) in the nucleus. Pre-miRNAs are transported to the cytoplasm where they are further processed into the mature miRNA, which associates with Argonaute 2 (Ago2) and a several accessory proteins to form the RNA-induced silencing complex (RISC). RISC then facilitates the suppression of mRNA expression.

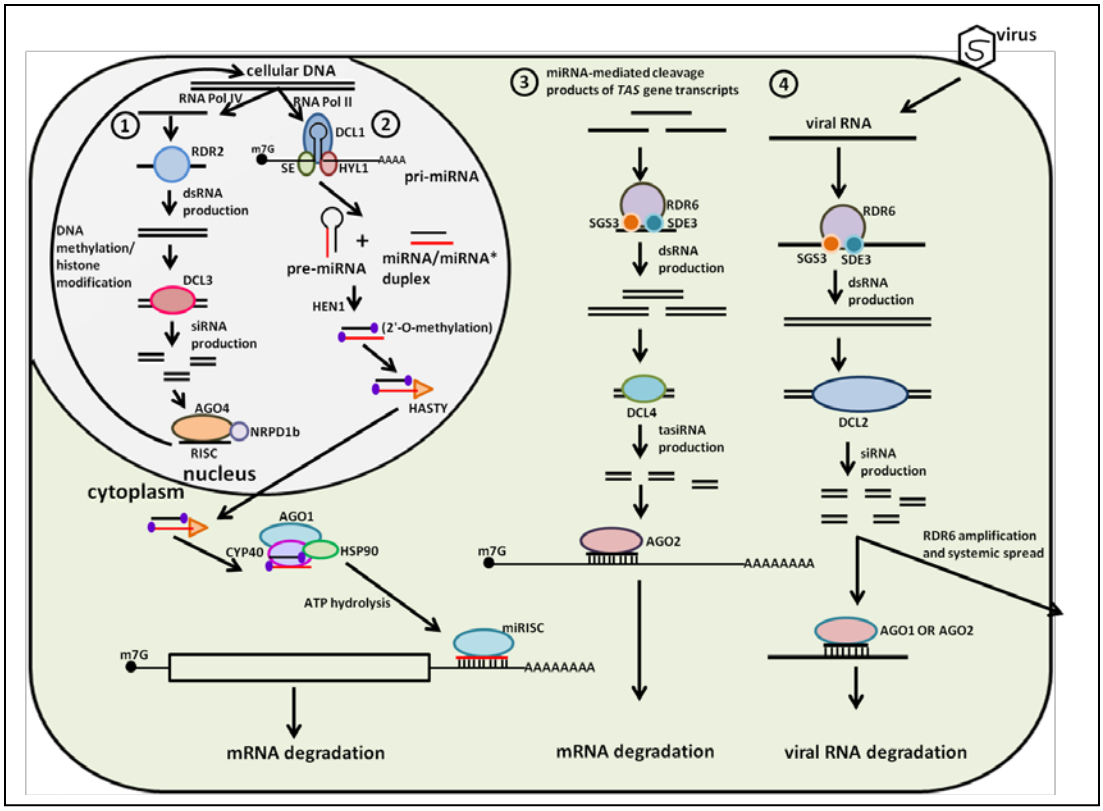
virus
cellular DNA
RNA Pol IV
RNA Pol II
1
2
RDR2
DCL1
m7G
SE
HYL1
AAAA
pri-miRNA
dsRNA production
DNA methylation/ histone modification
pre-miRNA
+
miRNA/miRNA* duplex
DCL3
HEN1
siRNA production
(2'-O-methylation)
HASTY
AGO4
NRPD1b
RISC
nucleus
cytoplasm
AGO1
CYP40
HSP90
ATP hydrolysis
miRISC
m7G
AAAAAAAA
mRNA degradation
3
miRNA-mediated cleavage products of TAS gene transcripts
RDR6
SGS3
SDE3
dsRNA production
DCL4
tasiRNA production
AGO2
m7G
AAAAAAAA
mRNA degradation
4
viral RNA
RDR6
SGS3
SDE3
dsRNA production
DCL2
siRNA production
RDR6 amplification and systemic spread
AGO1 OR AGO2
viral RNA degradation

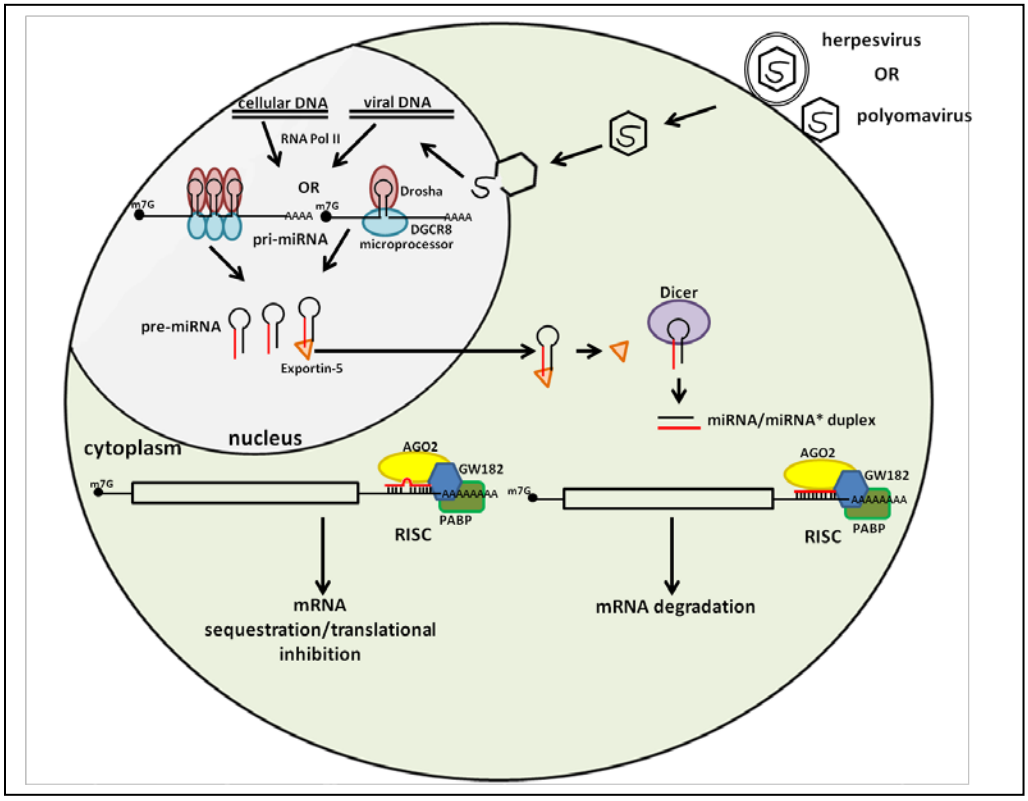
herpesvirus
OR
polyomavirus
cellular DNA
viral DNA
RNA Pol II
OR
Drosha
m7G
AAAA
m7G
AAAA
DGCR8
microprocessor
pri-miRNA
pre-miRNA
Exportin-5
Dicer
miRNA/miRNA* duplex
nucleus
cytoplasm
AGO2
GW182
m7G
AAAAAAAA
PABP
RISC
m7G
AGO2
GW182
AAAAAAA
PABP
RISC
mRNA
sequestration/translational
inhibition
mRNA degradation

Table 1.1 Examples of viral regulation of the host small RNA system

Virus	Effector molecule	Effect	References
Animals			
HSV1	*miR-H2-3p*	Targets viral *ICP0*-regulates latency	Umbach et al. 2008
KSHV	*miR-K12-4-5p*	Targets *RBL2*-modulates epigenetic regulation	Malkrer et al. 2011
KSHV	*miR-K12-5*	Targets viral *RTA*-regulates latency	Malkrer et al. 2011
KSHV	*miR-K12-11*	Host *miR-155* ortholog-regulates cell proliferation	Skalsky et al. 2007
MDV1	*miR-M4*	Host *miR-155* ortholog-regulates cell proliferation	Zhao et al. 2011
HIV	Host miRNAs (*miR-28*, *miR-125b*, *miR-150*, *miR-223*, and *miR-282*)	Target HIV mRNAs-involved in maintenance of viral latency	Huang et al. 2007
Influenza (highly pathogenic)	Host miRNAs (*miR-200a* and *miR-223*)	Target several immune response and cell death pathways	Li et al. 2010
Plants			
TSWV	Viral NS proteins	Binds to dsRNA and blocks Dicer mediated cleavage	Pantaleo et al. 2010
CMV	Viral protein 2b	Binds to and inhibits function of AGO1, also directly binds to small RNAs to block RISC function	Gonzalez et al. 2010
TEV	Viral helper component protease	Interacts with ds-siRNA and prevents strand separation	Kataya et al. 2009
TBSV	Viral protein p19	Blocks RISC loading by binding to small dsRNA duplexes	Yoon et al. 2012
RGDV	Viral protein Pns11	Alters levels of the host miRNAs *miR-160, miR-162, miR-167, miR-168*	Shen et al. 2012

References

Akula SM, Naranatt PP, Walia NS, Wang FZ, Fegley B, Chandran B. Kaposi's sarcoma-associated herpesvirus (human herpesvirus 8) infection of human fibroblast cells occurs through endocytosis. J Virol. 2003 77(14):7978-90.

Andersson ER. The role of endocytosis in activating and regulating signal transduction. Cell Mol Life Sci. 2012 69(11):1755-71.

Ansari IH, Kwon B, Osorio FA, Pattnaik AK. Influence of N-linked glycosylation of porcine reproductive and respiratory syndrome virus GP5 on virus infectivity, antigenicity, and ability to induce neutralizing antibodies. J Virol. 2006 80(8):3994-4004.

Anselmo, A.; Flori, L.; Jaffrezic, F.; Rutigliano, T.; Cecere, M.; Cortes-Perez, N.; Lefèvre, F.; Rogel-Gaillard, C.; Giuffra, E. Co-expression of host and viral microRNAs in porcine dendritic cells infected by the pseudorabies virus. PLoS One. 2011, 6, e17374.

Bauman, Y.; Nachmani, D.; Vitenshtein, A.; Tsukerman, P.; Drayman, N.; Stern-Ginossar, N.; Lankry, D.; Gruda, R.; Mandelboim, O. An identical miRNA of the human JC and BK polyoma viruses targets the stress-induced ligand ULBP3 to escape immune elimination. Cell Host Microbe. 2011, 9, 93-102.

Bautista EM, Molitor TW. Cell-mediated immunity to porcine reproductive and respiratory syndrome virus in swine. Viral Immunol. 1997 10(2):83-94.

Beura LK, Dinh PX, Osorio FA, Pattnaik AK. Cellular poly(c) binding proteins 1 and 2 interact with porcine reproductive and respiratory syndrome virus nonstructural protein 1β and support viral replication. J Virol. 2011 85(24):12939-49.

Bittel, P,; Robatzek, S. Microbe-associated molecular patterns (MAMPs) probe plant immunity. Curr Opin Plant Biol. 2007 10, 335-341.

Buddaert W, Van Reeth K, Pensaert M. In vivo and in vitro interferon (IFN) studies with the porcine reproductive and respiratory syndrome virus (PRRSV). Adv Exp Med Biol. 1998 440:461-7.

Burgyán, J.; Havelda, Z. Viral suppressors of RNA silencing. Trends Plant Sci. 2011, 16: 265-272.

Burnside, J.; Morgan, R. Emerging roles of chicken and viral microRNAs in avian disease. BMC Proc. 2011, 5 Suppl 4, S2.

Calarco, JP.; Martienssen, RA. Genome reprogramming and small interfering RNA in the Arabidopsis germline. Curr Opin Genet Dev. 2011, 21, 134-13.

Calisher CH, MC Horzinek. 100 years of virology : the birth and growth of a discipline Wien ; New York : Springer, c1999.
Calvert JG, Slade DE, Shields SL, Jolie R, Mannan RM, Ankenbauer RG, Welch SK. CD163 expression confers susceptibility to porcine reproductive and respiratory syndrome viruses. J Virol. 2007 81(14):7371-9.

Carlton JG, Martin-Serrano J. The ESCRT machinery: new functions in viral and cellular biology. Biochem Soc Trans. 2009 37(Pt 1):195-9.

Chambers R, Takimoto T. Trafficking of Sendai virus nucleocapsids is mediated by intracellular vesicles. PLoS One. 2010 Jun 7;5(6):e10994.

Chang, T.C.; Wentzel, E.A.; Kent, O.A.; Ramachandran, K.; Mullendore, M.; Lee, K.H.; Feldmann, G.; Yamakuchi, M.; Ferlito, M.; Lowenstein, C.J.; Arking, D.E.; Beer, M.A.; Maitra, A.; Mendell, J.T. Transactivation of miR-34a by p53 broadly influences gene expression and promotes apoptosis. Mol Cell. 2007, 26, 745-752.

Chen, C.J.; Kincaid, R.P.; Seo, G.J.; Bennett, M.D.; Sullivan, C.S. Insights into Polyomaviridae microRNA function derived from study of the bandicoot papillomatosis carcinomatosis viruses. J Virol. 2011, 85, 4487-4500.

Cheshenko N, Liu W, Satlin LM, Herold BC. Focal adhesion kinase plays a pivotal role in herpes simplex virus entry. J Biol Chem. 2005 280(35):31116-25.

Coll, N.S.; Epple, P.; Dangl, J.L. Programmed cell death in the plant immune system. Cell Death Differ. 2011, 18: 1247-1256.

Czech, B.; Hannon, G.J. Small RNA sorting: matchmaking for Argonautes. Nat Rev Genet. 2011, 12: 19-31.

Dea S, Gagnon CA, Mardassi H, Pirzadeh B, Rogan D. Current knowledge on the structural proteins of porcine reproductive and respiratory syndrome (PRRS) virus: comparison of the North American and European isolates. Arch Virol. 2000;145(4):659-88.

Delrue I, Van Gorp H, Van Doorsselaere J, Delputte PL, Nauwynck HJ. Susceptible cell lines for the production of porcine reproductive and respiratory syndrome virus by stable transfection of sialoadhesin and CD163. BMC Biotechnol. 2010 10:48.

Diermann, N., Matoušek, J.; Junge, M.; Riesner, D.; Steger, G. Characterization of plant miRNAs and small RNAs derived from potato spindle tuber viroid (PSTVd) in infected tomato. Biol Chem. 2010, 391, 1379-1390.

Ding, B. Viroids: self-replicating, mobile, and fast-evolving noncoding regulatory RNAs. Wiley Interdiscip Rev RNA. 2010, 1, 362-375.
Dokland T. The structural biology of PRRSV. Virus Res. 2010 154(1-2):86-97.

Drew TW. A review of evidence for immunosuppression due to porcine reproductive and respiratory syndrome virus. Vet Res. 2000 -31(1):27-39.
Earley, K.W.; Pontvianne, F.; Wierzbick,i A.T.; Blevins, T.; Tucker, S.; Costa-Nunes, P.; Pontes, O.; Pikaard, C.S. Mechanisms of HDA6-mediated rRNA gene silencing: suppression of intergenic Pol II transcription and differential effects on maintenance versus siRNA-directed cytosine methylation. Genes Dev. 2010, 24, 1119-1132.

Ellis, A. L.; Wang, Z.; Yu, X.; Mertz, J.E. Either ZEB1 or ZEB2/SIP1 can play a central role in regulating the Epstein-Barr virus latent-lytic switch in a cell type-specific manner. J. Virol. 2010, 84, 6139–6152.

Ellis-Connell, A.L.; Iempridee, T.; Xu, I.; Mertz, J.E. Cellular microRNAs 200b and 429 regulate the Epstein-Barr virus switch between latency and lytic replication. J Virol. 2010, 84, 10329-10343.

Fahlgren, N.; Howel,l M.D.; Kasschau, K.D.; Chapman, E.J.; Sullivan, C.M.; Cumbie, J.S.; Givan, S.A.; Law, T.F.; Grant, S.R.; Dangl, J.L.; Carrington, J.C. High-throughput sequencing of Arabidopsis microRNAs: evidence for frequent birth and death of MIRNA genes. PLoS One. 2007, 2, e219.

Fang M, Nie Y, Theilmann DA. AcMNPV EXON0 (AC141) which is required for the efficient egress of budded virus nucleocapsids interacts with beta-tubulin. Virology. 2009 385(2):496-504.

Fang Y, Snijder EJ. The PRRSV replicase: exploring the multifunctionality of an intriguing set of nonstructural proteins. Virus Res. 2010 154(1-2):61-76.

Fernández A, Suárez P, Castro JM, Tabarés E, Díaz-Guerra M. Characterization of regions in the GP5 protein of porcine reproductive and respiratory syndrome virus required to induce apoptotic cell death. Virus Res. 2002 26;83(1-2):103-18.

Forrest A.R.; Kanamori-Katayama, M.; Tomaru, Y.; Lassmann, T.; Ninomiya, N.; Takahashi, Y.; de Hoon, M.J.; Kubosaki, A.; Kaiho, A.; Suzuki, M.; Yasuda, J.; Kawai, J.; Hayashizaki, Y.; Hume, DA.; Suzuki, H. Induction of microRNAs, mir-155, mir-222, mir-

424 and mir-503, promotes monocytic differentiation through combinatorial regulation. Leukemia. 2010, 24, 460-466.

Forte, E.; Salinas, R.E.; Chang, C.; Zhou, T.; Linnstaedt, S.D.; Gottwein, E.; Jacobs, C.; Jima, D.; Li, Q.J.; Dave, S.S.; Luftig, M.A. The Epstein-Barr virus (EBV)-induced tumor suppressor microRNA MiR-34a is growth promoting in EBV-infected B cells. J Virol. 2012, 86, 6889-6898.
Fukuhara, T.; Kambara, H.; Shiokawa, M.; Ono, C.; Katoh, H.; Morita, E.; Okuzaki, D.; Maehara, Y.; Koike, K.; Matsuura, Y. Expression of MicroRNA miR-122 Facilitates an Efficient Replication in Nonhepatic Cells upon Infection with Hepatitis C Virus. J Virol. 2012, 86, 7918-7933.

Guo X, Zhang Q, Hou S, Zhai G, Zhu H, Sánchez-Vizcaíno JM. Plasmid containing CpG motifs enhances the efficacy of porcine reproductive and respiratory syndrome live attenuated vaccine. Vet Immunol Immunopathol. 2011 15;144(3-4):405-9.

Grant BD, Donaldson JG. Pathways and mechanisms of endocytic recycling. Nat Rev Mol Cell Biol. 2009 10(9):597-608.

González, I.; Martínez, L.; Rakitina, D.V.; Lewsey, M.G.; Atencio, F.A.; Llave, C.; Kalinina, N.O.; Carr, J.P.; Palukaitis, P.; Canto, T. Cucumber mosaic virus 2b protein subcellular targets and interactions: their significance to RNA silencing suppressor activity. Mol Plant Microbe Interact. 2010, 23, 294-303.

Greene W, Gao SJ. Actin dynamics regulate multiple endosomal steps during Kaposi's sarcoma-associated herpesvirus entry and trafficking in endothelial cells. PLoS Pathog. 2009 5(7):e1000512.

Grinberg, M.; Gilad, S.; Meiri, E.; Levy, A.; Isakov, O.; Ronen, R.; Shomron, N.; Bentwich, Z.; Shemer-Avni, Y. Vaccinia virus infection suppresses the cell microRNA machinery. Arch Virol. 2012 Jun 7 [Epub ahead of print]

Hernaez B, Alonso C. Dynamin- and clathrin-dependent endocytosis in African swine fever virus entry. J Virol. 2010 84(4):2100-9.

Hohn, T.; Vazquez, F. RNA silencing pathways of plants: silencing and its suppression by plant DNA viruses. Biochim Biophys Acta. 2011, 1809, 588-600.

Hou YH, Chen J, Tong GZ, Tian ZJ, Zhou YJ, Li GX, Li X, Peng JM, An TQ, Yang HC. 2008. A recombinant plasmid co-expressing swine ubiquitin and the GP5 encoding-gene of porcine reproductive and respiratory syndrome virus induces protective immunity in piglets. Vaccine.26(11):1438-49.

Huang, J.; Wang, F.; Argyris, E.; Chen, K.; Liang, Z.; Tian, H.; Huang, W.; Squires, K.; Verlinghieri, G.; Zhang, H. Cellular microRNAs contribute to HIV-1 latency in resting primary CD4+ T lymphocytes. Nat Med. 2007, 13, 1241-1247.
Izar, B.; Mannala, G.K.; Mraheil, M.A.; Chakraborty, T.; Hain, T. microRNA Response to Listeria monocytogenes Infection in Epithelial Cells. Int J Mol Sci. 2012, 13, 1173-1185.

Janga, S.C.; Vallabhaneni, S. MicroRNAs as post-transcriptional machines and their interplay with cellular networks. Adv Exp Med Biol. 2011, 722, 59-74.
Jaskiewicz, L.; Filipowicz, W. Role of Dicer in posttranscriptional RNA silencing. Curr Top Microbiol Immunol. 2008, 320, 77-97.

Jin, H. Endogenous small RNAs and antibacterial immunity in plants. FEBS Lett. 2008, 582, 2679-2684.

Jopling, C.L.; Yi, M.; Lancaster ,A.M.; Lemon, S.M.; Sarnow, P. Modulation of hepatitis C virus RNA abundance by a liver-specific MicroRNA. Science. 2005, 309, 1577-1581.

Karp CL, Murray PJ. Non-canonical alternatives: what a macrophage is 4. J Exp Med. 2012 Mar 12;209(3):427-31.

Kataya, A.R.; Suliman, M.N.; Kalantidis, K.; Livieratos, I.C. Cucurbit yellow stunting disorder virus p25 is a suppressor of post-transcriptional gene silencing. Virus Res. 2009, 145, 48-53.

Katiyar-Agarwal, S.; Gao, S.; Vivian-Smith, A,; Jin, H. A novel class of bacteria-induced small RNAs in Arabidopsis. Genes Dev. 2007, 21, 3123-3134.

Keffaber KK. Reproductive failure of unknown etiology. American Association of Swine Practitioners Newsletter 1989; 1: 1-19.

Kim JK, Fahad AM, Shanmukhappa K, Kapil S. Defining the cellular target(s) of porcine reproductive and respiratory syndrome virus blocking monoclonal antibody 7G10. J Virol. 2006 80(2):689-96.

Kiss AL, Botos E. Endocytosis via caveolae: alternative pathway with distinct cellular compartments to avoid lysosomal degradation? J Cell Mol Med. 2009 13(7):1228-37.

Kreutz LC. Cellular membrane factors are the major determinants of porcine reproductive and respiratory syndrome virus tropism. Virus Res. 1998 53(2):121-8.

Kuchen, S.; Resch, W.; Yamane, A.; Kuo, N.; Li, Z.; Chakraborty, T.; Wei, L.; Laurence, A.; Yasuda, T.; Peng, S.; Hu-Li, J.; Lu, K.; Dubois, W.; Kitamura, Y.; Charles, N.; Sun, H.W.;

Muljo, S.; Schwartzberg, P.L.; Paul, W.E.; O'Shea, J.; Rajewsky, K.; Casellas, R. Regulation of microRNA expression and abundance during lymphopoiesis. Immunity. 2010, 32, 828-839.

Lambeth, L.S.; Yao, Y.; Smith, L.P.; Zhao, Y.; Nair, V. MicroRNAs 221 and 222 target p27Kip1 in Marek's disease virus-transformed tumour cell line MSB-1. J Gen Virol. 2009, 90, 1164-1171.

Lambotin M, Baumert TF, Barth H. Distinct intracellular trafficking of hepatitis C virus in myeloid and plasmacytoid dendritic cells. J Virol. 2010 84(17):8964-9.
Lee, S.; Paulson, K.G.; Murchison, E.P.; Afanasiev, O.K.; Alkan, C.; Leonard, J.H.; Byrd, D.R.; Hannon, G.J.; Nghiem, P. Identification and validation of a novel mature microRNA encoded by the Merkel cell polyomavirus in human Merkel cell carcinomas. J Clin Virol. 2011, 52, 272-275.

Lee, S.H.; Kalejta, R.F.; Kerry, J.; Semmes, O.J.; O'Connor, C.M.; Khan, Z.; Garcia, B.A.; Shenk, T.; Murphy, E. BclAF1 restriction factor is neutralized by proteasomal degradation and microRNA repression during human cytomegalovirus infection. Proc Natl Acad Sci U S A. 2012, 109, 9575-9580.

Leopold PL, Crystal RG. Intracellular trafficking of adenovirus: many means to many ends. Adv Drug Deliv Rev. 2007 10;59(8):810-21.

Lewis, A.P.; Jopling, C.L. Regulation and biological function of the liver-specific miR-122. Biochem Soc Trans. 2010, 38, 1553-1557.

Li, Z.; Zhang, S.; Huang, C.; Zhang, W.; Hu, Y.; Wei, B. MicroRNAome of splenic macrophages in hypersplenism due to portal hypertension in hepatitis B virus-related cirrhosis. Exp Biol Med. 2008, 233, 1454-1461.

Li, Y.; Chan, E.Y.; Li, J.; Ni, C.; Peng, X.; Rosenzweig, E.; Tumpey, T.M.; Katze, M.G. MicroRNA expression and virulence in pandemic influenza virus-infected mice. J Virol. 2010, 84, 3023-3032.

Li, Y.; Li, J.; Belisle, S.; Baskin, C.R.; Tumpey, T.M.; Katze, M.G. Differential microRNA expression and virulence of avian, 1918 reassortant, and reconstructed 1918 influenza A viruses. Virology. 2011, 421, 105-113.

Llave, C. Virus-derived small interfering RNAs at the core of plant-virus interactions. Trends Plant Sci. 2010, 15, 701-707.

Loveday, E.K.; Svinti, V.; Diederich, S.; Pasick, J.; Jean, F. Temporal- and strain-specific host microRNA molecular signatures associated with swine-origin H1N1 and avian-origin H7N7 influenza A virus infection. J Virol. 2012, 86, 6109-6122.

Lu, F.; Weidmer, A.; Liu, C.G.; Volinia, S.; Croce, C.M.; Lieberman, P.M. Epstein-Barr virus-induced miR-155 attenuates NF-kappaB signaling and stabilizes latent virus persistence. J Virol. 2008, 82, 10436-10443.

Luers, A.J.; Loudig, O.D.; Berman, J.W. MicroRNAs are expressed and processed by human primary macrophages. Cell Immunol. 2010, 263, 1-8.

Luo R, Xiao S, Jiang Y, Jin H, Wang D, Liu M, Chen H, Fang L. Porcine reproductive and respiratory syndrome virus (PRRSV) suppresses interferon-beta production by interfering with the RIG-I signaling pathway. Mol Immunol. 2008 May;45(10):2839-46.

Malterer, G.; Dölken, L.; Haas, J. The miRNA-targetome of KSHV and EBV in human B-cells. RNA Biol. 2011, 8, 30-34.

Martínez de Alba, A.E.; Jauvion, V.; Mallory, A.C.; Bouteiller, N.; Vaucheret H. The miRNA pathway limits AGO1 availability during siRNA-mediated PTGS defense against exogenous RNA. Nucleic Acids Res. 2011, 39,9339-9344.

Miller LC, Laegreid WW, Bono JL, Chitko-McKown CG, Fox JM. Interferon type I response in porcine reproductive and respiratory syndrome virus-infected MARC-145 cells. Arch Virol. 2004 149(12):2453-63.

Miller LC, Lager KM, Kehrli ME Jr. Role of Toll-like receptors in activation of porcine alveolar macrophages by porcine reproductive and respiratory syndrome virus. Clin Vaccine Immunol. 2009 16(3):360-5.

Morgan, R.; Anderson, A.; Bernberg, E.; Kamboj, S.; Huang, E.; Lagasse, G.; Isaacs, G.; Parcells, M.; Meyers, B.C; Green, P.J.; Burnside, J. Sequence conservation and differential expression of Marek's disease virus microRNAs. J Virol. 2008, 82, 12213-12220.

Murtaugh MP, Xiao Z, Zuckermann F. Immunological responses of swine to porcine reproductive and respiratory syndrome virus infection. Viral Immunol. 2002 15(4):533-47.

Nauwynck HJ, Duan X, Favoreel HW, Van Oostveldt P, Pensaert MB. Entry of porcine reproductive and respiratory syndrome virus into porcine alveolar macrophages via receptor-mediated endocytosis. J Gen Virol. 1999 80 (Pt 2):297-305.

Navarro, B.; Pantaleo, V.; Gisel, A.; Moxon, S.; Dalmay, T.; Bisztray, G.; Di Serio, F.; Burgyán, J. Deep sequencing of viroid-derived small RNAs from grapevine provides new insights on the role of RNA silencing in plant-viroid interaction. PLoS One. 2009, 4, e7686.

Norman, K.L.; Sarnow, P. Modulation of hepatitis C virus RNA abundance and the isoprenoid biosynthesis pathway by microRNA miR-122 involves distinct mechanisms. J Virol. 2010, 84, 666-670.

Neumann E.J.,Kliebenstein J.B., Johnson C.D., Mabry J.W., Bush E.J., Seitzinger A.H., Green A.L. & Zimmerman J.J. Assessment of the economic impact of porcine reproductive and respiratory syndrome on swine production in the United States. Journal of the American Veterinary Medical Association. 2005 227(3): 385-392.

O'Connell, R.M.; Taganov, K.D.; Boldin, M.P.; Cheng, G.; Baltimore, D. MicroRNA-155 is induced during the macrophage inflammatory response. Proc Natl Acad Sci U S A. 2007, 104, 1604-1609.

Okamura, K. Diversity of animal small RNA pathways and their biological utility. Wiley Interdiscip Rev RNA. 2012, 3, 351-368.

O'Neill, L.A.; Sheedy, F.J.; McCoy, C.E. MicroRNAs: the fine-tuners of Toll-like receptor signalling. Nat Rev Immunol. 2011, 11, 163-175.

Osorio F. PRRSV infections: a world-wide update (2010) . Acta Scientiae Veterinariae. 38(Supl 1): s269-s275, 2010.

Pacheco, R.; García-Marcos, A.; Barajas, D.; Martiáñez, J.; Tenllado, F. PVX-potyvirus synergistic infections differentially alter microRNA accumulation in Nicotiana benthamiana. Virus Res. 2012, 165, 231-235.

Pantaleo, V.; Saldarelli, P.; Miozzi, L.; Giampetruzzi, A.; Gisel, A.; Moxon, S.; Dalmay, T.; Bisztray, G.; Burgyan, J. . Deep sequencing analysis of viral short RNAs from an infected Pinot Noir grapevine. Virology. 2010, 408, 49-56.

Parida R, Choi IS, Peterson DA, Pattnaik AK, Laegreid W, Zuckermann FA, Osorio FA. Location of T-cell epitopes in nonstructural proteins 9 and 10 of type-II porcine reproductive and respiratory syndrome virus. Virus Res. 2012 5. [Epub ahead of print]

Poole, E.; McGregor-Dallas, S.R.; Colston, J.; Joseph, R.S.; Sinclair, J. Virally induced changes in cellular microRNAs maintain latency of human cytomegalovirus in CD34+ progenitors. J Gen Virol. 2011, 92, 1539-1549.

Qin, Z.; Jakymiw, A.; Findlay, V.; Parsons, C. KSHV-Encoded MicroRNAs: Lessons for Viral Cancer Pathogenesis and Emerging Concepts. Int J Cell Biol. 2012, 2012, 603961.

Quinn, S.R.; O'Neill, L.A. A trio of microRNAs that control Toll-like receptor signalling. Int Immunol. 2011, 23, 421-425.

Rajaram, M.V.; Ni, B.; Morris, J.D.; Brooks, M.N.; Carlson, T.K.; Bakthavachalu, B.; Schoenberg, D.R.; Torrelles, J.B.; Schlesinger, L.S. Mycobacterium tuberculosis lipomannan blocks TNF biosynthesis by regulating macrophage MAPK-activated protein kinase 2 (MK2) and microRNA miR-125b. Proc Natl Acad Sci U S A. 2011, 108, 17408-17413.
Riley, K.J.; Rabinowitz, G.S.; Yario T.A.; Luna, J.M.; Darnell, R.B.; Steitz, J.A. EBV and human microRNAs co-target oncogenic and apoptotic viral and human genes during latency. EMBO J. 2012, 31, 2207-2221.

Rodemer C, Haucke V. Clathrin/AP-2-dependent endocytosis: a novel playground for the pharmacological toolbox? Handb Exp Pharmacol. 2008 (186):105-22

Sagong M, Lee C. Porcine reproductive and respiratory syndrome virus nucleocapsid protein modulates interferon-β production by inhibiting IRF3 activation in immortalized porcine alveolar macrophages. Arch Virol. 2011 156(12):2187-95

Saffert, R.T.; Kalejta, R.F. Inactivating a cellular intrinsic immune defense mediated by Daxx is the mechanism through which the human cytomegalovirus pp71 protein stimulates viral immediate-early gene expression. J Virol. 2006, 80, 3863-3871.

Samsom JN, de Bruin TG, Voermans JJ, Meulenberg JJ, Pol JM, Bianchi AT. Changes of leukocyte phenotype and function in the broncho-alveolar lavage fluid of pigs infected with porcine reproductive and respiratory syndrome virus: a role for CD8(+) cells. J Gen Virol. 2000 81(Pt 2):497-505.

Sattar, S.; Song, Y.; Anstead, J.A.; Sunkar, R.; Thompson, G.A. Cucumis melo microRNA expression profile during aphid herbivory in a resistant and susceptible interaction. Mol Plant Microbe Interact. 2012, 25, 839-848.

Sang Y, Ross CR, Rowland RR, Blecha F. Toll-like receptor 3 activation decreases porcine arterivirus infection. Viral Immunol. 2008 21(3):303-13.

Shen, W.J.; Ruan, X.L.; Li, X.S.; Zhao, Q.; Li, H.P. RNA silencing suppressor Pns11 of rice gall dwarf virus induces virus-like symptoms in transgenic rice. Arch Virol. 2012 [Epub ahead of print]

Shimakami, T.; Yamane, D.; Welsch, C.; Hensley, L.; Jangra, R.K.; Lemon, S.M. Base Pairing between Hepatitis C Virus RNA and MicroRNA 122 3' of Its Seed Sequence Is Essential for Genome Stabilization and Production of Infectious Virus. J Virol. 2012, 86, 7372-7383.

Shivaprasad, P.V.; Chen, H.M.; Patel, K.; Bond, D.M.; Santos, B.A.; Baulcombe D.C. A microRNA superfamily regulates nucleotide binding site-leucine-rich repeats and other mRNAs. Plant Cell. 2012, 24, 859-874.

Skalsky, R.L.; Samols, M.A.; Plaisance, K.B.; Boss, I.W.; Riva, A.; Lopez, M.C.; Baker, H.V.; Renne, R. Kaposi's sarcoma-associated herpesvirus encodes an ortholog of miR-155. J Virol. 2007, 81, 12836-12845.

Snijder EJ, JC Dobbe, and WJ M Spaan. Heterodimerization of the Two Major Envelope Proteins Is Essential for Arterivirus Infectivity. J Virol. 2003 January; 77(1): 97–104.

Song C, Krell P, Yoo D. Nonstructural protein 1α subunit-based inhibition of NF-κB activation and suppression of interferon-β production by porcine reproductive and respiratory syndrome virus. Virology. 2010 407(2):268-80.

St-Pierre, P.; Hassen, I.F.; Thompson, D.; Perreault, J.P. Characterization of the siRNAs associated with peach latent mosaic viroid infection. Virology. 2009, 383, 178-182.

Subramaniam S, Kwon B, Beura LK, Kuszynski CA, Pattnaik AK, Osorio FA. Porcine reproductive and respiratory syndrome virus non-structural protein 1 suppresses tumor necrosis factor-alpha promoter activation by inhibiting NF-κB and Sp1. Virology. 2010 25;406(2):270-9.

Suikkanen S, Antila M, Jaatinen A, Vihinen-Ranta M, Vuento M. Release of canine parvovirus from endocytic vesicles. Virology. 2003 25;316(2):267-80.

Sullivan, C.S.; Grundhoff, A.T.; Tevethia, S.; Pipas, J.M.; Ganem, D. SV40-encoded microRNAs regulate viral gene expression and reduce susceptibility to cytotoxic T cells. Nature. 2005, 435, 682-686.

Sullivan, C.S.; Sung, C.K.; Pack, C.D.; Grundhoff, A.; Lukacher, A.E.; Benjamin, T.L.; Ganem, D. Murine Polyomavirus encodes a microRNA that cleaves early RNA transcripts but is not essential for experimental infection. Virology. 2009, 387, 157-167.

Sur JH, Doster AR, Osorio FA. Apoptosis induced in vivo during acute infection by porcine reproductive and respiratory syndrome virus. Vet Pathol. 1998 35(6):506-14.

Thanawongnuwech R, Halbur PG, Thacker EL. The role of pulmonary intravascular macrophages in porcine reproductive and respiratory syndrome virus infection. Anim Health Res Rev. 2000 1(2):95-102.

Tsai B. Penetration of nonenveloped viruses into the cytoplasm. Annu Rev Cell Dev Biol. 2007;23:23-43.

Umbach, J.L.; Kramer, M.F.; Jurak, I.; Karnowski, H.W.; Coen, D.M.; Cullen, B.R. MicroRNAs expressed by herpes simplex virus 1 during latent infection regulate viral mRNAs. Nature. 2008, 454, 780-783.

Umbach, J.L.; Cullen, B.R. The role of RNAi and microRNAs in animal virus replication and antiviral immunity. Genes Dev. 2009, 23, 1151-1164.

Utley TJ, Ducharme NA, Varthakavi V, Shepherd BE, Santangelo PJ, Lindquist ME, Goldenring JR, Crowe JE Jr. Respiratory syncytial virus uses a Vps4-independent budding mechanism controlled by Rab11-FIP2. Proc Natl Acad Sci U S A. 2008 22;105(29):10209-14.
van der Schaar HM, Rust MJ, Chen C, van der Ende-Metselaar H, Wilschut J, Zhuang X, Smit JM. Dissecting the cell entry pathway of dengue virus by single-particle tracking in living cells. PLoS Pathog. 2008 4(12):e1000244.

Vanderheijden N, Delputte PL, Favoreel HW, Vandekerckhove J, Van Damme J, van Woensel PA, Nauwynck HJ. Involvement of sialoadhesin in entry of porcine reproductive and respiratory syndrome virus into porcine alveolar macrophages. J Virol. 2003 77(15):8207-15.

Vaz, C.; Mer, A.S.; Bhattacharya, A.; Ramaswamy, R. MicroRNAs modulate the dynamics of the NF-κB signaling pathway. PLoS One. 2011, 6, e27774.

Verheijea M.H, T.J.M. Weltinga, H.T. Jansena, P.J.M. Rottierb, J.J.M. Meulenberga. Chimeric Arteriviruses Generated by Swapping of the M Protein Ectodomain Rule Out a Role of This Domain in Viral Targeting. Virology 2002 303: 364–373

Verschoor CP, Puchta A, Bowdish DM. The macrophage. Methods Mol Biol. 2012 844:139-56.

Vu HL, Kwon B, Yoon KJ, Laegreid WW, Pattnaik AK, Osorio FA. Immune evasion of porcine reproductive and respiratory syndrome virus through glycan shielding involves both glycoprotein 5 as well as glycoprotein 3. J Virol. 2011 85(11):5555-64.

Wang, P.; Hou ,J.; Lin, L.; Wang, C.; Liu, X.; Li, D.; Ma, F.; Wang, Z.; Cao, X. Inducible microRNA-155 feedback promotes type I IFN signaling in antiviral innate immunity by targeting suppressor of cytokine signaling 1. J Immunol. 2010, 185, 6226-6233.

Welch SK, Jolie R, Pearce DS, Koertje WD, Fuog E, Shields SL, Yoo D, Calvert JG. Construction and evaluation of genetically engineered replication-defective porcine reproductive and respiratory syndrome virus vaccine candidates. 2004. Vet Immunol Immunopathol. 102(3):277-90.

Welch SK, Calvert JG. A brief review of CD163 and its role in PRRSV infection. Virus Res. 2010 154(1-2):98-103.

Wensvoort G, Terpstra C, Pol JM, ter Laak EA, Bloemraad M, de Kluyver EP, Kragten C, van Buiten L, den Besten A, Wagenaar F. Mystery swine disease in The Netherlands: the isolation of Lelystad virus. Vet Q. 1991 13(3):121-30.

Wissink EH, Kroese MV, Maneschijn-Bonsing JG, Meulenberg JJ, van Rijn PA, Rijsewijk FA, Rottier PJ. Significance of the oligosaccharides of the porcine reproductive and respiratory syndrome virus glycoproteins GP2a and GP5 for infectious virus production. J Gen Virol. 2004 85(Pt 12):3715-23.

Xiao, S.; Wang, W.; Yang, X. Evolution of Resistance Genes in Plants. In Innate Immunity of Plants, Animals Ed.; Heine, H. 2008.

Xiao S, Mo D, Wang Q, Jia J, Qin L, Yu X, Niu Y, Zhao X, Liu X, Chen Y. Aberrant host immune response induced by highly virulent PRRSV identified by digital gene expression tag profiling. BMC Genomics. 2010 11:544.

Xue Q, Zhao YG, Zhou YJ, Qiu HJ, Wang YF, Wu DL, Tian ZJ, Tong GZ. 2004. Immune responses of swine following DNA immunization with plasmids encoding porcine reproductive and respiratory syndrome virus ORFs 5 and 7, and porcine IL-2 and IFNgamma. Vet Immunol Immunopathol. 102(3):291-8.

Yu M, Levine SJ. Toll-like receptor, RIG-I-like receptors and the NLRP3 inflammasome: key modulators of innate immune responses to double-stranded RNA viruses. Cytokine Growth Factor Rev. 2011 22(2):63-72.

Zhao, Y.; Xu, H.; Yao, Y.; Smith, L.P.; Kgosana, L.; Green, J.; Petherbridge, L.; Baigent, S.J.; Nair, V. Critical role of the virus-encoded microRNA-155 ortholog in the induction of Marek's disease lymphomas. PLoS Pathog. 2011, 7, e1001305.

Zhang L, Tian X, Zhou F. Intranasal administration of CpG oligonucleotides induces mucosal and systemic Type 1 immune responses and adjuvant activity to porcine reproductive and respiratory syndrome killed virus vaccine in piglets in vivo. Int Immunopharmacol. 2007 7(13):1732-40

Zheng, S.Q.; Li, Y.X.; Zhang, Y.; Li, X.; Tang, H. MiR-101 regulates HSV-1 replication by targeting ATP5B. Antiviral Res. 2011, 89, 219-226.

Zhu H, D Yu and X Zhang. The spike protein of murine coronavirus regulates viral genome transport from the cell surface to the endoplasmic reticulum during infection. J. Virol. 2009, 83(20):10653.

Chapter Two: Identification of the interaction between the host membrane fusion protein snapin with PRRSV envelope proteins GP5 and M

Introduction

A key component to unraveling the pathogenesis of any virus is to identify viral and host cellular protein interaction networks. The field of proteomics, characterized as the study of the protein complement of a genome, is a continually growing field. There are currently many proteomic methods available for the elucidation of protein-protein interactions. A popular and commonly used method is the yeast two-hybrid assay (Y2H) (reviewed by Hamdi and Colas 2012). The Y2H assay was developed in the late 1980s and is based on the GAL4 transcription factor of yeast (Fields and Song 1989). GAL4 consist of two domains, one domain functions as a DNA-binding domain, which interacts with motifs in the promoters of GAL4- regulated genes. The other domain is termed an activation domain and functions in activating transcription from these promoters. In a standard Y2H assay, though today many variations exist, the protein of interest, known as the "bait" protein, is expressed as a fusion protein with the DNA-binding domain of GAL4. In addition a "prey" protein library, in which a cDNA library, generated from a cell population and/or tissue of interest, cloned into a vector to express prey proteins as fusion proteins containing the activation domain of GAL4. Yeast expressing the bait fusion protein and yeast expressing the prey fusion proteins are then mated. If the "bait" protein interacts with a particular prey protein, then the two domains of the GAL4 transcription will be brought into proximity to each other, creating a functional GAL4 protein that activates the expression of one or more reporter

genes that are under the control of the GAL4 promoter (Figure 2.1). The reporter genes typically include both nutrient selection and colorimetric genes. The popularity of theY2H assay is due to several factors, among these is the relatively low cost compared to other available technologies and minimal reagents and equipment requirements. Y2H assays also require little *a priori* knowledge of potential interactions of the bait protein.

Protein-protein interaction networks associated with a diverse range of viruses have been discovered using the Y2H methodology. A recent large scale Y2H analysis of interactions between proteins encoded by vaccina virus, a pox virus historically used as a smallpox vaccine, and a human protein library, revealed a total 109 interactions for 33 viral proteins (Zhang et al. 2009). Vaccinia virus proteins were found to interact with a functionally diverse set of human proteins, including proteins involved in cytokine signaling, immune signaling, and microtubule formation and transport. Analysis of interactions between 27 hepatitis C virus (HCV) proteins and human proteins discovered over 300 viral-host protein interactions (Bailer and Haas 2009). Some HCV proteins were found to have a large number of interacting partners, including the serine protease NS3, which was found to potentially interact with 214 human proteins.

Construction of protein-protein interaction networks has greatly assisted in determining transport and assembly of viruses. The virion tegument protein of human cytomegalovirus (HCMV), a herpesvirus, was found to interact with Bicaudal D1 (BicD1), an intracellular trafficking protein, in a Y2H screen (Indran et al. 2010). BicD1 is involved in the dynein-mediated secretory pathway. Transfection of a short interfering RNA (siRNA)

targeting BicD1 into human dermal fibroblasts significantly reduces production of HCMV. The decrease in virus productivity is due to the lack of trafficking of pp150, an HCMV tegument protein important in virion maturation (AuCoin et al. 2006), to sites of virion assembly in the cytoplasm, suggesting that dynein-mediated transport of virion components is required for proper assembly of HCMV particles. The assembly and release of retroviruses, such as HIV, is mediated by the virally-encoded GAG proteins. Y2H analysis of interacting partners of the GAG precursor protein of HIV1 found an interaction with the human protein filamin A (FLNA) (Cooper et al. 2011). FLNA is an actin binding protein which mediates the interaction between membrane glycoproteins and the actin cytoskeleton network (Nakamura et al. 2011). Knock-down of FLNA in HIV-infected HeLa cells via siRNA-mediated repression results in the accumulation of GAG in intracellular compartments and prevents its trafficking to the plasma membrane, which in turn reduces virus productivity. These observations suggest the GAG-FLNA interaction is needed for HIV particle release from infected cells. Dengue virus (DENV), a member of Flaviviridae family is the causative agent of Dengue hemorrhagic fever, a major illness in the tropics. DENV encodes a single envelope glycoprotein called E protein. An Y2H screening found that DENV E protein interacts with three human endoplasmic reticulum chaperone proteins, immunoglobulin heavy chain binding protein (BiP), calnexin and calreticulin, in an independent manner (Limjindaporn et al. 2009). Chaperone proteins mediate the proper folding and unfolding of proteins and the assembly of large macromolecules. SiRNA knock-down of the expression of any of these three cellular proteins, greatly reduces the production

of DENV virions. It was suggested that this loss of virus production may be due to improper folding of DENV E protein and/or mis-assembly of virion particles, both of which could require host cell chaperone proteins for proper formation.

Currently, little is known about the entry and exit strategies of PRRSV. PRRSV has a limited cell tropism (cells susceptible to virus entry and replication) and primarily, infects alveolar macrophages *in vivo* but is also able to infect the cell line MARC-145 (derived from the original cell line MA-104, an African green monkey kidney cell line). The steps of entry and uncoating of PRRSV into permissive cells are not completely understood. Evidence suggests that PRRSV first binds to heparan sulfate, after which sialic acids on the surface of the virion interact with the N-terminal sialic acid-binding domain of sialoadhesin on the host cell, which leads to internalization of the virus particle. The virus particle is thought to then be transported in an endosomal compartment where a drop in pH is needed for uncoating of the virus. The viral E protein (ORF2b) is thought to function as an ion channel and may be involved in this step (Lee and Yoo 2006). Recent work suggests that the scavenger receptor CD163 is involved in the disassembly of the virus and release of the viral genome, but is not required for entry (Delrue et al. 2010). However, the exact mechanism of and other viral and/or cellular factors involved in the entry of PRRSV into the host cell and virion disassembly are not known. Electron microscopy study of PRRSV virion assembly and release suggests that viral nucleocapsids become enveloped by budding through the smooth endoplasmic reticulum (Pol and Reus 1997). It has been suggested the virus particle obtains its envelope by budding into the Golgi apparatus (Dea et al. 1995). Mature virus particles

are then released from the cell by exocytosis. However, little else is known about the release of mature virus particles from PRRSV infected cells. The virally encoded GP5 and M proteins are the major envelope proteins of PRRSV. Together, these proteins form a heterodimer linked by a disulfide bond between cysteine in their respective N-termini. This heterodimer is thought to function in virion assembly and budding and possibly in entry of the virus into the host cell, however the exact role(s) that the GP5 and M proteins play in the PRRSV life cycle is unclear. Therefore, identifying potential host cell protein interacting partners with GP5 and M is vital to understanding the entry and exit of the PRRS virus. To this end we screened a porcine macrophage cDNA library to identify interacting partners of GP5 and M using a standard Y2H assay. This assay identified the host protein Snapin as a potential interacting partner of both of these PRRSV envelope proteins. Snapin is known to interact with the members of the SNARE complex, a group of related proteins that are involved in intracellular membrane fusion events. To further refine the region(s) of GP5 and M that interact with Snapin, epitope mapping was utilized to identify the specific interacting motifs.

Materials and Methods

Bait vector and prey library construction

PRRSV ORF5, GP5, and ORF6, M protein, were individually cloned into the yeast expression vector, pGBKT7-BD (Clontech) using the EcoRI and BamHI restriction sites. These vectors were then individually transformed into yeast strain AH109. A porcine macrophage “prey” library was constructed by Clontech using cDNA produced from total

RNA from uninfected/un-stimulated, infected and mitogen stimulated porcine macrophages. Primary alveolar macrophages (SAMs) were isolated from a 7-week-old pig by broncholavage. SAMs were cultured in RPMI1640 supplemented with 10% FBS. A group of SAMs were infected with VR2332 *in vitro* at multiplicity of infection (M.O.I.) 1. Another group of SAMs were stimulated with the mitogen, phorbol-12-myristate-13-acetate (PMA). Total RNA was extracted, using Tri-reagent (Sigma) at 3hr, 6hr, 12hr and 24hr post infection or stimulation. Total cDNA were produced for prey library construction, consisting of cDNA cloned into the pGADT7-rec vector by recombination and transformed into Y187 yeast (Clontech).

Yeast-two hybrid assay

The yeast-two hybrid assay was carried out according to the manufacturer's instructions (Clontech). A 50 ml overnight culture of the bait vector, for either GP5 or M protein, transformed AH109 yeast was resuspended in 5mL of growth media. The bait culture and 1mL of the prey vector library transformed Y187 yeast were combined in 50 ml of 2XYPDA (yeast extract, peptone, and dextrose media supplemented with adenine hemisulfate at a final concentration of 0.003%, Clontech) containing 50 μg/ml of kanamycin and grown overnight at 30°C. The culture was centrifuged at 1,000rpms for 10min and resuspended in 10 ml of 0.5X YPDA media containing kanamycin. In order to determine viability, mating efficiency, and the number of clones screened. Dilutions of 1:10, 1:100, 1:1,000, and 1:10,000 were plated on leucine deficient media (bait vector nutrient selector), tryptophan deficient media (prey vector nutrient selector) and leucine/tryptophan deficient media. The remaining culture

was grown on adenine, histidine, leucine and tryptophan deficient media to select for colonies with positive interactions. Colonies were allowed to grow 14 days of growth were streaked on adenine, histidine, leucine and tryptophan deficient media. Colonies that successfully grew were then subjected to a β-galactosidase assay to further confirm a positive protein-protein interaction. Colonies were transferred to whatman filter paper and flash frozen using liquid nitrogen. After thawing, another whatman filter paper soaked in Z buffer (sodium phosphate dibasic and monobasic, potassium chloride, magnesium sulfate, X-gal and β-mercaptoethanol) was applied. Positive colonies were then selected via their β-galactosidase activity, as a positive protein-protein interaction activates the expression of the β-galactosidase selector gene, resulting in a colorimetric change. Plasmids from positive colonies were isolated as follows. An individual colony was grown overnight in 0.5 ml of adenine, histidine, leucine and tryptophan deficient media. The cultures were centrifuged at maximum speed (~13000rpm) in a microcentrifuge for 5 minutes and resuspended in 50µl of growth media. Ten microliters of lyticase (5U/µl) were added and incubated at 37°C for 1 hour. Ten microliters of SDS (20%) were added to this mixture and the samples were then frozen at -20°C overnight. The plasmids were then purified using a Wizard miniprep plasmid isolation kit (Promega). Salt was removed from plasmid samples via dialysis using 0.025µm VSWP membrane filters (Millipore) and transformed into DH10B competent cells using a Biorad gene pulser II for electroporation (200Ω, 25uf and 2.5kv). Transformed bacteria were then plated on LB agar plates containing carbenicillin (100µg/mL) to select for bacteria containing pGADT7 (prey) plasmids. Plasmids were isolated from individual

bacterial colonies using a Wizard miniprep plasmid isolation kit (Promega) and subjected to sequencing. The identities of the prey proteins were determined using the GenBank Basic Local Alignment Search Tool (BLAST) from the National Center for Biotechnology Information (NCBI).

Epitope mating

Truncated regions of GP5 and M were designed based on the hydropathy profiles of each protein (FIGURE) and cloned in to the pGBKT7 vector using NdeI and EcoRI restriction endonucleases and then transformed into AH109 yeast. Transformed yeast were then mated with Y187 yeast transformed with pGADT7-Snapin as follows. A colony of AH109 of each epitope construct was mixed with a colony of Y187 pGADT7-Snapin yeast in 0.5mL of YPD media. Matings were then carried out at 30°C for 24hrs. Matings were then vortexed to resuspend cells and 100µl aliquots were grown on adenine, histidine, leucine and tryptophan deficient media ~5 days. Select colonies were then streaked on adenine, histidine, leucine and tryptophan deficient media and grown for ~5 days. Colonies which successfully grew were then subjected to a β-galatacosidase assay to further confirm positive protein-protein interactions, as described above.

Results

Yeast-two hybrid

To further understand to the protein interaction networks of the major envelope proteins of PRRSV, GP5 and M, these two viral proteins were used as “bait” in a yeast two-hybrid screening of “prey” proteins generated from uninfected, infected and stimulated

porcine macrophages. Macrophages were infected with VR2332 *in vitro* or stimulated with the mitogen, phorbol-12-myristate-13-acetate (PMA). Macrophages were infected or stimulated for 3hr, 6hr, 12hr and 24hr.

For the GP5 yeast two-hybrid approximately $4.5X10^6$ colonies were screened and for the M yeast two-hybrid approximately $3X10^6$ colonies were screened. Eight of the clones from the GP5 yeast two-hybrid assay were identified as the cellular membrane fusion accessory protein snapin, while 6 clones from the M protein yeast-two hybrid were also identified as snapin (Figure 2.4). As GP5 and M function as a heterodimer in PRRSV virions and both were found to interact with the host protein Snapin, this interaction is likely important in PRRSV pathogenesis.

Epitope mapping

To better characterize the interaction between PRRSV GP5/M and the cellular protein snapin, epitope mapping in conjunction with the yeast two-hybrid assay was employed. Truncated regions of GP5 and M based on the hydropathy profiles of each protein (Figure 2.2; Figure 2.3) were designed, with focus on the endo- and ecto-domains of each protein as these are the most probable sites of snapin interaction. For both GP5 and M protein the ecto-domain near the N-terminus of each protein were identified as the sites of the interaction with snapin (Figure 2.2; Figure 2.3; Figure 2.5). For GP5 the truncated version consisting of amino acids 31-60 was found to interact with snapin, while the other truncations failed to form diploids in the yeast two-hybrid assay. Similarly for M protein, the truncation

consisting of amino acids 1-22 was able to interact with snapin in the yeast two-hybrid experiment, while the other truncations were unable to form positive interactions.

Discussion

Currently little is known about the transport of PRRSV particles into and out of the cell. Several studies have suggested that the major PRRSV envelope proteins GP5 and M are involved in the intracellular transport of PRRSV particles. To further elucidate the involvement of GP5 and M in PRRSV pathogenesis, a yeast-two hybrid assay using a porcine alveolar macrophage prey library was carried out. The assay revealed that both viral proteins interact with a member of membrane fusion, Snapin. Further epitope mapping revealed that the ecto-domains of both viral proteins GP5 and M are the sites of Snapin interaction, suggesting that these particular viral/host protein interactions may be involved in virus transport.

SNARE Complex

Within the cell, molecules such as proteins and lipids are transported in vesicles that bud from the donor membrane and fuse with the acceptor membrane. This fusion is mediated by SNARE (soluble N-ethylmaleimide-sensitive fusion protein attachment protein receptor) proteins that are found in almost all eukaryotic cells. The SNARE complex functions to both position vesicles at and to fuse them with the target membrane (Parpura and Mohideen 2008). The SNARE complex is composed of three protein families; syntaxins (Syns), vesicle-associated membrane proteins (VAMPs), and SNAP-25 (synpatosome-assoicated protein-25) related proteins (Buxton et al. 2003). The ternary SNARE complex is

composed of proteins present in both the vesicle and in the membrane to which it is to be fused (Parpura and Mohideen 2008). SNARE components located in vesicle membranes include synaptobrevin protein 2 (which is also known as vesicle-associated membrane protein 2 (VAMP-2)) or in some cells, a homologous protein cellubrevin (aka VAMP3). While the SNARE proteins, such as syntaxin (Syn1) and SNAP-25 in neurons, or its ubiquitously expressed homolog SNAP-23, are located in the membrane to which the vesicle is to be fused. Each of these proteins contains a motif that is termed in the SNARE domain or motif which is the site of direct interaction between them. The structure of these motifs consists of coiled-coiled regions of ~60 residues (Fasshauer 2003). These sites are located adjacent to their C-terminal membrane anchors. For Syn1, SNAP-25, and Sb2, the SNARE domains are bundled together to form a long cylinder with a variable radius along its length. The SNAP-25 protein consists of two SNARE motifs (SN1 and SN2) connected by a linker peptide. Unlike other SNARE proteins SNAP25 does not contain a transmembrane (TM) domain but is thought to attach to membranes by palmitoyl modifications found in the linker region

Once assembled the SNARE domains form four coiled α-helices, Sx1 and Sb2 each contribute one helix, while two are from SNAP-25 (SN1 and SN2). The SNARE domains are arranged in parallel to each other with all their N-termini located at one end of the complex and all of the C-termini located at the other end (Figure 5). In the current model for SNARE-mediated membrane fusion the two membranes are brought together in a zippering process in which the N-termini of the helices interact first, after which the interaction then

proceeds down the domains, that once fully "zippered" bring the two membranes in close proximity (Parpura and Mohideen 2008). Eventually this process leads to the fusion of the lipid bilayers of the two membranes.

SNARE mediated fusion occurs in four steps (Söllner 2004). First, the transport vesicle is tethered to the targeted membrane. It is this tethering step that contributes to target specificity. Next, the SNARE fusion machinery is activated by the linking the two fusing membranes. Now folding, i.e. "zippering", of the SNARE proteins brings the membranes next to each other. Finally, the fusion pore forms and dilates which leads to the fusion of the two membranes and the release of the intravesicle components. In this step the vesicular membrane is often completely incorporated into the target membrane. The final zippering of the C-termini of the SNARE helices is the key step in membrane fusion and it likely a target for membrane fusion regulation. It is likely that SNARE proteins have multiple functions in SNARE complex formation such as, establishing close contact between the two fusing membranes, formation of the scaffolding needed for complex formation, and the binding of the lipid surfaces of the membranes.

Snapin

In addition to the major proteins that form the SNARE complex additional accessory factors are involved in regulating membrane fusion. These accessory proteins include Syn-1 binding proteins, munc18a, synaptotagmin 1, and Snapin. Munc18a likely functions to negatively regulate membrane fusion by blocking the interaction of SNAREs (Rodkey et al. 2008). Synaptotagmin 1 is a calcium binding protein that mediates the interaction of Syn1

with the core SNARE complex, in a calcium dependent manner (Koh and Bellen 2003). However the interaction of synaptotagmin 1 with the SNARE complex is also mediated by another accessory protein Snapin. Initially Snapin was suggested to be a neuron-specific component of the SNARE complex that regulates the function of the SNARE protein, SNAP-25 binding protein (Ilardi et al. 1999). However, later work found Snapin to be ubiquitously expressed in mouse tissues and it was proposed to function as general component of the SNARE complex in both neuronal and non-neuronal cells (Buxton et al. 2003). Moreover, this work also found Snapin functions as SNAP-23-binding protein. SNAP-23 is considered to be the homolog of the neuron-specific SNAP-25. Therefore, it was proposed that Snapin functions to mediate both SNAP-23 and SNAP-25 vesicle trafficking.

Analysis of the intracellular localization of Snapin suggests that it locates to multiple cellular membranes. Snapin was found to localize to both the cytosol, peripheral membrane, as well as at endosomal and Golgi membrane sites (Yuan et al., 2006, Buxton et al., 2003, Chen et al., 2005 and Vites et al., 2004). The expression of a Snapin-GFP fusion protein suggests that it may also localize to the plasma membrane. Analysis of the protein structure of Snapin suggests that it either consists of a single helical domain or possibly two helical motifs or does not likely contain a transmembrane domain (Gowthaman et al. 2006). Mutational studies suggest that a helical domain located at the C-terminus is essential for binding of Snapin to both SNAP-25 and SNAP-23. A genetic mouse model in which Snapin was deleted demonstrated that an absence of Snapin protein results in the accumulation of LAMP-1 (a late endocytic protein) and the late endosomal SNARE proteins, syntaxin 8 and

Vti1b, in endocytic organelles (Lu et al. 2009). The deletion of Snapin and the accumulation of LAMP-1, syntaxin8 and Vti1b, results in compensatory changes in late endosomal SNAREs, suggesting that Snapin may also regulate late endocytic membrane fusion. Snapin is enriched in late endocytic compartments and associates with the late endocytic trans-SNARE complex by binding to syntaxin 8. Late endocytic SNAREs function in the fusion of late endosomes with lysosomes. Lysosomes are acidic compartments that are involved in the degradation of macromolecules and organelles for endosomal pathways that are no longer needed. Thus an additional function of Snapin could be in the regulation of the transport of macromolecules to the lysosome for degradation and recycling.

SNARE complex utilization by viruses

Analysis of virus entry into and egress from host cells has shown that a number of viruses utilize SNARE-mediated fusion pathways for both viral protein trafficking as well as for the trafficking of virus particles. Recently, Herpes Simplex Virus-1 (HSV-1) was found to interact with a member of the SNARE complex to aid in the anterograde transport of viral proteins (Miranda-Saksena et al. 2009). Assembled herpesviruses consist of four major structures; an inner core, a capsid, a tegument and a host-derived envelope. Two models have been proposed for the anterograde transport of herpesviruses along the axon. In the "married" model a fully assembled capsid is formed within the cell body and is then transported within the host cell's vesicles until it is released from the axon. In the second model termed the subassembly model, structural components of the virus are transported separately. The unenveloped viral capsid is transported along microtubules, while the

envelope-associated and tegument-associated proteins are transported via host cell vesicles. Finally, the virus is fully assembled at the axon terminus before it is released. A recent study found evidence supporting the subassembly model for the axonal transport of herpesviruses (Miranda-Saksena et al. 2009). In this work it was shown that HSV-1 tegument and envelope proteins could be transported separately or together along the axon. Moreover, it was found that these viral proteins are transported in separate transport vesicles from those transporting viral capsids. The study also found that individual HSV-1 tegument and envelope proteins can interact with the SNARE protein SNAP-25, a component of SNARE complex associated with vesicular membranes, further supporting that these proteins are likely separately transported along the axon, and it that they use the host's membrane fusion pathway to achieve this transport.

The non-enveloped dsRNA virus Blue Tongue Virus (BTV) is a member of the Reoviridae virus family. BTV is the causative agent of blue tongue disease a vector-borne disease of ruminants that is endemic in many tropical locations and has recently spread to Europe. Two major BTV structural proteins are the outer capsid proteins, VP2 and VP5. These proteins are involved initial cell attachment and penetration of BTV. It is possible that the outer capsid assembly of BTV occurs prior to the transport of the mature virus to the plasma membrane. Evidence also suggests another assembly mechanism in which the assembled inner core virus particle is transported to the plasma membrane, where the outer core is now assembled (Grimes et al 1997). In order to develop a better understanding of the major structural proteins BTV assembly and transport, protein interaction studies have been

undertaken. Through the use of pull-down assays and confocal microscopy the BTV non-structural protein NS3 was found to interact with both VP2 and VP5 (Bhattacharya and Roy 2008). It was also found that the NS3 protein can interact with host proteins involved in exocytosis pathways. Confocal microscopy revealed that BTV NS3 is transported to the plasma membrane were it is involved in the release of mature virus particles from the infected cell. Therefore it was hypothesized that cellular trafficking machinery could be involved in the transport and release of BTV particles. Structural analysis of the VP5 protein identified a conserved membrane-docking domain similar to the host SNARE protein synaptoagmin. Site-directed mutagenesis of this VP5 domain suggests that it is essential for lipid raft association. This would suggest that the interaction of the outer capsid VP5 and the non-structural protein NS3 may be involved in the release of BTV from the host cell by interacting with cellular SNARE proteins, via a SNARE-like domain contained in the VP5 protein, and mediating membrane fusion between vesicles containing the virus particles and the plasma membrane.

In conclusion, both members of the PRRSV major envelope heterodimer, GP5 and M protein, were found to interact with a member of the host SNARE-dependent membrane fusion pathway snapin. More refined epitope mapping revealed that both proteins interact with snapin at sites within their ecto-domains near the N-terminus. This would suggest that the PRRSV may utilize the host cells SNARE machinery, via the interaction of the GP5/M heterodimer with snapin, to facilitate the transport of virus particles into and/or out of host cells.

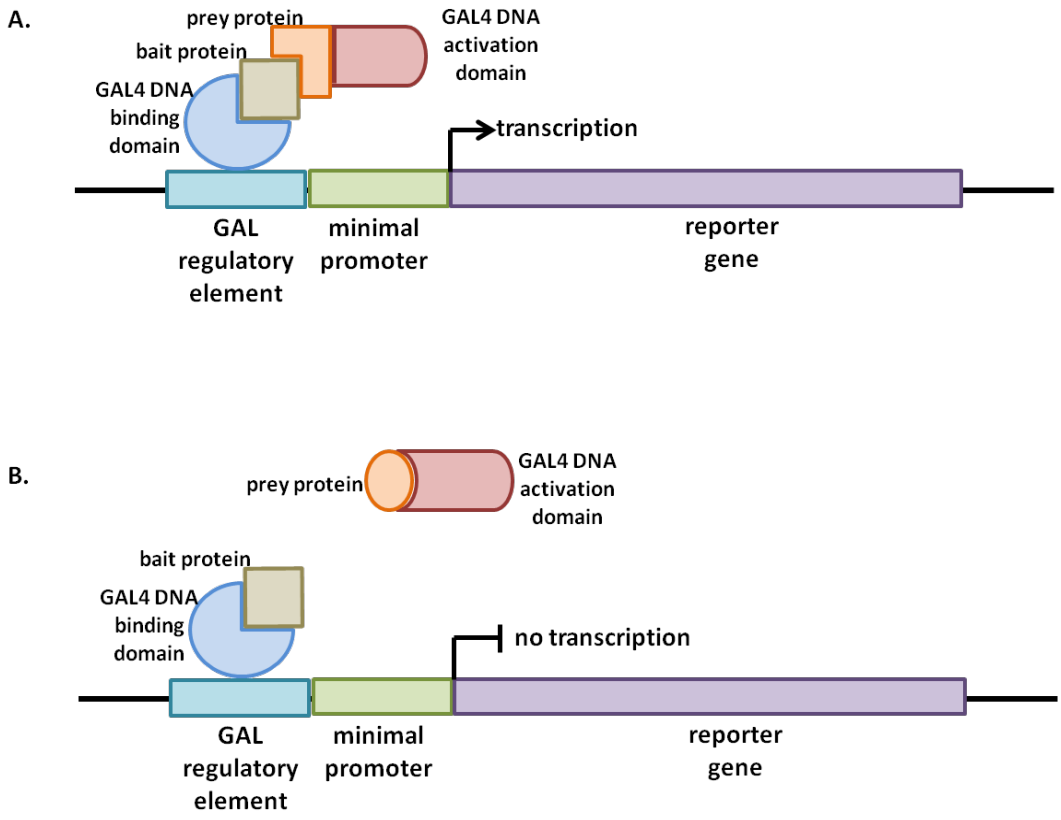

Figure 2.1. Diagram of the yeast two-hybrid assay.
The protein of interest, known as the "bait" protein, is expressed as a fusion protein with the DNA-binding domain of GAL4. A "prey" protein library generated from a cell population and/or tissue of interest and is expressed as fusion proteins containing the activation domain of GAL4. Yeast expressing the bait fusion protein and yeast expressing the prey fusion proteins are then mated. A. If the "bait" protein interacts with a particular prey protein, then the two domains of the GAL4 transcription will be brought into proximity to each other, creating a functional GAL4 protein which will then activate the expression of one or more reporter genes, which are under the control of the GAL4 promoter. B. If there is no interaction between the "bait" and "prey" a functional GAL4 transcription factor will not be produced preventing the transcription of the reporter genes.

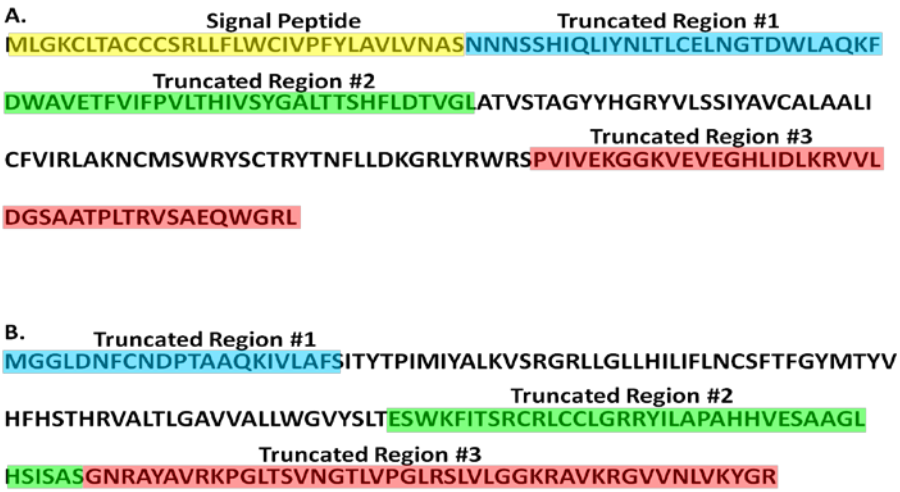

Figure 2.2. Truncated regions of PRRSV GP5 and M for epitope mapping. Truncated regions of GP5 and M were designed based on the hydropathy profiles of each protein with focus on the endo- and ecto-domains of each protein as these are the most probable sites of snapin interaction. A.GP5 epitopes. B. M epitopes.

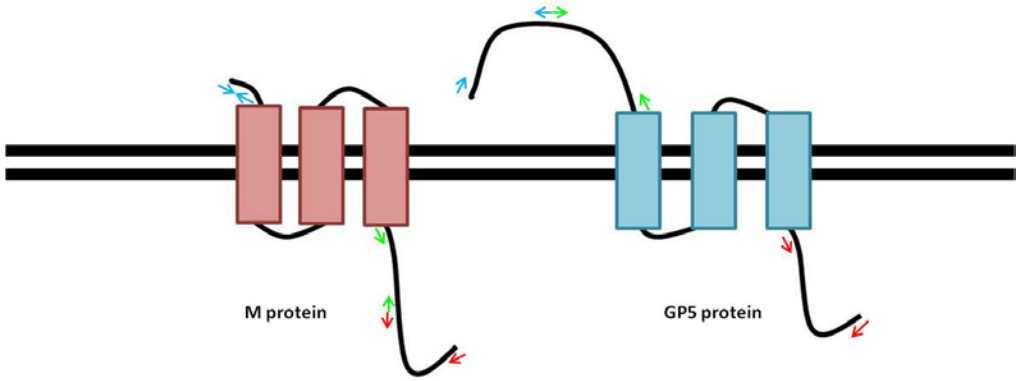

Figure 2.3. Diagram of truncated regions of PRRSV GP5 and M for epitope mapping.
Arrows represent approximant primer sites for truncated constructs of M and GP5 for epitope mapping. Arrow colors correspond to the coloring scheme in figure 2.2.

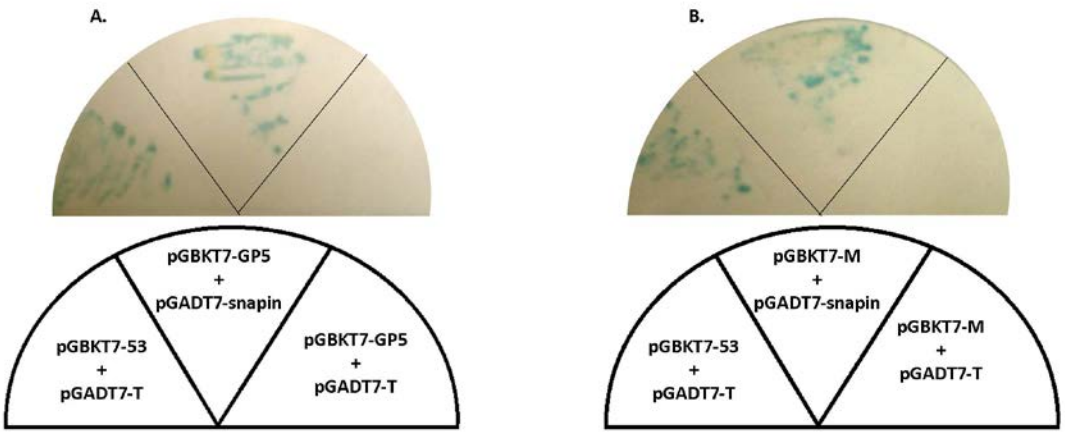

Figure 2.4. Confirmation of the full length PRRSV GP5 and M interaction with the host protein Snapin via a yeast two-hybrid β-galactosidase assay.
A. From left to right: pGBKT7-53 and pGADT7-T mating (positive control), pGBKT7-GP5 and pGADT7-Snapin mating, and PGBKT7-GP5 and pGADT7-T (negative control). B. From left to right: pGBKT7-53 and pGADT7-T mating (positive control), pGBKT7-M and pGADT7-Snapin mating, and PGBKT7-M and pGADT7-T (negative control).

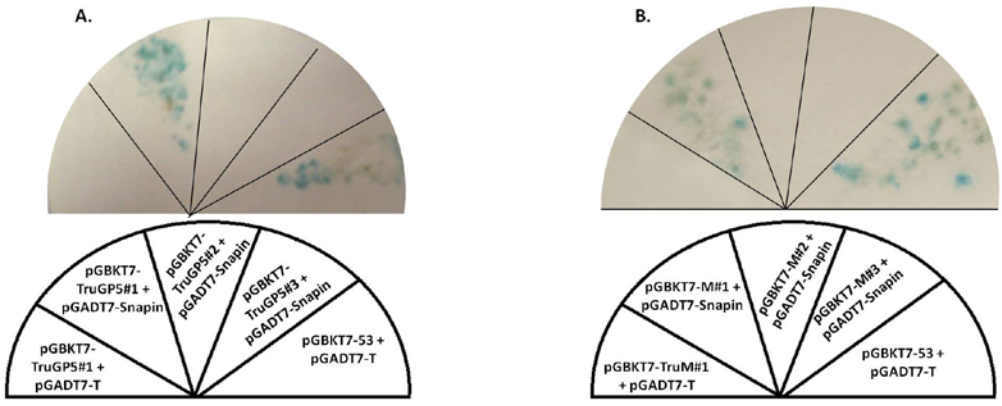

Figure 2.5. Epitope mapping of the interacting regions of PRRSV GP5 and M proteins with the host protein Snapin.
Epitope mapping was performed using the yeast two-hybrid system and confirmed via the β-galactosidase assay. Truncations of GP5 and M were designed based on the hydropathy profiles of each protein. A. Epitope mapping of GP5, left to right: pGBKT7-TruGP5(1) and pGADT7-T (negative control); pGBKT7-TruGP5(1) (aa 31-60) and pGADT7-Snapin; pGBKT7-TruGP5(2) (aa 61-92) and pGADT7-Snapin; pGBKT7-TruGP5(3) (aa 157-200) and pGADT7-Snapin; pGBKT7-53 and pGADT7-T (positive control. B. Epitope mapping of M, left to right: pGBKT7-TruM(1) and pGADT7-T (negative control); pGBKT7-TruM(1) (aa 1-22) and pGADT7-Snapin; pGBKT7-TruM(2) (aa 87-127) and pGADT7-Snapin; pGBKT7-TruGP5(M) (aa 128-173) and pGADT7-Snapin; pGBKT7-53 and pGADT7-T (positive control).

References

AuCoin DP, Smith GB, Meiering CD, Mocarski ES.Betaherpesvirus-conserved cytomegalovirus tegument protein ppUL32 (pp150) controls cytoplasmic events during virion maturation. J Virol. 2006 80(16):8199-210.

Bailer SM, Haas J. Connecting viral with cellular interactomes.Curr Opin Microbiol. 2009 12(4):453-9.

Bhattacharya B, Roy P.Bluetongue virus outer capsid protein VP5 interacts with membrane lipid rafts via a SNARE domain. J Virol. 2008 82(21):10600-12.

Buxton P, Zhang XM, Walsh B, Sriratana A, Schenberg I, Manickam E, Rowe T. 2003. Identification and characterization of Snapin as a ubiquitously expressed SNARE-binding protein that interacts with SNAP23 in non-neuronal cells. Biochem J. 375(Pt 2):433-40.

Chen M, Lucas KG, Akum BF, Balasingam G, Stawicki TM, Provost JM, Riefler GM, Jörnsten RJ, Firestein BL.A novel role for snapin in dendrite patterning: interaction with cypin. Mol Biol Cell. 2005 16(11):5103-14.

Cooper J, Liu L, Woodruff EA, Taylor HE, Goodwin JS, D'Aquila RT, Spearman P, Hildreth JE, Dong X.Filamin A protein interacts with human immunodeficiency virus type 1 Gag protein and contributes to productive particle assembly.J Biol Chem. 2011 286(32):28498-510.

Dea S, Sawyer N, Alain R, Athanassious R.Ultrastructural characteristics and morphogenesis of porcine reproductive and respiratory syndrome virus propagated in the highly permissive MARC-145 cell clone. Adv Exp Med Biol. 1995 380:95-8.

Delrue I, Van Gorp H, Van Doorsselaere J, Delputte PL, Nauwynck HJ.Susceptible cell lines for the production of porcine reproductive and respiratory syndrome virus by stable transfection of sialoadhesin and CD163. BMC Biotechnol. 2010 10:48.

Fasshauer D.Structural insights into the SNARE mechanism. Biochim Biophys Acta. 2003 1641(2-3):87-97

Fields S, Song O.A novel genetic system to detect protein-protein interactions. Nature. 1989 340(6230):245-6.

Gowthaman R, Silvester AJ, Saranya K, Kanya KS, Archana NR.Modeling of the potential coiled-coil structure of snapin protein and its interaction with SNARE complex.Bioinformation. 2006 1(7):269-75.

Grimes JM, Jakana J, Ghosh M, Basak AK, Roy P, Chiu W, Stuart DI, Prasad BV.An atomic model of the outer layer of the bluetongue virus core derived from X-ray crystallography and electron cryomicroscopy. Structure. 1997 5(7):885-93.
Hamdi A, Colas P.Yeast two-hybrid methods and their applications in drug discovery. Trends Pharmacol Sci. 2012 33(2):109-18.

Ilardi JM, Mochida S, Sheng ZH. 1999. Snapin: a SNARE-associated protein implicated in synaptic transmission. Nat Neurosci. 2(2):119-24.

Indran SV, Ballestas ME, Britt WJ.Bicaudal D1-dependent trafficking of human cytomegalovirus tegument protein pp150 in virus-infected cells.J Virol. 2010 84(7):3162-77.

Koh TW, Bellen HJ.Synaptotagmin I, a Ca2+ sensor for neurotransmitter release.Trends Neurosci. 2003 26(8):413-22.

Lee C, Yoo D.The small envelope protein of porcine reproductive and respiratory syndrome virus possesses ion channel protein-like properties. Virology. 2006 355(1):30-43

Limjindaporn T, Wongwiwat W, Noisakran S, Srisawat C, Netsawang J, Puttikhunt C, Kasinrerk W, Avirutnan P, Thiemmeca S, Sriburi R, Sittisombut N, Malasit P, Yenchitsomanus PT.Interaction of dengue virus envelope protein with endoplasmic reticulum-resident chaperones facilitates dengue virus production. Biochem Biophys Res Commun. 2009 379(2):196-200.

Lu L, Cai Q, Tian JH, Sheng ZH.Snapin associates with late endocytic compartments and interacts with late endosomal SNAREs. Biosci Rep. 2009 29(4):261-9.

Miranda-Saksena M, Boadle RA, Aggarwal A, Tijono B, Rixon FJ, Diefenbach RJ, Cunningham AL.Herpes simplex virus utilizes the large secretory vesicle pathway for anterograde transport of tegument and envelope proteins and for viral exocytosis from growth cones of human fetal axons. J Virol. 2009 83(7):3187-99.

Nakamura F, Stossel TP, Hartwig JH.The filamins: organizers of cell structure and function. Cell Adh Migr. 2011 5 (2):160-9.

Parpura V, Mohideen U.Molecular form follows function: (un)snaring the SNAREs. Trends Neurosci. 2008 31(9):435-43.

Pol JM, Wagenaar F, Reus JE.Comparative morphogenesis of three PRRS virus strains.Vet Microbiol. 1997 55(1-4):203-8.

Rodkey TL, Liu S, Barry M, McNew JA. 2008. Munc18a scaffolds SNARE assembly to promote membrane fusion. Mol Biol Cell. 2008 19(12):5422-34.
Söllner TH. 2004. Intracellular and viral membrane fusion: a uniting mechanism. Curr Opin Cell Biol. 16(4):429-35.

Vites O, Rhee JS, Schwarz M, Rosenmund C, Jahn R. 2004. Reinvestigation of the role of snapin in neurotransmitter release. J Biol Chem. 279: 26251-26256.
Yuan X, Shan Y, Zhao Z, Chen J, Cong Y.Interaction between Snapin and G-CSF receptor.Cytokine. 2006 33(4):219-25.

Zhang L, Villa NY, Rahman MM, Smallwood S, Shattuck D, Neff C, Dufford M, Lanchbury JS, Labaer J, McFadden G.Analysis of vaccinia virus-host protein-protein interactions: validations of yeast two-hybrid screenings.J Proteome Res. 2009 (9):4311-8.

Chapter Three: Characterizing the interaction between Porcine Reproductive and Respiratory Syndrome Virus envelope proteins, GP5 and M and a member of the SNARE membrane fusion complex, Snapin.

Introduction

The serendipitous discovery that introduction of additional copies of the chalcone synthase into petunias results in suppression of color pigmentation, rather that enhancement as expected, opened a new field of gene regulation termed RNA interference (RNAi) (reviewed by Matzke and Matzke 2004). As reviewed earlier, many endogenous RNAi pathways exist in eukaryotes; however these pathways are also used to introduce exogenous small RNAs, both *in vitro* and *in vivo*, for the study of specific gene functions. Small RNAs provide a relatively simple way to reduce gene expression compared to other gene inhibitory methods, such as deletion mutagenesis. In addition these small RNAs can be transiently introduced allowing for knock-down at a specific experimental stage, such as during a particular point of a virus infection. As exogenously introduced small RNAs are transient in nature this means that the knock-down its self is reversible, though the use of retroviral vectors and transgenics can be used to stabily express siRNAs. Commercially available siRNA screens allow for the concurrent knock-down of thousands of genes allows researchers to identify genes involved in their phenotype of interest, with little *a priori* knowledge required. These characteristics provide much flexibility in RNAi assays.

One area that has benefited greatly from RNAi technology is virology. The above described characteristics make siRNA ideal for identifying both viral and cellular genes involved at specific stages of the virus life cycle. An accessory protein of HIV-1, Nef, is

known to interfere with host cell cholesterol and lipid raft formation. This is achieved by the interaction of Nef with the cellular protein ABCA1 (ATP-binding cassette, sub-family A (ABC1), member 1). Recently it was demonstrated that siRNA knock-down of ABCA1 in RAW264.7 cells (mouse macrophage cell line) stably expressing HIV-1 nef (an accessory protein involved in virus replication) and HIV-1 and in human monocyte-derived macrophages results in an increase in both cholesterol delivery to lipid rafts and in HIV-1 replication (Cui et al. 2012). The Tax oncogene of another human retrovirus, human T-cell leukemia virus type 1 (HTLV-1), is modified by the cellular ubiquitin ligase, Really Interesting New Gene Finger protein 4 (RNF4). RNF4-modified Tax is relocated from the nucleus to the cytoplasm. SiRNA-mediated knock-down of RNF4 prevents transport of Tax to the cytoplasm, resulting in increased apoptosis of HTLV-1 infected cells (Fryrear et al. 2012). During retroviral infections viral DNA is synthesized and associates with viral proteins in the cytoplasm to form the pre-integration complex, which is then transported into the nucleus. RNAi knock-down of RanBP2, a member of the nuclear pore complex, reduces transport of the pre-integration complex into the nucleus which in turn, reduces HIV-1 production (Zhang et al. 2010). An RNAi screen in which members of cellular secretory pathways were knock-downed during hepatitis C virus (HCV) infection, identified several host proteins that are critical for HCV intracellular transport (Coller et al. 2012). For example, siRNA knock-down of Rab11a, a member of the recycling endosome, prevents budding of the HCV core from the Golgi. In another large scale siRNA screening to ascertain cellular proteins associated with negative sense RNA viral infections, 72 cellular

genes were found to be required for productive infections (Panda et al. 2012). Knock-down of several members of the coatomer complex I, a protein complex that coats transport vesicles, as well as its effector proteins, ARF1 and GBF1, decreases production of three negative sense RNA viruses, vesicular stomatitis virus (VSV), lymphocytic choriomeningitis virus (LCMV) and human parainfluenza virus type 3 (hPIV-3). Further characterization of the function of the coatomer complex I in VSV infection discovered that siRNA knock-down of the complex member ε-COP prevents internalization of VSV particles (Cureton et al. 2012). The chicken anemia virus (CAV) protein Apoptin displays differential localization depending on cell type: in primary cells apoptin localizes to the cytoplasm, while it is found in the nucleus of transformed cells, where it induces apoptosis. SiRNA targeting of either ATM or DNA-PK, two proteins involved in the DNA damage response, prevents nuclear localization of apoptin in transformed cells and increases apoptosis of these cells (Kucharski et al. 2011).

The Nidoviridae virus order is comprised of the two major virus families coronaviridae and arteriviridae. More is known about the involvement of intracellular transport during coronavirus infections than during arterivirus infections, though neither mechanism of virally induced perturbation has been completely elucidated. Severe acute respiratory syndrome coronavirus (SARS-CoV) is a human pathogen first discovered in 2003. It was quickly identified as a coronavirus. Numerous studies have been undertaken to elucidate the mechanisms involved in the intracellular movement of SARS-CoV particles and their components. Treatment of cells with the SARS-CoV spike protein or with pseudo-virus

particles containing the SARS-CoV spike protein, the SARS-CoV receptor 2CACE21, is transported from the cell surface to endosomes. This phenomenon suggests a receptor-mediated endocytosis mechanism for entry of SARS-CoV (Wang et al. 2008). Furthermore, the spike protein of the pseudoviruses also is known to co-localize with early endosome markers. This entry mechanism is independent of both clathrin and caveolae mediated pathways. Analysis of the movement of individual SARS-CoV proteins within the host cell found that viral nucleocapsid and glycoproteins accumulate at the Golgi where nascent virus particles are formed, which then bud through the membranes of the ER-Golgi intermediate compartment (ERGIC) (Stertz et al. 2007). This particle formation and budding occurs as early as 3 hours post infection. Intracellular tracking of the SARS-CoV surface proteins, S, M, and E revealed that these proteins localize to several intracellular regions (Nal et al. 2005). The S protein localizes to several regions of the secretory pathway ranging from the ER to the plasma membrane. Meanwhile, the M protein localizes to the Golgi and E localizes to perinuclear patches near the ER. Though all coronaviruses share aspects of intracellular transport, they can also use unique mechanisms as well. Functional analysis of the S protein of two coronaviruses, SARS-CoV and transmissible gastroenteritis virus (TGEV), a porcine coronavirus, revealed that they possessed individual intracellular localization patterns (Schwegmann-Wessels et al. 2004). It was discovered that unlike the S protein of SARS-CoV, the S protein of TGEV is not transported to plasma membrane. This intracellular retention of TGEV S protein is linked to a tyrosine-dependent signal in its cytoplasmic tail not present in the SARS-CoV S protein. Modification of the SARS-CoV S

protein to contain the signal domain results in loss of its transport to the cell surface. The S protein of the avian coronavirus infectious bronchitis virus (IBV) also contains a tyrosine motif its cytoplasmic tail (Winter et al. 2008). Similar to the TGEV S protein, this tyrosine motif serves as signal for intracellular retention of the S protein. Furthermore, IBV S is specifically retained at the late Golgi compartment. One function of the S protein of coronaviruses is likely in the uncoating and transport of the viral genome to the ER (Zhu et al. 2009). There are both fusogenic (induces syncytium formation) and non-fusogenic strains of mouse hepatitis virus (MHV). Nonfusogenic MHV grows to higher titers than non-fusogenic MHV. A hybrid MHV consisting of the genome of a fusogenic strain expressing the S protein of a non-fusogenic strain displayed non-fusogenic growth kinetics (Zhu et al, 2009). This would suggest that the S protein is associated with the enhanced growth seen in non-fusogenic strains. It was further demonstrated that recombinant virus was able to initiate viral transcription and translation much faster than the original fusogenic strain. When the recombinant virus was treated with trypsin there was reduced transport of the viral genome to the ER. Though both TEGV and MHV infect epithelial cells they exit from opposite ends, with TEGV exiting from the apical surface and MHV exiting from the basolateral surface. To further characterize these different transport mechanisms, a porcine epithelial cell line expressing the MHV receptor was generated (Rossen et al. 1996). This cell line is permissive to both viruses. Interestingly the viruses still displayed opposite exiting strategies, indicating that the exiting signal is viral rather than cellular specific. It was suggested that this difference may be due to the different infection strategies of these two

viruses, as TGEV is mainly associated with enteric infections, while MHV infections are more system wide.

Treatment of MARC-145 cells with chemicals that disrupt pH-dependent intracellular trafficking revealed that PRRSV virions entry into these cells requires a pH shift (Kreutz and Ackermann et al. 1996). In alveolar macrophages it was demonstrated that the PRRSV major envelope proteins interact with sialoadhesin, and this interactions aids in virion entry (Delputte and Nauwynck 2004). However, the importance of this interaction was recently disputed (Tian et al. 2012). The macrophage specific molecule CD163 was also identified as a cellular PRRSV receptor (Calvert et al. 2007) via interactions with the minor envelope proteins GP4 and GP2 (Das et al. 2010). Additionally it was recently demonstrated that GP4 and CD163 co-localize in lipid rafts at the plasma membrane (Du et al. 2012).

The use of chimeric PRRS viruses to elucidate the involvement of the minor PRRSV structural proteins in receptor recognition, in which the minor envelope proteins were substituted with the minor proteins from EAV, suggests that the minor envelope proteins are the key to PRRSV tropism, as the chimeric viruses can infect EAV permissive cells (Tian et al. 2012). Further evidence that major PRRSV envelope proteins are not major factors in receptor recognition is the fact that chimeric PRRS viruses in which the M ectodomain of other arteriviruses, including LDV and EAV, was substituted for the ectodomain of PRRSV M protein do not have altered cellular tropisms (Verheije et al. 2002). A similar result was found when the ectodomains of GP5 of PRRSV and LDV were substituted for the ectodomain of EAV GP5 (Dobbe et al. 2001). Taken together these studies indicate that the

main function of the major PRRSV envelope proteins, GP5 and M may not be receptor recognition, however as they are present on the virion surface they likely play key roles in virion transport.

In the previous chapter we used a yeast two-hybrid approach to show that both major PRRSV envelope proteins GP5 and M interact with the cellular protein snapin. Snapin is a component of the SNARE complex, which functions in intracellular membrane fusion events (Buxton et al. 2003). In order to further understand the role(s) of the GP5/M interaction with snapin in PRRSV replication, RNAi technology was used to target snapin and knock-down its expression at key stages of the PRRSV life cycle. Multiple techniques including, real-time PCR, western blotting, and virus titration, were also used to characterize the effect of snapin knock-down on PRRSV production.

Material and Methods

pCDNA3 vector construction

PRRSV GP5 and M were individually cloned into the PCDNA3 vector (Invitrogen); primers were designed so that each protein would have a C-terminal His tag. Primers were also designed to contain either HindIII (forward primers) or EcoRI (reverse primers) restriction sites. Primer sequences were as follows: GP5 forward primer: 5′-AAAAGCTTATGTTGGGGAAGTGCTTG-3′, GP5 reverse primer: 5′-GGGAATTCCTAGGTGGTGGTGGTGGTGAGACGACCCCATTG-3′, M forward primer: 5′-AAAAGCTTATGGGGTCGTCTCTAGAC-3′, M reverse primer-5′-GGGAATTCTTAGTGGTGGTGGTGGTGGTGTTTGGCATATTTAAC-3′. For PCR

amplification PRRSV VR-2332 GP5 and M previously cloned into the pGBKT7 vector were used for template DNA. Each 25µl PCR reaction consisted of the following: 5µl of 5X GoFlex PCR buffer (Promega), 1µl of the forward primer (10pmol), 1µl of the reverse primer (10pmol), 0.2µl of template DNA (10ng), 0.8µl of dNTPs (8mM), 2.5µl of $MgCl_2$ (2.5mM), 0.2µl tag (1U), and 14.3µl of nuclease-free water. PCR amplification was carried out as follows: 95°C for 5 minutes, followed by 35 cycles of 95°C for 30 seconds; 55°C for 30 seconds; 72°C for 30 seconds, and finally 72°C for 5 minutes. PCR product amplification was confirmed by separating 3µl of PCR reactions on a 1% agarose gel and ethidium bromide staining Next PCR products were purified using an Ultra Clean PCR clean-up kit (MO BIO) following the manufacturer's instructions with the exception that the PCR products were eluted in 30µl of nuclease-free water. Next, the PCR product and the pCDNA3 vector were sequentially digested with HindIII and EcoRI. The PCR product was digested with HindIII in a 30µl reaction as follows: 3µl of 10X NEB Buffer 2 (New England Biolabs), 1µl of HindIII (New England Biolabs), and 26µl of the purified PCR product. The pCDNA3 vector as digested with HindIII in a 30µl reaction as follows: 3µl of 10X NEB Buffer 2 (New England Biolabs), 1µl of HindIII (New England Biolabs), 4µl of pCDNA3 vector (1µg) and 22µl of nuclease-free water. Reactions were maintained at 37°C for 2.5 hours. Digestion reactions were separated on a 1% agarose gel and the digested products were purified using a QIAquick gel extraction kit (Qiagen) following the manufacturer's instructions with the exception that the DNA was eluted in 30µl of nuclease-free water. The DNA was then digested with EcoRI. Each 30µl digestion included, 3µl of 10X EcoR buffer

(NEB), 1µl of EcoRI, and 26µl of purified DNA (both PCR products and the pCDNA3 vector). Reactions were maintained at 37°C for 2.5 hours. Digestion reactions were then separated on a 1% agarose gel and the digested products were purified using a QIAquick gel extraction kit (Qiagen) following the manufacturer's instructions with the exception that the DNA was eluted in 30µl of nuclease-free water. For DNA ligation, 30µl reactions, consisting of 3µl of 10X ligase buffer (NEB), 1µl of T4 DNA ligase (New England Biolabs), 3µl of digested pCDNA3 vector, and 23µl of digested GP5 or M his tag PCR products, were maintained at 14°C overnight. The entire ligation reaction was mixed with 50µl of DH5α chemically-competent cells and kept on ice for 20 minutes. The bacteria were then heat-shocked for 45 seconds in a 42°C waterbath. The bacteria were added to 250µl of SOC media and placed in a 37°C shaking incubator for 1 hour. Fifty microliters and 100µl of the bacterial cultures were plated on LB agar containing 100µg/ml of carbenicillin and kept at 37°C overnight. Two colonies for each construct were selected and grown overnight in 5ml of LB broth with 100µg/ml of carbenicillin in a 37°C shaking incubator. Plasmids were purified from the cultures using a Wizard Plus SV miniprep kit (Promega) following the manufacturer's instructions with the exception that the plasmids were eluted in 30µl of nuclease-free water. For each clone 1µg of DNA was digested with HindIII and EcoRI to confirm proper insertion of the GP5 and M genes. One positive clone for GP5-his and one for M-his were sequenced.

pCDNA3 tranfection

Marc-145 cells were seeded at a density of $3X10^5$ cells per well in a six-well plate. The following day 3 wells were tranfected with pCDNA3-GP5-his and 3 wells were transfected with pCDNA3-M-his using Fugene 6 at a ratio of 3:1 (3µl of Fugene 6 to 1µg of DNA) (Roche). For each transfection reaction 3µl of Fugene 6 reagent was added to 97µl of serum and antibiotic free RPMI1640 media and incubated at room temperature for 5 minutes. Next, 1µg of the pCDNA3 construct was added and mixed by flicking and maintained at room temperature for 15 minutes. The reagent/DNA complex was then added to the cells and the cells were maintained in RPMI1640 with 5% FBS, L-glutamine, penicillin (100 U/ml), streptomycin (100 µg/ml) and fungizone (4µg/ml) at 37°C with 5% CO_2 for 72 hours. Each well was collected in 50µl of lysis buffer (50mM Tris-HCl pH 7.6, 150mM NaCl, 2mM EDTA, and 0.2% NP-40).

Pull-down assay

Cell lysates were briefly centrifuged to remove non-soluble debris. Lysates were then mixed with 20µl of washed and calibrated nickel beads (Qiagen) on a rotor at 4°C overnight. The beads were centrifuged at 2,000rpm for 10 minutes and supernatant was removed. The beads were then washed three times in 200µl of 1XPBS. The beads were then resuspended in 20µl of 2X SDS-loading buffer. For western blotting 10µl of the bead/dye mixture were loaded per well.

Western Blotting

For all western blotting samples were maintained at 95°C for 10 minutes prior to loading. For all blots 12% SDS PAGE gels were used and proteins were separated at 110V until the dye front reached the bottom of the gel (~90 minutes) using a mini protean 3 cell protein cell system (BioRad). Gels were soaked in Tris-Glycine transfer buffer for 5 minutes and proteins were transferred to PVDF using a Trans-Blot SD semi-dry transfer cell (Bio-Rad) at 22V for 1 hour. All blots were blocked in 1% non-fat milk in 1X PBS for 1 hour at room temperature. The rabbit anti-Snapin antibodies were used at a dilution of 1:500 and incubated at 4°C overnight. The mouse anti-N protein (Rural Technologies Inc) was used at a dilution of 1:1000 and incubated at room temperature for 1 hour. All other antibodies, mouse anti-his tag (Novagen), rabbit anti-GAPDH (Sigma), goat anti-mouse HRP conjugate (Novagen), and goat anti-rabbit HRP conjugate (Novagen) were used at a dilution of 1:1500 and incubated at room temperature for 1.5 hours. All blots were developed using an ECL western blot substrate kit (Pierce) following the manufacturer's instructions. Blots were exposed to X-OMAT film (Kodak) between 30 seconds and 2 minutes depending on signal intensity. Films were developed on a Konica Minolta SRX-101A film processor.

RNA isolation and Real-Time PCR analysis

For all RNA isolations sample was collected in 1 mL of Tri-Reagent (Sigma) and homogenized by repeated passage thru a 23G needle. Next, 200µl of chloroform was added, mixed and the samples were kept at room temperature for ~5 minutes. The samples were then centrifuged at 13,000 rpm for 15 minutes. The aqueous layer was transferred to a new

tube and 500µl of 100% EtOH was added. RNA was precipitated at room temperature for 15 minutes. RNA was pelleted at 13,000 rpm for 20 minutes. The RNA pellets were washed in 1ml of 75% EtOH and centrifuged at 13,000 rpm for 10 minutes. The RNA pellets were then air dried and reconstituted in 30µl of DEPC-treated water (Ambion). RNA was quantified using a nanodrop ND-1000 spectrophotometer and quality was assessed using agarose gel electrophoresis. The RNA was then DNase-treated using a Turbo DNase kit (Ambion) For cDNA synthesis a SuperScript III cDNA synthesis kit was used. The cDNA synthesis was carried following the manufacturer's instructions and using1µg of DNase-treated total RNA. Primers for PRRSV N-protein, Snapin and β-actin were designed using primer blast (http://www.ncbi.nlm.nih.gov/tools/primer-blast/index.cgi?LINK_LOC=BlastHome). The primer sequences are as follows: Snapin forward primer: 5′-AGAGCTCCGGGAACAAATTGAC-3′, Snapin reverse primer: 5′-CGTCGCCGGGCATTAAGTA-3′, β-actin forward primer: 5′-AGGAGCACCCCGTGCTGC-3′, β-actin reverse primer: 5′-TAGCACAGCCTGGATAGCAACGT-3′, PRRSV N forward primer: 5′-ACCCCTAGTGAGCGGCATTGT-3′, PRRSV N reverse primer: 5′-CCTCCCTGAATCTGACAGGGTGCA-3′. Real-Time PCR reactions were performed in duplicate. Each reaction contained 40ng of cDNA, 1X iQ SYBR super mix (Bio-Rad), 500nM of both the forward and reverse primers. Cycles were performed as follows: 95°C for 10 minutes, followed by 40 cycles of 95°C for 10 seconds and 58°C for 50 seconds on a MyiQ real-time PCR detection system. Disassociation curve analysis was utilized to ensure

gene specific amplification. Data was normalized to the β-actin housekeeping gene. Data was transformed to relative expressions using the $2^{-\Delta\Delta Ct}$ method (Livak and Schmittgen 2001).

Virus titration

Marc-145 cells were seeded at a density of $2X10^5$ per well in 6-well plates. Cells were cultured in RPMI1640 media (MediaTech) supplemented with 5% FBS,, L-glutamine, penicillin (100 U/ml), streptomycin (100 μg/ml) and fungizone (4μg/ml) at 37°C with 5% CO_2. PRRSV strain VR-2332 was obtained from ATCC. The virus was titered on Marc-145 cells using $TCID_{50}$ (Reed Muench method). For virus titration, $5X10^4$ cells were seeded per well in 96-well plates. The following day, stock virus was serially diluted from 10^{-1} to 10^{-10} and each dilution was added to an 8-well column and cells were maintained for 5 days. The cells were then fixed in 100% methanol at -20°C for 10 minutes and air dried. Cells were rehydrated in 1XPBS for 5 minutes. Anti-PRRSV N protein mouse monoclonal antibodies (SDOW17; Rural Technologies) were added at a dilution of 1:2500 and incubated at room temperature for 1.5 hours. Cells were repeatedly washed with 1XPBS and goat anti-mouse FITC conjugated antibodies (Invitrogen) were added at a dilution of 1:200 and incubated at room temperature for 1 hour. Cells were repeatedly washed with 1XPBS and fluorescence was determined using a Leica fluorescence microscope. $TCID_{50}$ was calculated using the Reed-Muench method. All titrations were performed in duplicate. $TCID_{50}$ calculations were converted to MOIs for subsequent experiments (http://atcc.custhelp.com/app/answers/detail/a_id/410/~/converting-tcid%5B50%5D-to-moi).

siRNA design

Four siRNA were designed to target Snapin (Table 3.1). Two siRNAs (siRNA 17 and siRNA 45) were designed using the siDESIGN Center (http://www.dharmacon.com/designcenter/DesignCenterPage.aspx), one (siRNA 156) was designed using the BLOCK-IT RNAi designer (http://rnaidesigner.invitrogen.com/rnaiexpress/) and one (siRNA 368) was designed using siRNA_profile (http://bonebiology.utu.fi/pimaki/main.html). The miRNA target prediction algorithm miRanda (http://www.microrna.org/microrna/home.do) was utilized to confirm that the siRNAs did not have a high degree of complementarity to any other host genes. The Silencer negative control siRNA #1 was purchased from Ambion. The sequences for the siRNAs are given in Table 3.1.

siRNA transfection

For each siRNA transfection (triplicates for each siRNA) 2 x 10^5 Marc-145 cells were seeded per well of a 6-well plate. The next day for each transfection, 5µl of siPORT Amine siRNA tranfection reagent (Ambion) was diluted into 100µl of serum and antibiotic free RPMI1640 media and incubated for 10 minutes at room temperature. For each siRNA, 12.5µl of 10µM siRNA was diluted into 100µl of serum and antibiotic free RPMI1640 media. The diluted transfection reagent and the diluted siRNA were mixed and incubated at room temperature for 10 minutes. The mixture was then added to the cells for 48 hours. Cells from each well was collected in 1mL of Tri-Reagent (Sigma).

Snapin expression determination using immunofluorescence

MARC-145 cells transfected with either a snapin-specific siRNA or a negative control siRNA were fixed in 100% cold methanol for 10 minutes at -20°C. The cells were air dried and then rehydrated in 1XPBS for 5 minutes at room temperature. Rabbit anti-snapin antibodies were then added at a dilution of 1:500 and maintained at room temperature, with gentle rocking, for 2 hours. Cells were repeatedly washed with 1XPBS and goat anti-rabbit texas red conjugated antibodies (Invitrogen) were added at a dilution of 1:200 and incubated at room temperature for 1 hour. Cells were repeatedly washed with 1XPBS and fluorescence was determined using a Leica fluorescence microscope.

siRNA-mediated snapin knock-down during a PRRSV infection

The siRNA "368" was determined to be the most effective and least detrimental to host cells and so was chosen for use in all subsequent experiments. Tranfection reactions were setup as described above. In the first experiment, $2X10^5$ MARC-145 cells were seeded per well in 6-well plates. The following day the cells were transfected with either 50nM of siRNA "368" or 50nM negative control siRNA. Twenty-four hours post-transfection the cells were infected with PRRSV VR-2332 at MOIs of 0.1, 1 and 5 or mock infected. At 12 hours, 24 hours and 48 hours post-infection, the cells were either collected in 1 mL of Tri-Reagent (Sigma) for mRNA quantification or 50µl of lysis buffer for protein quantification. Each MOI and timepoint was performed in triplicate. In the second experiment, 2×10^5 MARC-145 cells were seeded per well in 6-well plates. The following day the cells were infected with PRRSV VR-2332 at a MOI of 0.1, 1, or 5 or mock infected for 12 hours. The cells were

then transfected with either 50nM of siRNA "368" or 50nM negative control siRNA for either 12 hours, 24 hours or 48hours. At the given timepoints the cells were either collected in 1 mL of Tri-Reagent (Sigma), or 50µl of lysis buffer. Each MOI and timepoint was performed in triplicate.

Results

Confirmation of the GP5 and M interaction with cellular snapin

In order to confirm the interaction between PRRSV GP5 and M and the cellular membrane fusion protein snapin, GP5 and M were expressed as his fusion proteins in the MARC-145 cells. After transient transfection of MARC-145 cells with either pCDNA3-GP5-his, pCDNA3-M-his, or mock transfected, cells were collected and subjected to pull-down analysis. Western blot analysis confirmed the transient expression of both GP5-his (Figure 3.1a) and M-his in transfected cells (Figure 3.1b). No fusion proteins were detected in mock transfected cells. The transfected cells were lysed in a mild lysis buffer, allowing for the maintenance of protein interactions and subjected to his-fusion protein purification using nickel beads. Western blot analysis confirmed the co-purification the cellular protein snapin with MARC-145 cells transfected with either pCDNA3-GP5-his or pCDNA3-M-his (Figure 3.2).

Knock-down of snapin prior to PRRSV infection

To determine the effect if any, of the interaction between GP5 and M with the cellular protein snapin on PRRSV entry into host cells, siRNA technology was used to knock-down snapin prior to PRRSV infection in MARC-145 cells. Twenty-four hours post siRNA

transfection the cells were infected at one of three MOIs, 0.1, 1, and 5. The effect on PRRSV N protein expression, often used as an indicator of PRRSV replication, was determined at 12, 24, and 48 hours post infection. The effect on N RNA expression was determined using real-time PCR and the effect on N protein expression was determined using western blotting. Both real-time and western blot analysis confirmed that the siRNA efficiently knocked-down snapin expression (Figures 3.3-3.5 and Figure 3.9). Overall the snapin-specific siRNA down-regulated snapin mRNAs levels between ~15-30 fold compared to cells transfected with the negative control siRNA (Figures 3.3-3.5). Snapin protein expression was also drastically reduced (Figure 3.9). Knock-down of snapin expression resulted in decreased PRRSV replication, particularly at the later stages of infection as evidenced by a decrease in both PRRSV N mRNA and protein levels (Figure 3.3-3.5 and Figure 3.9). There was ~ 5 fold decrease in the titer of PRRSV (48hpi) in cells transfected with snapin-specific inhibitor compared to cells transfected with a negative control siRNA (Table 3.2).

Knock-down of snapin after PRRSV infection

To further characterize the interaction between PRRSV GP5 and M with the cellular protein snapin a second experiment was carried in which MARC-145 cells were first infected with PRRSV VR-2332 at MOIs of 0.1, 1, and 5 for 12 h and then transfected with either the snapin specific siRNA or a negative control siRNA. Both mRNA and protein levels were assayed at 12 hpt (hours post transfection), 24 hpt, and 48 hpt. Virus titration was performed to further determine the effects of snapin knock-down on PRRSV production. At the 12 hpt time point there was a modest effect on snapin expression, with a decrease in snapin mRNA

levels of ~3-5 fold knock-down of snapin expression. By 48 hpt transfection snapin mRNA were greatly reduced ranging from ~25-35 fold decrease in snapin mRNA levels in cells transfected with the snapin-specific inhibitor compared to cells transfected with the negative control siRNA (Figures 3.6-3.8). At the 12 hpt transfection there was only a significant difference in N mRNA levels in cells infected with PRRSV at an MOI of 1, but not in cells infected with MOIs of 0.1 or 5 (Figures 3.6-3.8). However, at the later timepoints snapin knock-down had a significant negative impact on N mRNAs, at 48hpi there was average of ~15 fold decrease in N mRNAs in cells transfected with the snapin specific siRNA compared to the cells transfected with the negative control siRNA (Figures 3.6-3.8). Western blot analysis also demonstrated decreased N protein levels in cells transfected with the snapin siRNA compared to cells containing the negative control siRNA (Figure 3.10). Again a ~5 fold decrease in PRRSV titers (at 48hpt) was found in cells transfected with the snapin specific inhibitor compared to cells possessing the negative control siRNA (Table 3.3).

Discussion

One of the key factors in understanding viral pathogenesis is identifying the underlying mechanisms of viral intracellular transport. As GP5 and M of the arterivirus PRRSV are considered the major viral envelope proteins, it is likely that they are somehow involved in the intracellular transport of PRRSV virions and/or its components. To better understand the functional roles of GP5 and M in the PRRSV lifecycle we utilized a yeast-two hybrid screen to discover which if any, host cell proteins interact with these viral envelope proteins. This screening revealed that both GP5 and M interact with the host membrane

fusion associated protein snapin. To identify functional role(s) of this interaction snapin expression was knocked-down during key PRRSV infection stages using a siRNA designed to specifically target the snapin mRNA. In addition imunofluorescence analysis revealed that siRNA 368 effectively reduced snapin expression in transfected cells (Figure 3.11). In addition both mRNA and protein expression analysis confirmed the down-regulation of snapin expression in cells transfected with siRNA 368 compared those transfected with the negative control. The down regulation had a negative impact on PRRSV replication as evidenced by the fact that PRRSV N mRNA and protein expression levels as well as PRRSV titers were significantly decreased in cells transfected with a snapin specific siRNA inhibitor compared to cells transfected with a negative control siRNA.

Several factors have been identified that are key to designing an effective siRNA. First it has been shown that siRNAs targeting the ORF of the mRNA rather than in the untranslated regions (UTRs) tend be more potent, as the UTRs often interact with regulatory proteins which may interfere with siRNA binding (Elbashir et al. 2002). It is also important that siRNAs binding sites bypass intron/exon boundaries, which due to mRNA splicing may result in mis-pairing between the siRNA and mRNA (Celotto and Graveley 2002). It has been found that a dinucleotide overhang, particularly, UU at the 3′ end of the siRNA often increases its effectiveness (Elbashir et al. 2001a). Typically the best performing siRNAs are between 21-22 nucleotides (Elbashir et al. 2001b). The thermodynamic stability of siRNA also has an effect on its function. Most effectual siRNAs possess GC content between 30%-53%, siRNAs with extreme GC contents tend to interact poorly with targeted mRNA

(Reynolds et al. 2004). Also the best functioning siRNAs often have internal stability at the 3′ end (Shabalina et al. 2006). In support of this well functioning siRNAs have an A/U rich 5′ end and G/C rich 3′ end (Shabalina et al. 2006). Numerous publicly available algorithms are available that take into account different combinations these criteria. As unpredictable biological factors also contribute to siRNA function it is impossible to predict exactly which siRNA sequence will be the most effective and least toxic to the target cell. It is thus generally recommended that multiple siRNAs be designed and tested. Of the four siRNAs designed in this experiment (Table 3.1) based on the above criteria, one in particular siRNA 368, so named because its target site lies between nucleotides 368-387, was very effective in down-regulating snapin expression. Transfection of siRNA 368 in MARC-145 cells knocked-down snapin expression up to ~30 fold compared to cells transfected with the negative control siRNA.

The arteriviridae family of the order nidoviridae consists of four members, equine arteritis virus (EAV), lactate dehydrogenase elevating virus (LDV), simian hemorrhagic fever virus (SHFV), and porcine reproductive and respiratory syndrome virus (PRRSV). It is thought that these viruses enter host cells in a clathrin-dependent manner. For example, interference of clathrin-mediated endocytosis, via chemicals or siRNA, blocks EAV infection of BHK cells (Nitschke et al. 2008). In PAMs PRRSV co-localizes with clathrin and treatment of the cells with cytochalasin D, an inhibitor of the clathrin pathway, prevents virion uptake (Nauwynck et al. 1999). A drop in vesicle pH is required for PRRSV virion entry as the number of infected MARC-145 cells decreases when the cells are treated

cytochalasin B and phenylarsine oxide, which maintain intracellular pH levels, prior to PRRSV infection (Kreutz and Ackermann 1996). PRRSV is thought to enter the clathrin-dependent endocytic pathway after the interaction of the minor envelope proteins and the cellular receptor CD163 (Calvert et al. 2007). Secondary interactions between virion and sialoadhesin and vimentin also likely engage in PRRSV virus uptake (Vanderheije et al. 2002; Kim et al. 2006). PRRSV M protein also binds heparin-like molecules present on the surface of PAMs (Delputte et al. 2002).

Snapin is a member of the SNARE complex, a group of proteins that mediate the fusion between vesicles and their target compartments by bringing their membranes into close proximity to one another (Risselada and Grubmüller 2012). Snapin is an accessory protein involved in mediating the interaction of synaptotagmin 1 with core SNARE complex (Buxton et al. 2003). Snapin is widespread throughout the cell localizing to multiple cell membrane boundaries including the peripheral membrane, as well as at endosomal and Golgi membrane sites (Yuan et al., 2006, Buxton et al., 2003, Chen et al., 2005 and Vites et al., 2004). Snapin is also found to be enriched in late endocytic compartments suggesting that it may also aid in the fusion of late endosomes with lysosomes organelles (Lu et al. 2009).

As SNARE complex mediated fusion is major component of intracellular trafficking pathways, it is not surprising that viruses have developed mechanisms to subvert its functions for their own benefit. It was recently shown that SNARE-mediated fusion is important in the assembly of HIV-1 virus particles (Garg and Joshi 2012). Interruption of SNARE function prevents Gag trafficking to the plasma membrane, the site of virion assembly. During

HCMV infection the SNARE component SNAP-23 localizes to intracellular sites of virion assembly (Liu et al. 2011). Reduction of SNAP-23 expression in HCMV-infected cells does not produce productive virus, suggesting an important role of the SNARE-fusion complex in the HCMV lifecycle. Another member of the SNARE complex, syntaxin 3 has also been linked to HCMV infection (Cepeda and Fraile-Ramos 2011). Synaxin 3 co-localizes with HCMV assembly sites and with virus wrapping membranes. Knock-down of synaxin 3 expression decreases production of HCMV virions. One of the capsid proteins of bovine papillomavirus type 1 (BPV1), L2 interacts with SNARE component syntaxin 18 (Laniosz et al. 2007). Mutational disruption of the L2-syntaxin 18 interaction negates BPV1 infectivity. Parainfluenza virus 5 (PIV5) encodes a fusogenic protein F which structurally is very similar to SNARE proteins, containing a coiled coil "zipper" domain (Donald et al. 2011). One function of the F protein is to mediate membrane fusion events during a PIV5 infection. Blue tongue virus (BTV), a reovirus, also encodes a protein that is structurally similar to SNARE proteins, the outer capsid protein VP5 (Bhattacharya and Roy 2008). Functional analysis revealed that VP5 associates with lipid rafts and is thus thought to be involved in mediating viral transport. The non-structural protein p48 of Norwalk virus interacts with cellular vesicle-associated membrane protein-associated protein A (VAP-A), a regulator of SNARE-mediated vesicle transport (Ettayebi and Hardy 2003). Exogenous expression of p48 in COS-7 cells, a monkey fibroblast cell line, disturbs intracellular trafficking pathways. Two HCV non-structural proteins, NS5A, a trans-activator, and NS5B, the viral RNA-dependent RNA polymerase, interact with the SNARE protein vesicle-associated membrane

protein-associated protein of 33kDa (VAP-33) (Tu et al. 1999). It has been suggested that this interaction may serve to anchor these viral proteins at the membrane sites of the HCV RNA replication complex. A member of the cowpea mosaic virus (CPMV), RNA1-encoded 60kDa nucleotide-binding protein (60k), interacts with two SNARE-like proteins, VP27-1 and VP27-2, which are considered homologs of animal VAP-33 (Carette et al. 2002). The 60k protein is thought to induce membrane rearrangements during CPMV viral RNA replication and it is possible that VP27-1 and VP27-2 aid in this function. The expression of the SNARE protein NAPA, which is involved in vesicle transport between the ER and the Golgi, is affected by Epstein-Barr virus (EBV) latent membrane protein 1 (LMP1) (Wu et al. 2011). LMP1 increases levels of the NF-κB subunit p50, which increases binding of p50 homodimers on the *NAPA* promoter and thereby blocking expression from the NAPA promoter.

Both GP5 and M proteins are important in PRRSV virion assembly as viral genomes lacking either of the genes encoding these proteins do not release functional virus particles (Wissink et al. 2005). It was further shown that individually GP5 and M are targeted to the endoplasmic reticulum, however together they localizes to the Golgi. In the current experiment we determined that both PRRSV GP5 and M interact with the host cellular membrane fusion protein snapin. We utilized RNAi technology to specifically knock-down snapin expression during the course of PRRSV *in vitro* infection on the PRRSV permissive cell line MARC-145. The decrease in both mRNA and protein expression of the PRRSV nucleocapsid protein, N, which is commonly used as an indicator of PRRSV replication, in

MARC-145 cells transfected with the snapin specific siRNA, suggests the interaction GP5/M and snapin is critical for productive PRRSV infection. Based on snapin's involvement in intracellular membrane fusion, its localization to both the ER and Golgi, sites of GP5 and M localization, along with the fact that is thought that PRRSV is transported through these organelles to obtain its envelope, is an indicator that the GP5/M/snapin interaction is likely an important part of the intracellular transport of PRRSV. In the future it will be interesting to see if the interactions between the major envelope proteins with snapin or other members of the SNARE complex are conserved between arteriviruses and/or coronaviruses or if this is a PRRSV specific mechanism.

Table 3.1. Snapin-specific siRNA sequences.

siRNA 17	UAGCUAGGUUGUCAAUUUG
siRNA 45	AAUCCAGCAUUGCCCUCCU
siRNA 156	GCUCCGGGAACAAAUUGACUU
siRNA 368	UGCUGGAUUCGGGAAUUUAUU

Underlined bases are dinucleotide 3′ overhangs

Table 3.2. Effect of pre-snapin-specific siRNA transfection* on PRRSV titers at 48 hpi.

	MOI 0.1	**MOI 1**	**MOI 5**
	TCID50	TCID50	TCID50
siRNA 368	$10^{1.7}$ ±1.99**	$10^{3.6}$ ± 2.27**	$10^{6.9}$ ± 1.69**
Neg. Con	$10^{2.5}$ ± 1.38	$10^{4.3}$ ± 1.63	$10^{7.5}$ ± 1.98

*The siRNA was transfected (in triplicate) into MARC-145 cells for 24 h prior to PRRSV infection.

**Significant difference in PRRSV compared to MARC-145 cells transfected with a negative control siRNA, $p<0.05$. Values are given as the mean$TCID_{50}$ of three replicates ± S.D.

Table 3.3. Effect of post-snapin-specific siRNA transfection* on PRRSV titers at 48 hpi.

	MOI 0.1	**MOI 1**	**MOI 5**
	TCID50	TCID50	TCID 50
siRNA 368	10^{2} ± 2.15	$10^{3.2}$ ± 2.26**	$10^{5.5}$ ± 2.31**
Neg. Con	$10^{2.1}$ ± 1.76	$10^{4.6}$ ± 1.67	$10^{6.2}$ ± 2.06

* MARC-145 were infected (in triplicate) with PRRSV for 12 h prior to transfection of siRNA

**Significant difference in PRRSV compared to MARC-145 cells transfected with a negative control siRNA, $p<0.05$. Values are given as the mean$TCID_{50}$ of three replicates ± S.D.

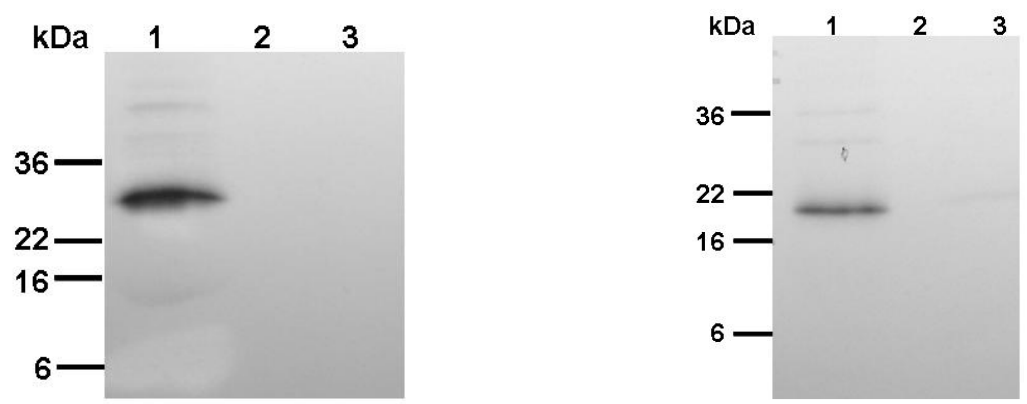

Figure 3.1. Exogenous expression of PRRSV GP5 and M his-tag fusion proteins in MARC-145 cells.
MARC-145 cells were transfected with either pCDNA3-GP5-his or pCDNA3-M-his. At 72 hours post transfection his-tag fusion proteins were purified with nickel beads. A. GP5-his fusion protein purification. Lane 1: GP5-his bound beads, Lane 2: flow through, Lane3: untransfected MARC-145 lysate. B. M-his fusion protein purification. Lane 1: M-his bound beads, Lane 2: flow through, Lane3: untransfected MARC-145 lysate. Mouse-anti-his tag antibodies were used at a dilution of 1:1500 and incubated at room temperature for 1.5 hours, goat-anti-mouse HRP conjugated antibodies were used at a dilution of 1:1500 and incubated at room temperature for 1.5 hours. Blots were developed using ECL substrate.

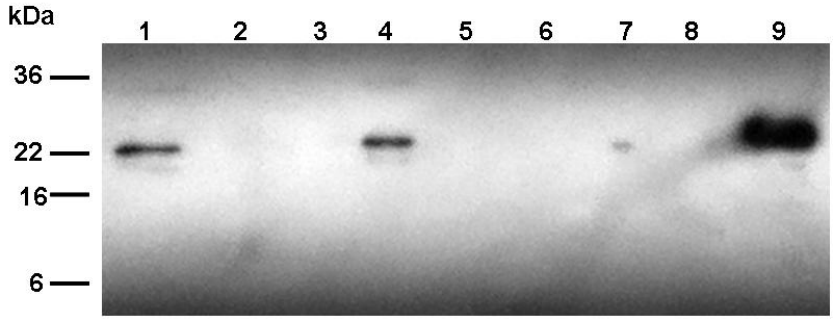

Figure 3.2. Co-purification of the cellular protein snapin with PRRSV GP5 and M his fusion proteins expressed in MARC-145 cells.
MARC-145 cells were transfected with either pCDNA3-GP5-his or pCDNA3-M-his. At 72 hours post transfection cells were lysed and mixed with nickel beads for the purification of the his fusion proteins and their interacting partners. Rabbit-anti-snapin antibodies were used at a 1:500 dilution overnight and goat-anti-mouse HRP conjugated antibodies were used at 1:1500 for 1.5 hours. Blots were developed using ECL substrate. Lanes: 1. GP5-his beads, 2. flow through from GP5-his lysate, 3. empty, 4, M-his beads, 5. flow through from M-his lysate, 6. empty, 7. MARC-145 cell lysate, 8. empty, 9. purified snapin protein (used in antibody production).

Figure 3.3. Effect of pre-transfection of snapin-specific siRNA on snapin and N mRNA expression in MARC-145 cells infected with PRRSV at M.O.I. of 0.1.
Either a snapin-specific siRNA or a negative control siRNA were transfected into MARC-145 cells for 24 h. The cells were then either mock infected or infected with PRRSV VR-2332 at an MOI of 0.1. RNA was collected at 12 hpi, 24 hpi, and 48 hpi and used for RT-PCR quantification. Tranfections were performed in triplicate. All expression values were normalized to β-actin expression. Expression is given as snapin expression relative to time-matched mock-infected cells transfected with the negative control siRNA. Relative N expression is given as N expression relative to VR-2332 infected time-matched transfected with the negative inhibitor. *$p<0.05$, **$p<.01$

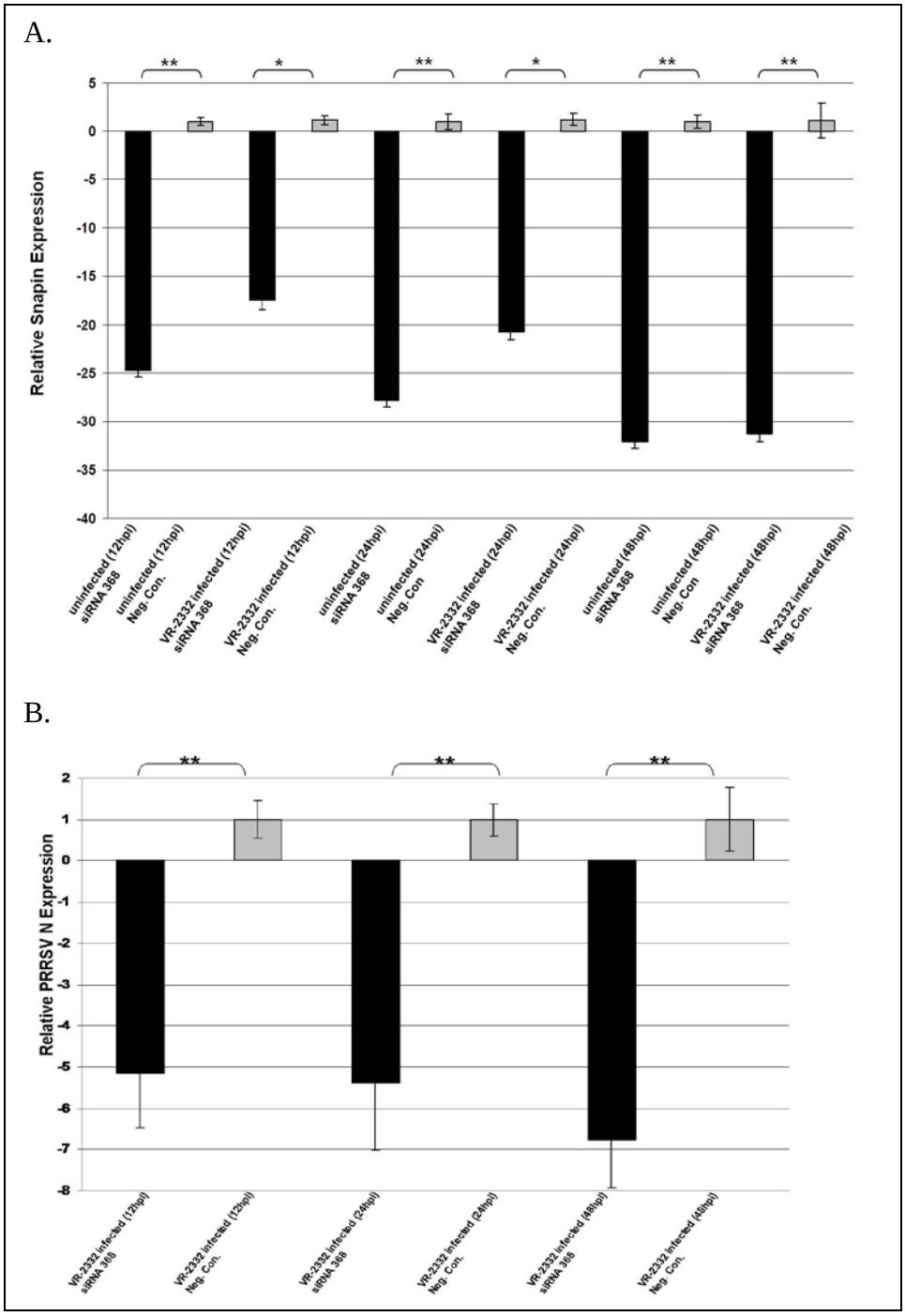
A.
Relative Snapin Expression
5
0
-5
-10
-15
-20
-25
-30
-35
-40
**
*
**
*
**
**
uninfected (12hpi) siRNA 368
uninfected (12hpi) Neg. Con.
VR-2332 infected (12hpi) siRNA 368
VR-2332 infected (12hpi) Neg. Con.
uninfected (24hpi) siRNA 368
uninfected (24hpi) Neg. Con
VR-2332 infected (24hpi) siRNA 368
VR-2332 infected (24hpi) Neg. Con.
uninfected (48hpi) siRNA 368
uninfected (48hpi) Neg. Con
VR-2332 infected (48hpi) siRNA 368
VR-2332 infected (48hpi) Neg. Con.
B.
Relative PRRSV N Expression
2
1
0
-1
-2
-3
-4
-5
-6
-7
-8
**
**
**
VR-2332 infected (12hpi) siRNA 368
VR-2332 infected (12hpi) Neg. Con.
VR-2332 infected (24hpi) siRNA 368
VR-2332 infected (24hpi) Neg. Con.
VR-2332 infected (48hpi) siRNA 368
VR-2332 infected (48hpi) Neg. Con.

Figure 3.4. Effect of pre-transfection of a snapin-specific siRNA on snapin and N mRNA expression in MARC-145 cells infected with PRRSV at M.O.I. of 1.
Either a snapin-specific siRNA or a negative control siRNA were transfected into MARC-145 cells for 24 h. The cells were then either mock infected or infected with PRRSV VR-2332 at an MOI of 1. RNA was collected at 12 hpi, 24 hpi, and 48 hpi and used for RT-PCR quantification. Tranfections were performed in triplicate. All expression values were normalized to β-actin expression. Expression is given as snapin expression relative to time-matched mock-infected cells transfected with the negative control siRNA. Relative N expression is given as N expression relative to VR-2332 infected time-matched transfected with the negative inhibitor. *$p<0.05$, **$p<.01$

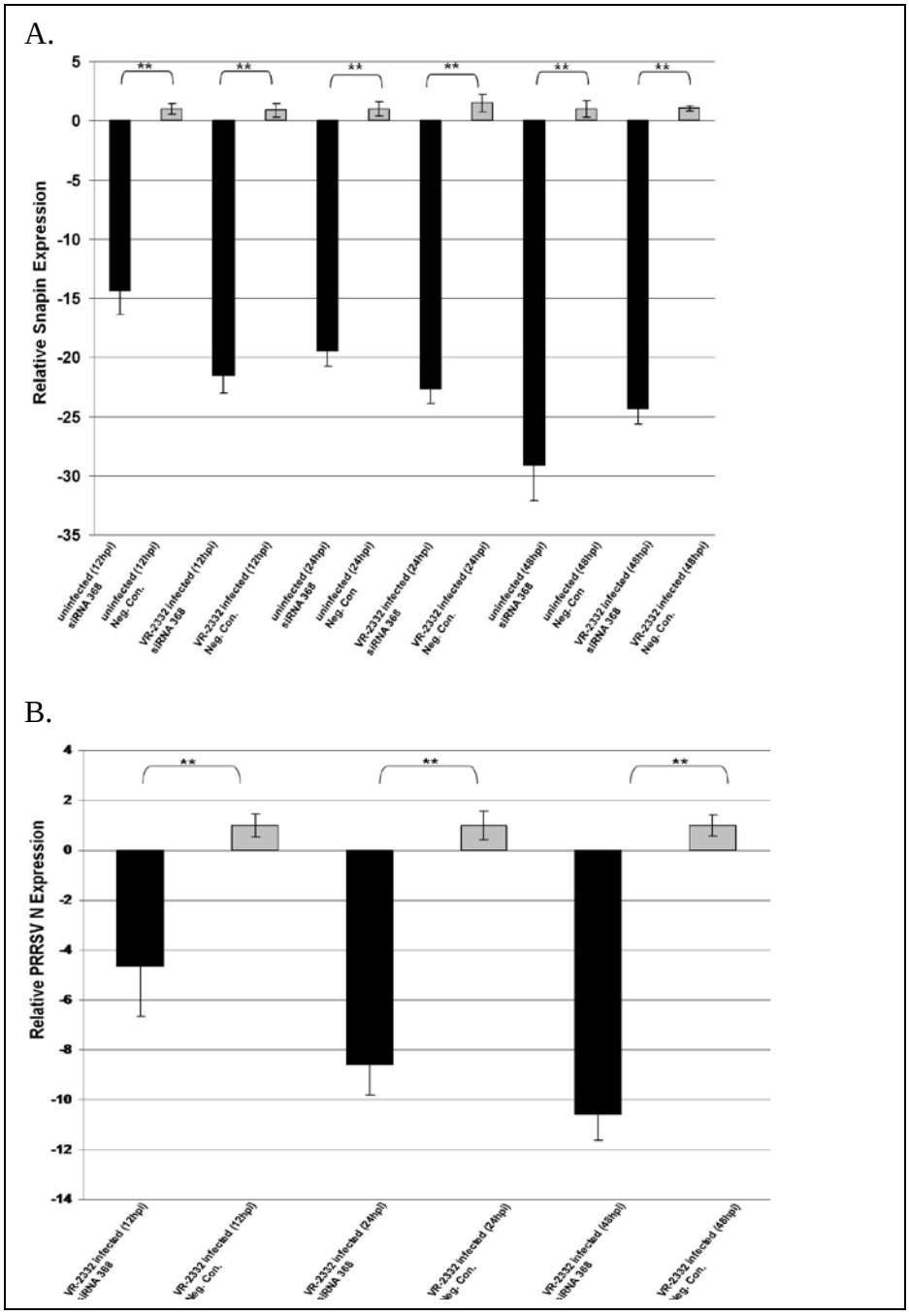
A.
Relative Snapin Expression
5
0
-5
-10
-15
-20
-25
-30
-35
**
uninfected (12hpi) siRNA 388
uninfected (12hpi) Neg. Con.
VR-2332 infected (12hpi) siRNA 388
VR-2332 infected (12hpi) Neg. Con.
uninfected (24hpi) siRNA 388
uninfected (24hpi) Neg. Con
VR-2332 infected (24hpi) siRNA 388
VR-2332 infected (24hpi) Neg. Con.
uninfected (48hpi) siRNA 388
uninfected (48hpi) Neg. Con
VR-2332 infected (48hpi) siRNA 388
VR-2332 infected (48hpi) Neg. Con.
B.
Relative PRRSV N Expression
4
2
0
-2
-4
-6
-8
-10
-12
-14
**
VR-2332 infected (12hpi) siRNA 388
VR-2332 infected (12hpi) Neg. Con.
VR-2332 infected (24hpi) siRNA 388
VR-2332 infected (24hpi) Neg. Con.
VR-2332 infected (48hpi) siRNA 388
VR-2332 infected (48hpi) Neg. Con.

Figure 3.5. Effect of pre-transfection of a snapin-specific siRNA on snapin and N mRNA expression in MARC-145 cells infected with PRRSV at M.O.I. of 5.
Either a snapin-specific siRNA or a negative control siRNA were transfected into MARC-145 cells for 24 h. The cells were then either mock infected or infected with PRRSV VR-2332 at an MOI of 5. RNA was collected at 12 hpi, 24 hpi, and 48 hpi and used for RT-PCR quantification. Tranfections were performed in triplicate. All expression values were normalized to β-actin expression. Expression is given as snapin expression relative to time-matched mock-infected cells transfected with the negative control siRNA. Relative N expression is given as N expression relative to VR-2332 infected time-matched transfected with the negative inhibitor. *$p<0.05$, **$p<.01$

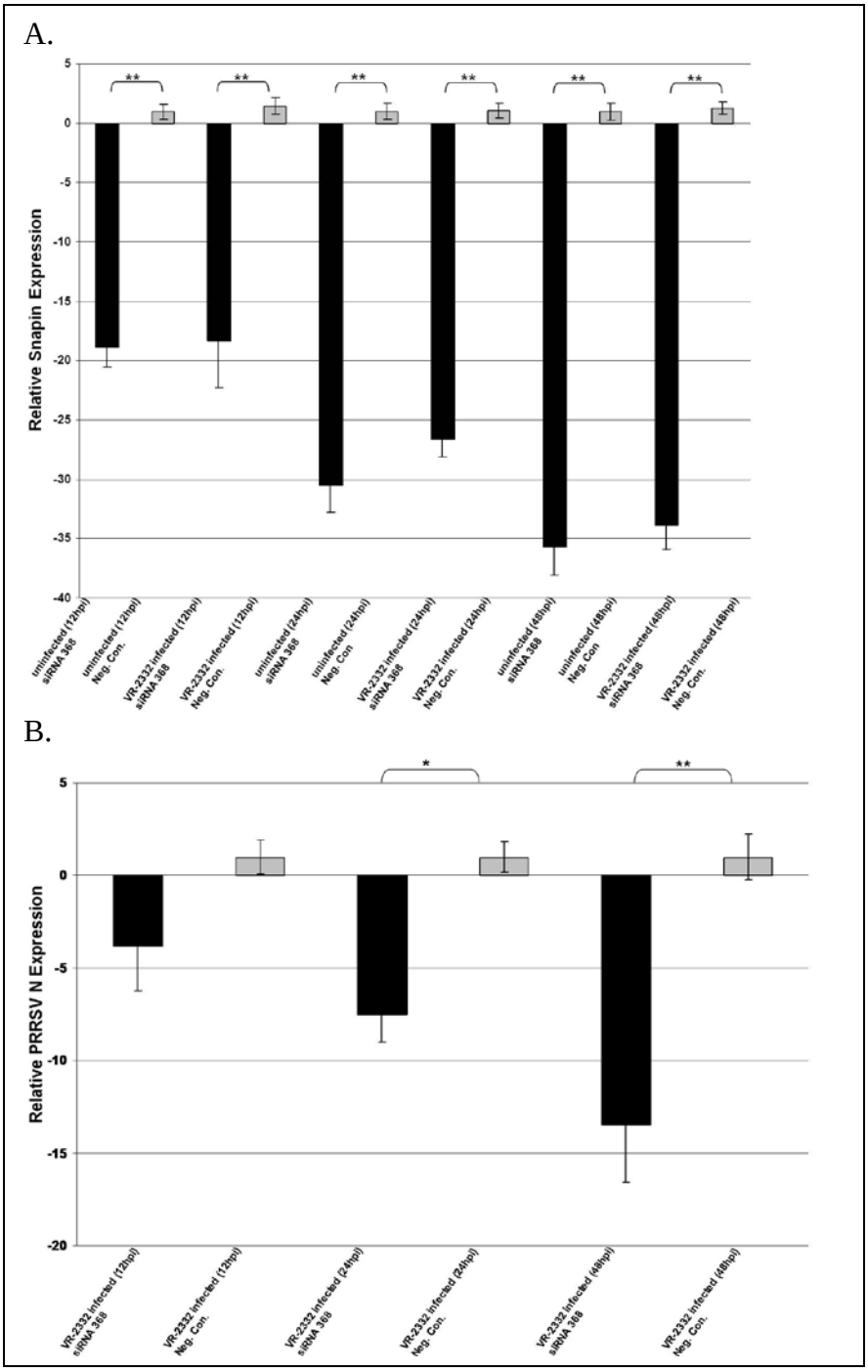
A.
Relative Snapin Expression
5
0
-5
-10
-15
-20
-25
-30
-35
-40
**
**
**
**
**
**
uninfected (12hpi) siRNA 368
uninfected (12hpi) Neg. Con.
VR-2332 infected (12hpi) siRNA 368
VR-2332 infected (12hpi) Neg. Con.
uninfected (24hpi) siRNA 368
uninfected (24hpi) Neg. Con.
VR-2332 infected (24hpi) siRNA 368
VR-2332 infected (24hpi) Neg. Con.
uninfected (48hpi) siRNA 368
uninfected (48hpi) Neg. Con.
VR-2332 infected (48hpi) siRNA 368
VR-2332 infected (48hpi) Neg. Con.
B.
Relative PRRSV N Expression
5
0
-5
-10
-15
-20
*
**
VR-2332 infected (12hpi) siRNA 368
VR-2332 infected (12hpi) Neg. Con.
VR-2332 infected (24hpi) siRNA 368
VR-2332 infected (24hpi) Neg. Con.
VR-2332 infected (48hpi) siRNA 368
VR-2332 infected (48hpi) Neg. Con.

Figure 3.6. Effect of post-transfection of a snapin-specific siRNA on snapin and N mRNA expression in MARC-145 cells infected with PRRSV at M.O.I. of 0.1.
Marc-145 cells were either mock infected or infected with VR-2332 at an MOI of 0.1 for 12 h. Then either a snapin-specific siRNA or a negative control siRNA were transfected into the cells. RNA was collected at 12 hpt (hours post transfection), 24 hpt, and 48 hpt and used for RT-PCR quantification. Tranfections were performed in triplicate. All expression values were normalized to β-actin expression. Expression is given as snapin expression relative to time-matched mock-infected cells transfected with the negative control siRNA. Relative N expression is given as N expression relative to VR-2332 infected time-matched transfected with the negative inhibitor. *$p<0.05$, **$p<.01$.

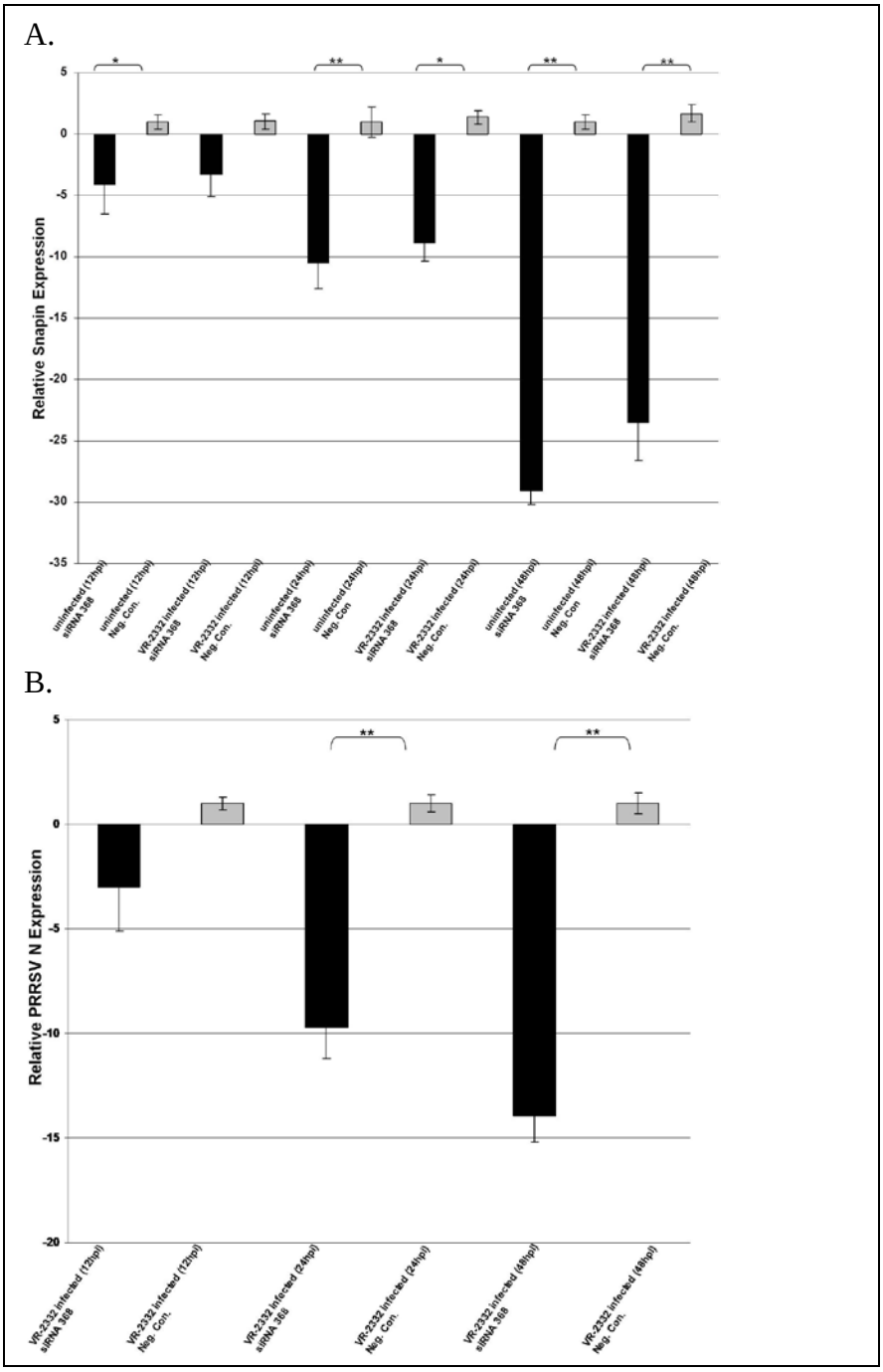
A.
Relative Snapin Expression
5
0
-5
-10
-15
-20
-25
-30
-35
*
**
*
**
**
uninfected (12hpi) siRNA 368
uninfected (12hpi) Neg. Con.
VR-2332 infected (12hpi) siRNA 368
VR-2332 infected (12hpi) Neg. Con.
uninfected (24hpi) siRNA 368
uninfected (24hpi) Neg. Con
VR-2332 infected (24hpi) siRNA 368
VR-2332 infected (24hpi) Neg. Con.
uninfected (48hpi) siRNA 368
uninfected (48hpi) Neg. Con
VR-2332 infected (48hpi) siRNA 368
VR-2332 infected (48hpi) Neg. Con.
B.
Relative PRRSV N Expression
5
0
-5
-10
-15
-20
**
**
VR-2332 infected (12hpi) siRNA 368
VR-2332 infected (12hpi) Neg. Con.
VR-2332 infected (24hpi) siRNA 368
VR-2332 infected (24hpi) Neg. Con.
VR-2332 infected (48hpi) siRNA 368
VR-2332 infected (48hpi) Neg. Con.

Figure 3.7. Effect of post-transfection of a snapin-specific siRNA on snapin and N mRNA expression in MARC-145 cells infected with PRRSV at M.O.I. of 1.
Marc-145 cells were either mock infected or infected with VR-2332 at an MOI of 1 for 12 h. Then either a snapin-specific siRNA or a negative control siRNA were transfected into the cells. RNA was collected at 12 hpt (hours post transfection), 24 hpt, and 48 hpt and used for RT-PCR quantification. Tranfections were performed in triplicate. All expression values were normalized to β-actin expression. Expression is given as snapin expression relative to time-matched mock-infected cells transfected with the negative control siRNA. Relative N expression is given as N expression relative to VR-2332 infected time-matched transfected with the negative inhibitor. *$p<0.05$, **$p<.01$.

A.

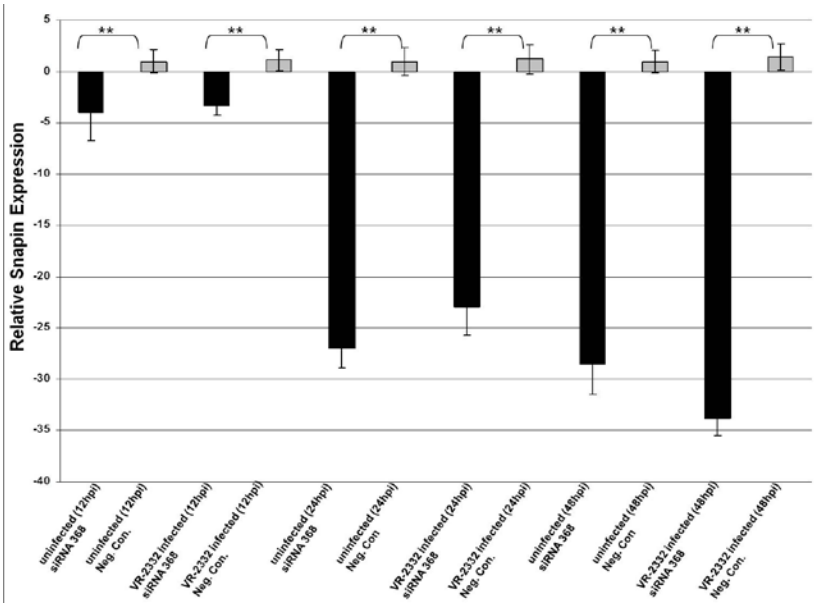
Relative Snapin Expression
5
0
-5
-10
-15
-20
-25
-30
-35
-40
**
uninfected (12hpi) siRNA 368
uninfected (12hpi) Neg. Con.
VR-2332 infected (12hpi) siRNA 368
VR-2332 infected (12hpi) Neg. Con.
uninfected (24hpi) siRNA 368
uninfected (24hpi) Neg. Con
VR-2332 infected (24hpi) siRNA 368
VR-2332 infected (24hpi) Neg. Con.
uninfected (48hpi) siRNA 368
uninfected (48hpi) Neg. Con
VR-2332 infected (48hpi) siRNA 368
VR-2332 infected (48hpi) Neg. Con.

B.

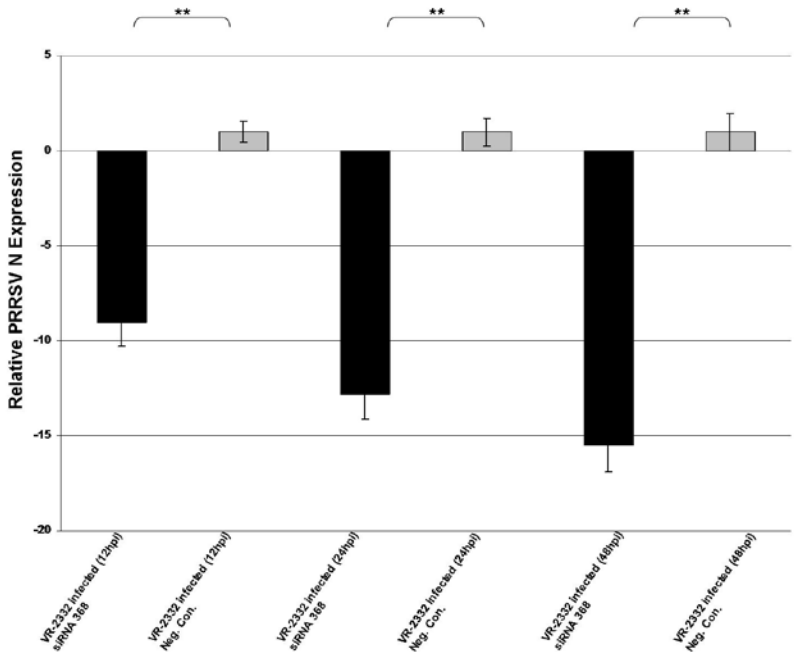
Relative PRRSV N Expression
5
0
-5
-10
-15
-20
**
VR-2332 infected (12hpi) siRNA 368
VR-2332 infected (12hpi) Neg. Con.
VR-2332 infected (24hpi) siRNA 368
VR-2332 infected (24hpi) Neg. Con.
VR-2332 infected (48hpi) siRNA 368
VR-2332 infected (48hpi) Neg. Con.

Figure 3.8. Effect of post-transfection a snapin-specific siRNA on snapin and N mRNA expression in MARC-145 cells infected with PRRSV at M.O.I. of 5.
Marc-145 cells were either mock infected or infected with VR-2332 at an MOI of 5 for 12 h. Then either a snapin-specific siRNA or a negative control siRNA were transfected into the cells. RNA was collected at 12 hpt (hours post transfection), 24 hpt, and 48 hpt and used for RT-PCR quantification. Tranfections were performed in triplicate. All expression values were normalized to β-actin expression. Expression is given as snapin expression relative to time-matched mock-infected cells transfected with the negative control siRNA. Relative N expression is given as N expression relative to VR-2332 infected time-matched transfected with the negative inhibitor. *$p<0.05$, **$p<.01$.

A.

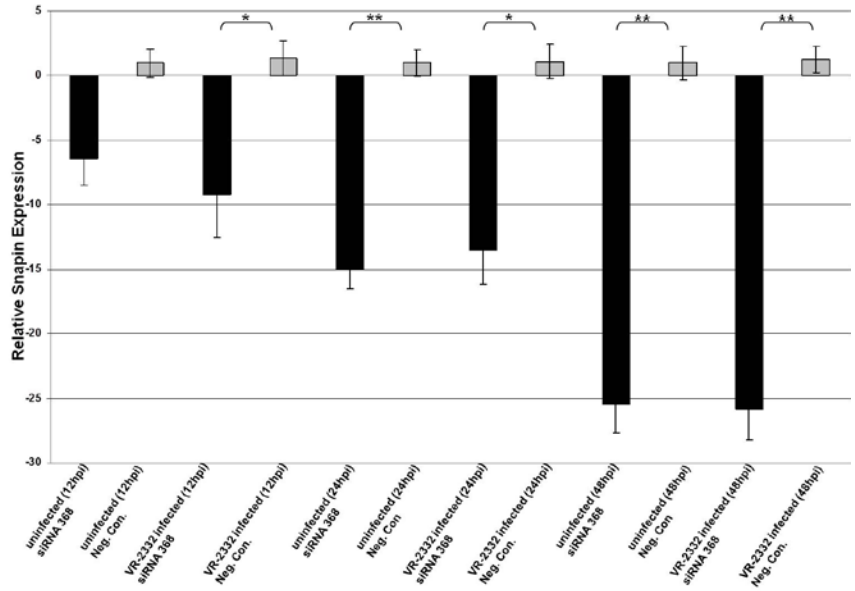
Relative Snapin Expression
5
0
-5
-10
-15
-20
-25
-30
*
**
*
**
**
uninfected (12hpi) siRNA 368
uninfected (12hpi) Neg. Con.
VR-2332 infected (12hpi) siRNA 368
VR-2332 infected (12hpi) Neg. Con.
uninfected (24hpi) siRNA 368
uninfected (24hpi) Neg Con
VR-2332 infected (24hpi) siRNA 368
VR-2332 infected (24hpi) Neg. Con.
uninfected (48hpi) siRNA 368
uninfected (48hpi) Neg. Con
VR-2332 infected (48hpi) siRNA 368
VR-2332 infected (48hpi) Neg. Con.

B.

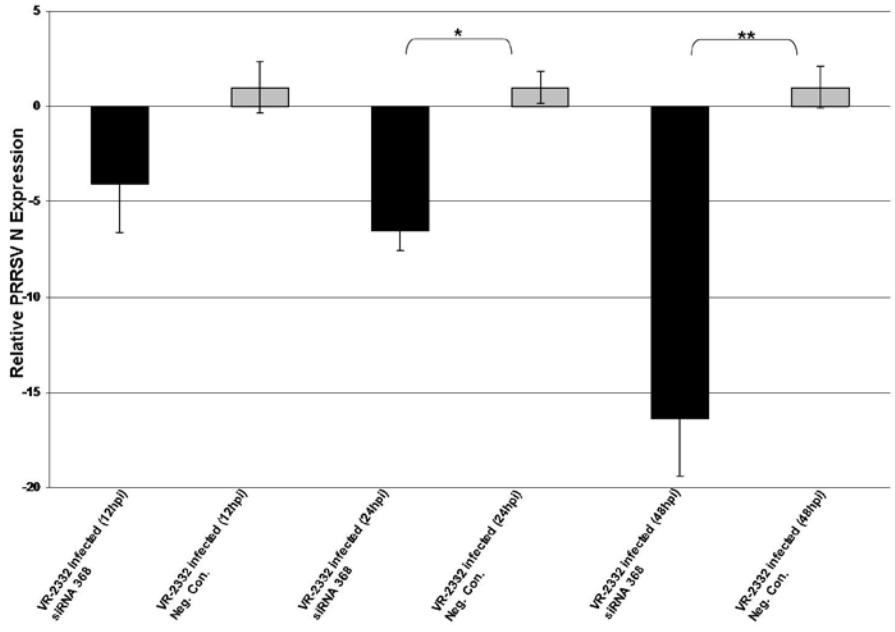
Relative PRRSV N Expression
5
0
-5
-10
-15
-20
*
**
VR-2332 Infected (12hpi) siRNA 368
VR-2332 infected (12hpi) Neg. Con.
VR-2332 infected (24hpi) siRNA 368
VR-2332 infected (24hpi) Neg. Con.
VR-2332 infected (48hpi) siRNA 368
VR-2332 infected (48hpi) Neg. Con.

Figure 3.9. Effect of pre-transfection of a snapin-specific siRNA on snapin and N protein expression in MARC-145 cells infected with PRRSV.
Either a snapin-specific siRNA or a negative control siRNA were transfected into MARC-145 cells for 24 h. The cells were then either mock infected or infected with PRRSV VR-2332. Protein was collected at 12 hpi, 24 hpi, and 48 hpi and used for western blotting. Tranfections were performed in triplicate. Representative blots from each experimental group are shown. GAPDH was used as a loading control. Panel A: Detection of snapin protein expression in cells transfected with either a snapin specific control or a negative control siRNA. 1: mock infected MARC-145 cells transfected with the snapin specific inhibitor, 2: PRRSV VR-2332 infected MARC-145 cells infected with a snapin specific inhibitor, 3: mock infected MARC-145 cells transfected with a negative control siRNA, 4: PRRSV VR-2332 infected MARC-145 cells transfected with a negative control siRNA. Panel B: Detection of PRRSV N protein expression in cells transfected with either a snapin specific control or a negative control siRNA. 5: MARC-145 cells transfected with a snapin specific siRNA inhibitor and infected with VR-2332 for 12 h, 6: MARC-145 cells transfected with a snapin specific siRNA inhibitor and infected with VR-2332 for 24 h, 7: : MARC-145 cells transfected with a snapin specific siRNA inhibitor and infected with VR-2332 for 48 h, 8: MARC-145 cells transfected with a negative control siRNA and infected with VR-2332 for 12 h, 9: MARC-145 cells transfected with a negative control siRNA and infected with VR-2332 for 24 h, 10: MARC-145 cells transfected with a negative control siRNA and infected with VR-2332 for 48 h.

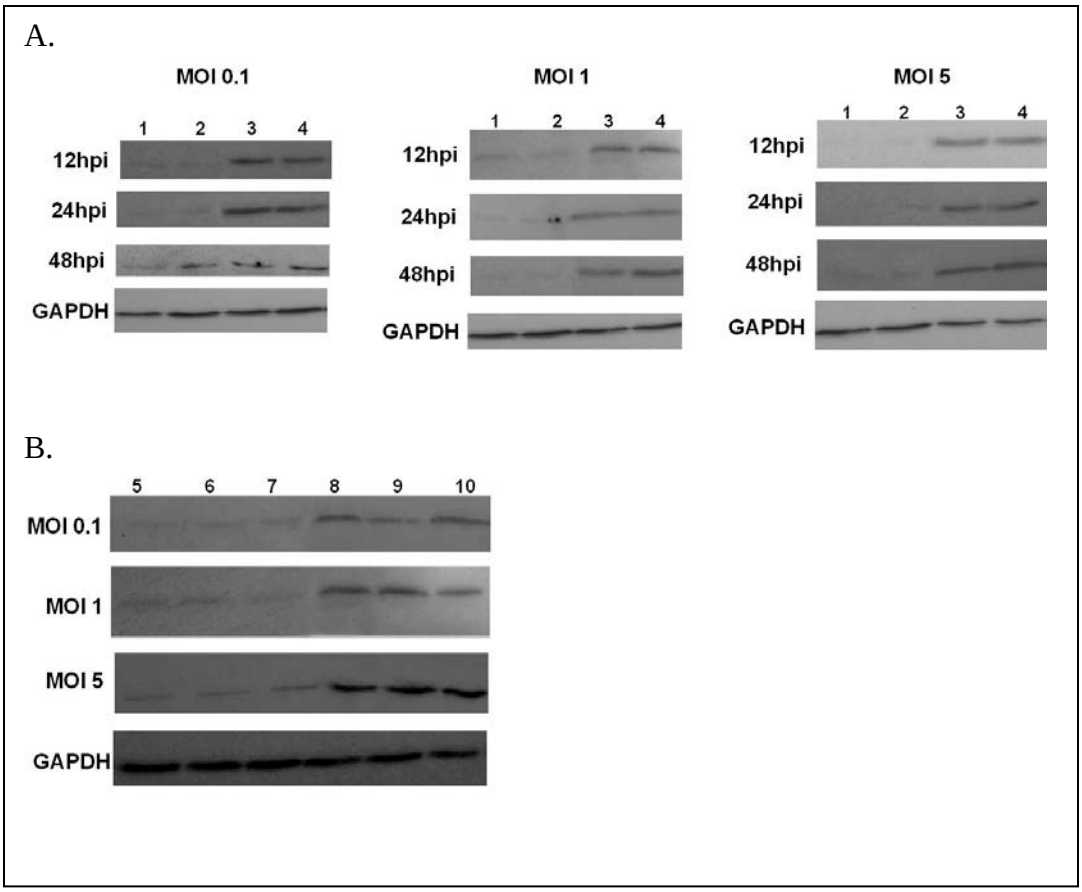
A.
MOI 0.1
MOI 1
MOI 5
1 2 3 4
12hpi
24hpi
48hpi
GAPDH
B.
5 6 7 8 9 10
MOI 0.1
MOI 1
MOI 5
GAPDH

Figure 3.10. Effect of post-transfection of a snapin-specific siRNA on snapin and N protein expression in MARC-145 cells infected with PRRSV.
Marc-145 cells were either mock infected or infected with VR-2332 for 12 h. Then either a snapin-specific siRNA or a negative control siRNA were transfected into the cells. Protein was collected at 12 hpt, 24 hpt, and 48 hpt and used for western blotting. Tranfections were performed in triplicate. Representative blots from each experimental group are shown. GAPDH was used as a loading control. Panel A: Detection of snapin protein expression in cells transfected with either a snapin specific control or a negative control siRNA. 1: mock infected MARC-145 cells transfected with the snapin specific inhibitor, 2: PRRSV VR-2332 infected MARC-145 cells infected with a snapin specific inhibitor, 3: mock infected MARC-145 cells transfected with a negative control siRNA, 4: PRRSV VR-2332 infected MARC-145 cells transfected with a negative control siRNA. Panel B: Detection of PRRSV N protein expression in cells transfected with either a snapin specific control or a negative control siRNA. 5: MARC-145 cells transfected with a snapin specific siRNA inhibitor and infected with VR-2332 for 12 h, 6: MARC-145 cells transfected with a snapin specific siRNA inhibitor and infected with VR-2332 for 24 h, 7: : MARC-145 cells transfected with a snapin specific siRNA inhibitor and infected with VR-2332 for 48 h, 8: MARC-145 cells transfected with a negative control siRNA and infected with VR-2332 for 12 h, 9: MARC-145 cells transfected with a negative control siRNA and infected with VR-2332 for 24 h, 10: MARC-145 cells transfected with a negative control siRNA and infected with VR-2332 for 48 h.

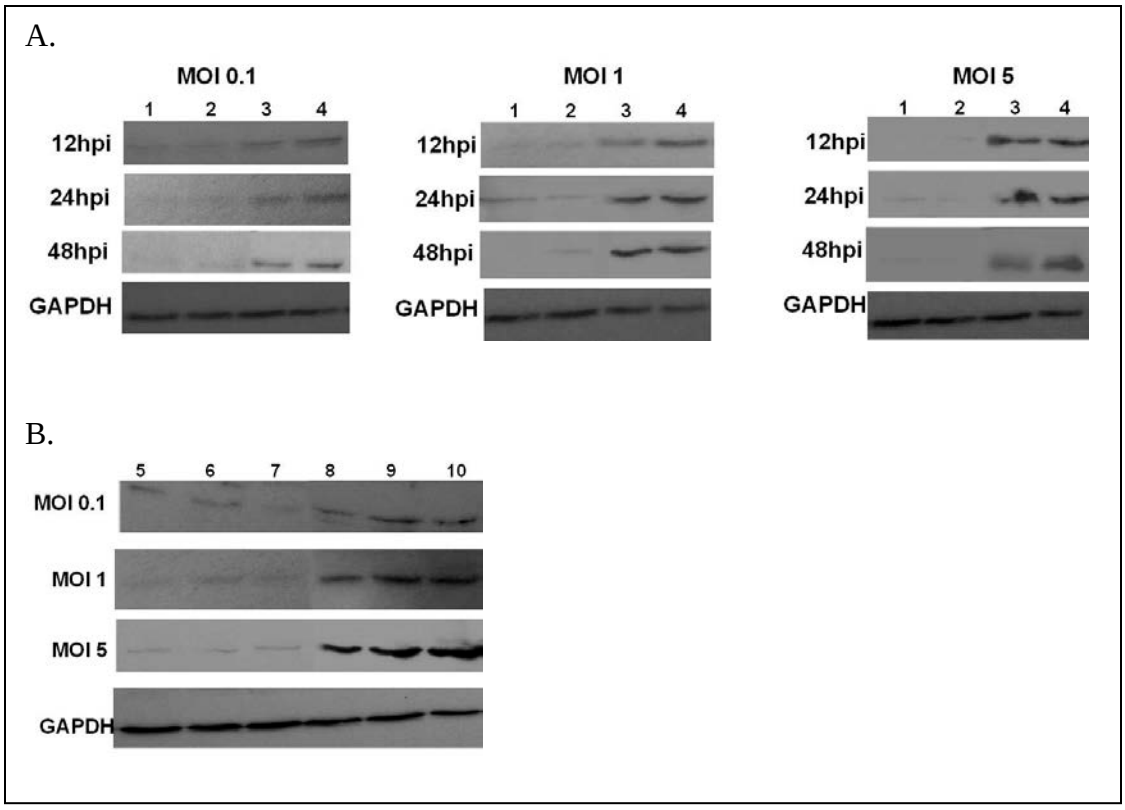
A.
MOI 0.1
MOI 1
MOI 5
1 2 3 4
12hpi
24hpi
48hpi
GAPDH
B.
5 6 7 8 9 10
MOI 0.1
MOI 1
MOI 5
GAPDH

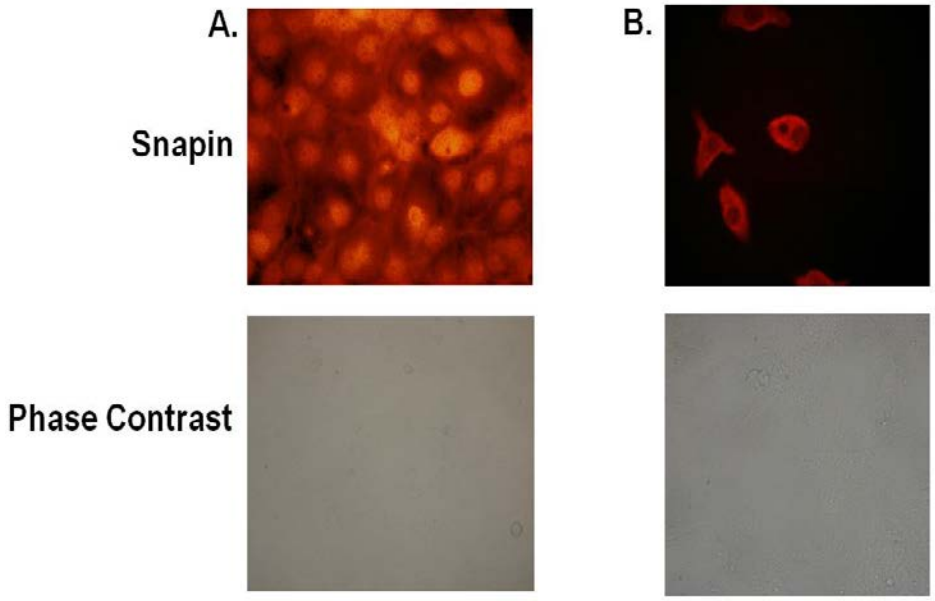

Figure 3.11. Confirmation of reduced snapin expression in MARC-145 cells tranfected with a snapin specific siRNA.
Marc-145 cells were transfected with either a snapin specific siRNA or a negative control siRNA. Cells were fixed used immunofluorescence detection of snapin expression. Panel A: MARC-145 cells were transfected with a negative control siRNA. Panel B: MARC-145 cells were transfected with the snapin-specific siRNA, siRNA 368.

References

Bhattacharya B, Roy P.Bluetongue virus outer capsid protein VP5 interacts with membrane lipid rafts via a SNARE domain. J Virol. 2008 82(21):10600-12.

Buxton P, Zhang XM, Walsh B, Sriratana A, Schenberg I, Manickam E, Rowe T. 2003. Identification and characterization of Snapin as a ubiquitously expressed SNARE-binding protein that interacts with SNAP23 in non-neuronal cells.Biochem J. 375(Pt 2):433-40.

Calvert JG, Slade DE, Shields SL, Jolie R, Mannan RM, Ankenbauer RG, Welch SK.CD163 expression confers susceptibility to porcine reproductive and respiratory syndrome viruses. J Virol. 2007 81(14):7371-9.

Carette JE, Verver J, Martens J, van Kampen T, Wellink J, van Kammen A.Characterization of plant proteins that interact with cowpea mosaic virus '60K' protein in the yeast two-hybrid system.
J Gen Virol. 2002 83(Pt 4):885-93.

Cepeda V, Fraile-Ramos A.A role for the SNARE protein syntaxin 3 in human cytomegalovirus morphogenesis. Cell Microbiol. 2011 13(6):846-58.

Chen M, Lucas KG, Akum BF, Balasingam G, Stawicki TM, Provost JM, Riefler GM, Jörnsten RJ, Firestein BL.A novel role for snapin in dendrite patterning: interaction with cypin. Mol Biol Cell. 2005 16(11):5103-14.

Coller KE, Heaton NS, Berger KL, Cooper JD, Saunders JL, Randall G.Molecular determinants and dynamics of hepatitis C virus secretion. PLoS Pathog. 2012 8(1):e1002466.

Cui HL, Grant A, Mukhamedova N, Pushkarsky T, Jennelle L, Dubrovsky L, Gaus K, Fitzgerald ML, Sviridov D, Bukrinsky M.HIV-1
Nef mobilizes lipid rafts in macrophages through a pathway that competes with ABCA1-dependent cholesterol efflux. J Lipid Res. 2012 53(4):696-708.

Cureton DK, Burdeinick-Kerr R, Whelan SP.Genetic inactivation of COPI coatomer separately inhibits vesicular stomatitis virus entry and gene expression. J Virol. 2012 86(2):655-66.

Das PB, Dinh PX, Ansari IH, de Lima M, Osorio FA, Pattnaik AK.The minor envelope glycoproteins GP2a and GP4 of porcine reproductive and respiratory syndrome virus interact with the receptor CD163.J Virol. 2010 84(4):1731-40.

Delputte PL, Nauwynck HJ.Porcine arterivirus infection of alveolar macrophages is mediated by sialic acid on the virus. J Virol. 2004 78(15):8094-101.
Donald JE, Zhang Y, Fiorin G, Carnevale V, Slochower DR, Gai F, Klein ML, DeGrado WF.Transmembrane orientation and possible role of the fusogenic peptide from parainfluenza virus 5 (PIV5) in promoting fusion. Proc Natl Acad Sci U S A. 2011 Mar 8;108(10):3958-63.

Dobbe JC, van der Meer Y, Spaan WJ, Snijder EJ. Construction of chimeric arteriviruses reveals that the ectodomain of the major glycoprotein is not the main determinant of equine arteritis virus tropism in cell culture.Virology. 2001 288(2):283-94.

Du Y, Qi J, Lu Y, Wu J, Yoo D, Liu X, Zhang X, Li J, Sun W, Cong X, Shi J, Wang J.Evaluation of a DNA vaccine candidate co-expressing GP3 and GP5 of porcine reproductive and respiratory syndrome virus (PRRSV) with interferon α/γ in immediate and long-lasting protection against HP-PRRSV challenge.Virus Genes. 2012 Epub ahead of print

Elbashir SM, Harborth J, Lendeckel W, Yalcin A, Weber K, Tuschl T.Duplexes of 21-nucleotide RNAs mediate RNA interference in cultured mammalian cells. Nature. 2001a 411(6836):494-8.

Elbashir SM, Lendeckel W, Tuschl T.RNA interference is mediated by 21- and 22-nucleotide RNAs. Genes Dev. 2001b 15(2):188-200.

Elbashir SM, Harborth J, Weber K, Tuschl T.Analysis of gene function in somatic mammalian cells using small interfering RNAs. Methods. 2002 26(2):199-213.

Ettayebi K, Hardy ME.Norwalk virus nonstructural protein p48 forms a complex with the SNARE regulator VAP-A and prevents cell surface expression of vesicular stomatitis virus G protein. J Virol. 2003 77(21):11790-7.

Fryrear KA, Guo X, Kerscher O, Semmes OJ.The Sumo-targeted ubiquitin ligase RNF4 regulates the localization and function of the HTLV-1 oncoprotein Tax. Blood. 2012 119(5):1173-81.

Garg H, Joshi A. SNAREs in HIV-1 assembly. Commun Integr Biol. 2012 5(2):172-4.

Kim JK, Fahad AM, Shanmukhappa K, Kapil S.Defining the cellular target(s) of porcine reproductive and respiratory syndrome virus blocking monoclonal antibody 7G10. J Virol. 2006 80(2):689-96.

Kreutz LC, Ackermann MR.Porcine reproductive and respiratory syndrome virus enters cells through a low pH-dependent endocytic pathway. Virus Res. 1996 42(1-2):137-47.

Kucharski TJ, Gamache I, Gjoerup O, Teodoro JG. DNA damage response signaling triggers nuclear localization of the chicken anemia virus protein Apoptin. J Virol. 2011 85(23):12638-49.
Laniosz V, Nguyen KC, Meneses PI. Bovine papillomavirus type 1 infection is mediated by SNARE syntaxin 18. J Virol. 2007 81(14):7435-48.

Liu ST, Sharon-Friling R, Ivanova P, Milne SB, Myers DS, Rabinowitz JD, Brown HA, Shenk T.Synaptic vesicle-like lipidome of human cytomegalovirus virions reveals a role for SNARE machinery in virion egress. Proc Natl Acad Sci U S A. 2011 2;108(31):12869-74.

Lu L, Cai Q, Tian JH, Sheng ZH.Snapin associates with late endocytic compartments and interacts with late endosomal SNAREs. Biosci Rep. 2009 29(4):261-9.

Matzke MA, Matzke AJ.Planting the seeds of a new paradigm.PLoS Biol. 2004 May;2(5):E133.

Nal B, Chan C, Kien F, Siu L, Tse J, Chu K, Kam J, Staropoli I, Crescenzo-Chaigne B, Escriou N, van der Werf S, Yuen KY, Altmeyer R. Differential maturation and subcellular localization of severe acute respiratory syndrome coronavirus surface proteins S, M and E. J Gen Virol. 2005 May;86(Pt 5):1423-34.

Nauwynck HJ, Duan X, Favoreel HW, Van Oostveldt P, Pensaert MB.Entry of porcine reproductive and respiratory syndrome virus into porcine alveolar macrophages via receptor-mediated endocytosis. J Gen Virol. 1999 80 (Pt 2):297-305.

Nitschke M, Korte T, Tielesch C, Ter-Avetisyan G, Tünnemann G, Cardoso MC, Veit M, Herrmann A.Equine arteritis virus is delivered to an acidic compartment of host cells via clathrin-dependent endocytosis. Virology. 2008 377(2):248-54.

Panda D, Das A, Dinh PX, Subramaniam S, Nayak D, Barrows NJ, Pearson JL, Thompson J, Kelly DL, Ladunga I, Pattnaik AK.RNAi screening reveals requirement for host cell secretory pathway in infection by diverse families of negative-strand RNA viruses. Proc Natl Acad Sci U S A. 2011 108(47):19036-41.

Reynolds A, Leake D, Boese Q, Scaringe S, Marshall WS, Khvorova A.Rational siRNA design for RNA interference. Nat Biotechnol. 2004 22(3):326-30.

Risselada HJ, Grubmüller H.How SNARE molecules mediate membrane fusion: recent insights from molecular simulations. Curr Opin Struct Biol. 2012 22(2):187-96.

Rossen JW, Bekker CP, Strous GJ, Horzinek MC, Dveksler GS, Holmes KV, Rottier PJ.A murine and a porcine coronavirus are released from opposite surfaces of the same epithelial cells. Virology. 1996 224(1):345-51.

Schwegmann-Wessels C, Bauer S, Winter C, Enjuanes L, Laude H, Herrler G.The sialic acid binding activity of the S protein facilitates infection by porcine transmissible gastroenteritis coronavirus. Virol J. 2011 8:435.
Shabalina SA, Spiridonov AN, Ogurtsov AY.Computational models with thermodynamic and composition features improve siRNA design. BMC Bioinformatics. 2006 7:65.

Stertz S, Reichelt M, Spiegel M, Kuri T, Martínez-Sobrido L, García-Sastre A, Weber F, Kochs G.The intracellular sites of early replication and budding of SARS-coronavirus.Virology. 2007 361(2):304-15.

Tian D, Wei Z, Zevenhoven-Dobbe JC, Liu R, Tong G, Snijder EJ, Yuan S.Arterivirus minor envelope proteins are a major determinant of viral tropism in cell culture. J Virol. 2012 86(7):3701-12.

Tu H, Gao L, Shi ST, Taylor DR, Yang T, Mircheff AK, Wen Y, Gorbalenya AE, Hwang SB, Lai MM.Hepatitis C virus RNA polymerase and NS5A complex with a SNARE-like protein. Virology. 1999 263(1):30-41.

Verheije MH, Welting TJ, Jansen HT, Rottier PJ, Meulenberg JJ. Chimeric arteriviruses generated by swapping of the M protein ectodomain rule out a role of this domain in viral targeting. Virology. 2002 303(2):364-73.

Vites O, Rhee JS, Schwarz M, Rosenmund C, Jahn R. 2004. Reinvestigation of the role of snapin in neurotransmitter release. J Biol Chem. 279: 26251-26256.

Wang H, Yang P, Liu K, Guo F, Zhang Y, Zhang G, Jiang C.SARS coronavirus entry into host cells through a novel clathrin- and caveolae-independent endocytic pathway. Cell Res. 2008 18(2):290-301.

Winter C, Schwegmann-Wessels C, Neumann U, Herrler G.The spike protein of infectious bronchitis virus is retained intracellularly by a tyrosine motif. J Virol. 2008 82(6):2765-71.

Wissink EH, Kroese MV, van Wijk HA, Rijsewijk FA, Meulenberg JJ, Rottier PJ. Envelope protein requirements for the assembly of infectious virions of porcine reproductive and respiratory syndrome virus. J Virol. 2005 79(19):12495-506.

Wu ZZ, Chow KP, Kuo TC, Chang YS, Chao CC.Latent membrane protein 1 of Epstein-Barr virus sensitizes cancer cells to cisplatin by enhancing NF-κB p50 homodimer formation and downregulating NAPA expression. Biochem Pharmacol. 2011 82(12):1860-72.

Yuan X, Shan Y, Zhao Z, Chen J, Cong Y.Interaction between Snapin and G-CSF receptor.Cytokine. 2006 33(4):219-25.

Zhang R, Mehla R, Chauhan A.Perturbation of host nuclear membrane component RanBP2 impairs the nuclear import of human immunodeficiency virus -1 preintegration complex (DNA). PLoS One. 2010 5(12):e15620.

Zhu H, Yu D, Zhang X.The spike protein of murine coronavirus regulates viral genome transport from the cell surface to the endoplasmic reticulum during infection. J Virol. 2009 83(20):10653-63.

Chapter Four: Discovery of differentially expressed microRNAs in Porcine Reproductive and Respiratory Syndrome virus infected alveolar macrophages

Introduction

For many years it was thought that gene regulation occurs solely at the transcription level. However, about a decade ago a new class of gene regulators was discovered that function at the post transcriptional level, small regulatory RNA. It is now known that there are many types of small regulatory RNAs, a major group of which is termed microRNA (miRNA). In 1993 the *C.elegans lin-4* gene was discovered to encode small RNAs that are complementary to sequences in the 3′UTR (3′untranslated region) of *lin-14* encoded mRNA. These small RNAs were subsequently discovered to function as suppressors of *lin-14* expression (Lee et al. 1993). This discovery provided the first example of a novel regulatory mechanism that is mediated by small, non-coding RNAs. These non-coding RNAs, termed microRNA (miRNA), comprise a class of small RNAs the majority of which are found either in the introns of protein-coding genes or in intergenic regions where they are under the control of their own promoters (reviewed in Ying and Lin 2009). However, some are found in the exons of protein coding genes. Hundreds of miRNAs have been found to be encoded in most eukaryotic genomes, and it is likely that many miRNAs have yet to be discovered. MiRNAs regulate many biological processes, such as cell proliferation and differentiation, and are particularly important in gene regulation during development (reviewed in Carthew and Sontheimer 2009). Most miRNAs are expressed in a spatio-temporal manner, suggesting that they have very specific functions.

MiRNA biogenesis is relatively well understood and has been reviewed extensively elsewhere (e.g. Winter et al. 2009). MiRNAs are initially transcribed as long primary transcripts termed primary-miRNA (pri-miRNA), which can be several kilobases long, by RNA polymerase II (Cai et al. 2004). These pri-miRNAs can consist of a single miRNA or be composed of multiple miRNA sequences. Drosha, an RNA III family endonuclease, then processes these pri-miRNAs into ~70 nucleotide-long stem loop precursor miRNAs (pre-miRNAs) (Lee et al. 2003). Exportin-5 exports the pre-miRNA into the cytoplasm (Yi et al. 2003). Dicer, also a member of the RNA III endonuclease family, cleaves the pre-miRNA hairpin to produce a double stranded miRNA duplex, which ranges in size from 19-24 nucleotides (Ketting et al. 2001). It is now thought that Dicer also contains a helicase domain, which is involved in separating the miRNA duplex to produce two single-stranded RNA molecules, the mature miRNA and its complementary star strand (which is usually degraded) (Soifer et al. 2008). One strand, the mature miRNA, is then preferentially loaded onto the RNA-induced silencing complex (RISC), which is formed by the interaction of argonaute proteins with the mature miRNA (Hammond et al. 2001). RISC is composed of multiple proteins, which includes members of the argonaute protein family, RNA binding proteins such as R2D2, TRBP and PACT, and Dicer (for review see Yang and Yuan 2009). RISC then mediates the post-transcriptional inhibition of expression of the targeted mRNA, which is either degraded or sequestered within a cytoplasmic vesicle termed a processing-body (P-body) (Behm-Ansmant et al. 2006). A recent caveat has been added to the canonical miRNA pathway. Though miRNAs most often function as suppressors of gene expression, it

appears that they can also activate gene expression under certain circumstances, including during cell cycle arrest (Vasudevan et al. 2007; Buchan and Parker 2007).

MiRNAs regulate gene expression through the recognition of miRNAs to their respective target sites. The majority of miRNA target sites lie within the 3′UTR of the targeted mRNA. Many studies have found that a partial sequence complementarity between a miRNA and its target sites is sufficient for a miRNA to knockdown the expression of its target genes. This partial complementarity, along with miRNAs' small size, makes prediction of authentic miRNA target genes difficult. Criteria have been developed to aid in predicting miRNA target sites, however, no definitive set of rules currently exist. A major determinant in miRNA targeting is prefect complementarity between the first 6-8 nucleotides of the 5′end of the miRNA and 3′ end of the mRNA target site, which is referred to as the "seed" region or "seed" match (Brenneck et al. 2005). Though a perfect seed match is found between many miRNAs and their respective target sites, it is not an absolute requirement for miRNA targeting. Study of the *C. elegans lys-6* miRNA revealed that a perfect seed match does not necessarily lead to mRNA targeting, and that having G:U wobble pairing in the seed region is not detrimental to miRNA targeting as was previously thought (Didiano and Hobert 2006). The thermodynamic stability of the miRNA:mRNA duplex, which is calculated as the free energy of the duplex, is another determining factor in miRNA targeting (Watanabe et al. 2007). The majority of miRNA target site predicting algorithms use the seed match and miRNA:mRNA duplex thermodynamic stability as the two major rules in determining target sites. Though both seed pairing and thermodynamic stability are important determinants of

miRNA target sites, other factors must also be involved, as miRNA prediction algorithms can have a false discovery rate of up to 30% (Lewis et al. 2003). It was suggested that additional factors such as sequence-dependent accessibility or protein cofactors are likely also involved in mediating miRNA targeting (Didiano and Hobert 2006). An additional requirement of many miRNA target prediction algorithms is target site conservation across multiple genomes. If a miRNA target site is evolutionarily conserved, then it is more likely to be an authentic miRNA target. Though target site conservation increases the identification of legitimate miRNA targets, it limits the ability to discover species-specific miRNA targeting, as these targets will be discarded. Almost all current miRNA target prediction algorithms focus on the 3′UTRs of potential target genes, as it is well accepted that is the location of the majority of miRNA binding sites. However, a recent report suggests miRNA binding sites may also lie within the coding regions (CDS) of targeted genes (Tay et al. 2008). It was discovered that the mouse genes *Nanog*, *Oct4*, and *Sox2* contain multiple miRNA target sites within their coding regions. The CDS of *Nanog* contains six *miR-470* and two *miR-296* binding sites, while the CDS of *Oct4* contains three *miR-470* binding sites and the *Sox2* CDS contains five *miR-134* sites. This would imply that legitimate miRNA target sites could lie in regions other than the 3′UTR and that these sites need to be taken into consideration when predicting miRNA target genes.

One major role of miRNAs is in the regulation of immune cell differentiation and the immune response (reviewed by Petrocca and Lieberman 2009). Several studies have demonstrated that miRNA-mediated gene regulation is an important part in immune cell fate

determination. It was recently shown that the miRNA *miR-146a* works in conjugation with the NF-κB related protein NFKB1 to modulate the function of both mast cells and T-cells (Rusca et al. 2012). Mast cells in which NFKB1 expression is abated do not induce *miR-146a* expression, which in turn results in prolonged mast cell survival due to the dysregulation of *miR-146a* targeted genes, including those associated with apoptosis. In T-cells it was demonstrated that NFKB1 and miR-146a work concordantly to regulate the expansion and activation of T-cells in response to TCR stimulation. *MiR-146a* has also been linked to myeloid cell development. The absence of *miR-146a* expression in mice results in increased myeloid cell proliferation (Boldin et al. 2011). During the maturation of a functional invariant of natural killer T-cells (iNKT) in the mouse thymus there is increased expression of *miR-150* (Zheng et al. 2012). In mice lacking miR-150, iNKT are unable to complete the final steps of the maturation process. The regulation of signaling by Notch1 by miR-181 was found to be an important aspect of human NK cell maturation (Cichocki et al. 2011). MiR-181a is also involved in regulating TCR signal transduction (Li et al. 2007). The miRNA miR-155 is a well characterized immune miRNA that has been found to be involved in the regulation of multiple aspects of the immune system. Deletion of miR-155 results in impaired immune responses (reviewed by Tili et al. 2009). MiR-155 is up-regulated during the inflammatory response in several immune cell populations, including monocytes. Murine macrophages stimulated with either LPS or poly I:C display decreased expression of miR-223 (Chen et al. 2012). This decrease in miR-223 expression was linked to a subsequent increase in the expression of its target STAT3, which results in the increase

in expression of the pro-inflammatory cytokines IL-6 and IL-1β. IL-6 was ultimately found to be part of a positive feedback loop by directing the decrease in miR-223 expression in stimulated macrophages. Unlike miR-223, the miRNA miR-210 is induced upon LPS stimulation of murine macrophages (Qi et al. 2012). Over expression of miR-210 in murine macrophages reduced the expression of pro-inflammatory cytokines. It was further suggested that miR-210 may function to regulate cytokine production by modulating the expression of NFKB1 and this TLR4 signaling. Together these studies demonstrate that miRNA-mediated gene regulation is vital part of immune cell development and function.

As reviewed earlier alterations in cellular miRNA expression and thus function are also involved in the host viral response and in viral pathogenesis. In HIV-1 infected patients 59 miRNAs were found be to down-regulated in peripheral blood mononuclear cells (PBMLs) compared to healthy controls (Houzet et al. 2008). In addition the expression of cellular miRNAs was found to differ between HIV-1 patients depending on the state of disease progression (Bignami et al. 2012). It was demonstrated that expression of the immune miRNA family miR-17-92 in HIV-1 infected cells is closely linked to virus production (Triboulet et al. 2007). Other cellular miRNAs which normally function in T-cell activation, *miR-28*, *miR-125b*, *miR-150*, *miR-223* and *miR-382*, are much higher expressed in resting versus activated CD4+ T-cells and thus, likely to regulate HIV-1 gene expression via miRNA binding sites in the 3UTRS of HIV-1 mRNAs (Huang et al. 2007). In diffuse large B-cell lymphomas (DLBCLs) induced by the gamma herpesvirus Epstein-Barr virus (EBV), numerous host miRNAs are differentially expressed compared to EBV-negative B-cells

(Imig et al. 2011). Up-regulated miRNAs include *miR-424, -223, -199a-3p, -199a-5p, -27b, -378, -26b, -23a,* and *-23b* and down-regulated miRNAs include, *miR-155, -20b, -221, -151-3p, -222, -29a*/*c*, and *-106a*. Target prediction suggests that *miR-424* targets the tumor suppressor SIAH1, and *miR-155* regulates c-MYB, which is a regulator of lymphocyte proliferation. This would suggest that alteration of host miRNA expression involved in cell growth regulation contributes to EBV transformation. The oncogene of the avian herpesvirus Marek's disease virus serotype 1 (MDV-1), MEQ, was found to modulate the expression of the cellular miRNA *miR-21,* via interaction with the *miR-21* promoter (Stik et al. 2012). *In vivo* knockout in mice of Dicer, a key enzyme in miRNA processing, increases their susceptibility to vesicular stomatitis virus (VSV) infection, suggesting that cellular miRNAs are involved in the anti-viral response to VSV (Otsuka et al. 2007). In hepatitis C virus (HCV) infections, INFβ was found to promote the expression of five cellular miRNAs, *miR-448, miR-431, miR-351, miR-296,* and *miR-196,* which have potential binding sites within the HCV genome (Pedersen et al. 2007). These miRNAs were found to possess the ability to interact with their respective bindings sites and reduce HCV replication. These are just a few examples of the numerous studies demonstrating the impact of viral infections on cellular miRNA expression. Overall, many different virus types are now known to induce changes in cellular miRNA expression profiles during infection, suggesting that miRNAs are a key aspect of the response to and manipulation by viruses.

Currently little is known about the effect of PRRSV infection on the cellular miRNome of its host cell, alveolar macrophages. However, based on our current knowledge

of the interplay between miRNA regulatory pathways and viruses in general, it is likely that cellular miRNAs are involved to some degree in PRRSV infections. In order to begin to elucidate the role(s) miRNAs play in PRRSV infections the first is to identify which miRNAs have altered expressed in PRRSV infected cells. To this end, we generated miRNA profiles of PRRSV infected swine alveolar macrophages (SAMs) *in vitro* at 12hpi, 24hpi, and 48hpi and analyzed the profiles using Illumina deep sequencing technology. We found that the expression of ~40 cellular miRNAs is altered in PRRSV infected SAMs at one or more of these time points. Analysis of the potential genes and pathways regulated by these differentially expressed miRNAs suggests that they are involved in regulating multiple cellular pathways including the immune related and intracellular trafficking pathways.

Materials and Methods

Cells and virus

Primary alveolar macrophages (SAMs) were collected from three 7-week old pigs via bronchoalveolar lavage and cultured in RPMI 1640 supplemented with L-glutamine, penicillin (100 U/ml), streptomycin (100 μg/ml) and fungizone (4μg/ml) and 10% FBS. For each pig 14 plates of $2X10^7$ cells per plate were maintained for 24 hours 37°C with 5% CO_2. SAMs were then either mock infected or infected with PRRSV strain VR-2332 at an M.O.I. of 10 in duplicate and maintained at 4°C for 4 hrs. SAMs were washed with 1XPBS and fresh media was added. The SAMs were then maintained at 37°C with 5% CO_2. Each plate was then collected in 2ml of Tri-Reagent (Sigma) at 0hpi, 12hpi, 24hpi, or 48hpi. Total RNA was purified and RNA from duplicate plates was pooled.

RNA isolation

For all RNA isolations each mL of Tri-Reagent (Sigma) were homogenized by repeated passage thru a 23G needle. Next, 200µl of chloroform was added, mixed and the samples were kept at room temperature for ~5 minutes. The samples were then centrifuged at 13,000 rpm for 15 minutes. The aqueous layer was transferred to a new tube and 500µl of 100% EtOH was added. RNA was precipitated at room temperature for 15 minutes. RNA was pelleted at 13,000 rpm for 20 minutes. The RNA pellets were washed in 1ml of 75% EtOH and centrifuged at 13,000 rpm for 10 minutes. The RNA pellets were then air dried and reconstituted in 30µl of DEPC-treated water (Ambion). RNA was quantified using a nanodrop ND-1000 spectrophotometer and quality was assessed using agarose gel electrophoresis. Small RNAs were enriched using a miRVana miRNA isolation kit (Ambion) and samples were subjected to on column DNase treatment. Small RNA was quantified using a nanodrop ND-1000 spectrophotometer.

Deep sequencing small RNA library construction

A total of 21 (7 libraries per pig, 3 pigs total) small RNA libraries representing 0hpi, 12hpi (mock and VR-2332 infected), 24hpi (mock and VR-2332 infected), and 48hpi (mock and VR-2332 infected). The small RNA libraries were generated using a TruSeq Small RNA sample preparation kit (Illumina) and barcode indices RPI1-RPI21 following the manufacturer's instructions. For each library 1µg of enriched small RNAs was used. For each library 1µl of the supplied RNA 3′RNA adapter (RA3) was mixed with the RNA and the volume was brought to 6µl with nuclease-free water and kept at 70°C for 2 minutes and

then maintained on ice. Next, 2µl of 5X HM ligation buffer (HML), 1µl of RNase inhibitor and 1µl of T4 RNA ligase 2, truncated (NEB) was added and the reaction was maintained at 28°C for 1 hour and then placed on ice. Next the supplied RNA 5′RNA adapter (RA5) was ligated to the RNA. First, 23.1µl of the 5′RNA adapter was maintained at 70°C for 2 minutes and then placed on ice. Next 23.1µl of 10mM ATP added followed by 23.1µl of T4 RNA ligase. Next, 3µl of this mix was added to each 3′ adapter ligation reaction and incubated at 28°C for 1 hour and then placed on ice. For reverse transcription 6µl of each 5′ and 3′ adapter-ligated RNA was mixed with 1µl of the supplied RNA RT Primer (RTP) and maintained at 70°C for 2 minutes and them placed on ice. Next 2µl of First Strand Buffer, 0.5µl of 12.5 mM dNTPs, 1µl of 100mM DTT, 1µl RNase Inhibitor, and 1µl of SuperScript II Reverse Transcriptase (Invitrogen) was added to each sample and maintained at 50°C for 1 hour and then placed on ice. Next the cDNA libraries were PCR amplified. To each reverse transcription reaction 22.5µl of ultra pure water, 10µl of 5X Phusion HF Buffer, 2µl of the RNA PCR Primer (RP1), 2µl of an RNA PCR primer Index (each library received a single unique index), 0.5µl of 25mM dNTP, and 0.5µl of Phusion DNA polymerase (total reaction volume is now 50µl) were added. PCR cycling conditions were as follows: 30 seconds at 98°C followed by 11 cycles of 98°C for 10 seconds, 60°C for 30 seconds, 72°C for 15 seconds and one cycle of 72°C for 10 minutes. Each library PCR reaction was separated on a 6 % polyacrylamide gel and the band corresponding to the supplied custom 145-160 bp DNA ladder was excised and precipitated in 2µl of glycogen (Ambion), 30µl of 3M NaOAc and 975µl of 100% EtOH at -80°C for 30 minutes. DNA was then pelleted by centrifugation at

20,000Xg for 20 minutes at 4°C and washed in 70% EtOH. The pellet was reconstituted in 10µl of 10 mM Tris-HCl (pH 8.5) and quality and quantity of the libraries were assessed on an Agilent Technologies 2100 Bioanalyzer using a high sensitivity DNA chip.

Small RNA library sequencing

Based on DNA chip concentrations, each library was diluted to 10nM using 10 mM Tris-HCl (pH 8.5) and then 4µl of each library were pooled into a single microcentrifuge tube and mixed. A total of 25µl of pooled DNA was submitted to NCSU Genomic Sciences Laboratory (GSL) for sequencing on a single lane of the Illumina Genome Analyzer IIx (GAIIx). GSL then sorted the reads according to the barcode index and trimmed adapter sequences. Only high quality reads (overall Phred ≥ 20) were selected. The data was supplied as FASTQ files.

Data Analysis

First the FASTQ files were converted to FASTA files using the conversion tool from the free public server of GLAXAY bioinformatics tools (https://main.g2.bx.psu.edu/). Next identical sequences in each library were grouped using the collapse function (GLAXAY). The collapsed sequences were then submitted to DSAP small RNA sequence analysis pipeline (http://dsap.life.nthu.edu.tw/) for identification of known porcine miRNAs as well homologous miRNAs from other species not yet present in the pig database in miRBase (the miRNA database; http://www.mirbase.org) and Rfam (database of RNA families; http://rfam.sanger.ac.uk/). MiRNA read numbers were normalized using counts per million (CPM). Differentially expressed miRNAs were determined using the edgeR: Bioconductor

package for differential expression analysis of digital gene expression data for R statistical software using the Cox-Reid common dispersion analysis and the negative binomial general linear model (NB GLM) likelihood ratio test. (Robinson et al. 2010). Only miRNAs represented by >20 reads were selected for differential expression testing. Pairwise differential expression comparisons were made between time-matched mock and VR-2332 infected SAMs. Values are presented as log fold differences.

miRNA target prediction analysis

Computational target prediction for selected significantly differentially expressed miRNA was performed using the miRanda algorithm (version 3.3; http://www.microrna.org) with the following parameter settings: score threshold >130 and free energy threshold < -16 kCal/mol. The pig (*Sus scrofa*) Unigene (NCBI) database was utilized to identify target genes. The list of potential target genes was further filtered using the following higher stringency methods: (1) a match between nucleotides 2-8 of the miRNA with the target sequence or (2) a match between nucleotides 2-7 and 13-16 of the miRNA with the target sequence (G:U wobble tolerance) and (3) miRNA binding sites must lie within the 3´UTR. To identify potential miRNA targeted pathways the DAVID (http://david.abcc.ncifcrf.gov/) and KEGG (http://www.genome.jp/kegg/pathway.html) analysis tools were used. A selected set of potential targets (Table 1) meeting these criteria was selected for experimental validation by a dual luciferase reporter assay. For each potential target gene, the 3´UTR flanking the binding site(s) for either *ssc-miR-147*, *ssc-miR-24* or *ssc-miR-146a* were PCR amplified from pig genomic DNA (from SAMs) using gene specific primers (Table 4.1). Each PCR product

was cloned into the 3´ UTR of the *Renilla* reporter gene in the psiCHECK-2 vector (Promega, 6273bp) using the NotI and XhoI restriction sites (Figure 4.1).

Construction of RCAS expressing pig miRNAs vectors

The RCASBP(A)-miR vector (11600bp) previously described by Chen *et al.* (2008) was utilized to ectopically express either *ssc-miR-147*, *ssc-miR-24*, *ssc-miR146a* or a scrambled control sequence (SC) in the chicken cell line DF1 (Figure 4.1). Primers for construction were designed based on the porcine precursor sequences for each miRNA. The RCAS-*miR* expressing viruses were generated as follows. Forward (68-nt) and reverse (76-nt) primers were synthesized and PAGE purified by Invitrogen (Table 1). To generate a short double-stranded DNA fragment, the primers were mixed at a final concentration of 1 μM, denatured at 95 °C for 20 sec and annealed at RT. The DNA fragment was then cloned into the pENTR3C-miR-SphNgo vector at the SphI and NgoMIV restriction sites. To generate the RCASBP(A)-*miR* vector, a recombination between the pENTR3C-*miR* entry vector and RCASBP(A)-YDV gateway destination vector was performed using a LR clonase kit (Invitrogen). The RCASBP(A)-*miR* vector was then transfected into DF1 cells using FuGENE 6 (Promega). Infection was confirmed and the virus was titered by immunofluorescence staining with the mouse monoclonal 3C2 antibody against viral gag protein (Developmental Studies Hybridoma Bank at University of Iowa) and FITC-conjugated goat anti mouse IgG (Invitrogen). Ectopic expression of miRNA expression was validated using real-time PCR.

Dual luciferase reporter assay

DF1 cells were infected with either RCAS-*ssc-miR-147*, RCAS-*ssc-miR-24*, RCAS-*ssc-miR146a* or RCAS-*SC* (M.O.I. of 1) and maintained in a 96-well plate in RPMI 1640 with 1 % heat-inactivated FBS, L-glutamine, penicillin (100 U/ml), streptomycin (100 µg/ml), and fungizone (4 µg/ml), at 37 °C with 5% CO_2. At 3 dpi, each psiCHECK-2 target construct (100 ng) was transfected (in triplicate) into the DF1 cells using FuGENE 6 (Promega). Forty-eight hours post-transfection, cells were lysed in Passive Lysis Buffer (Promega), firefly and *Renilla* luciferase activities were then assessed using the Dual-Luciferase Reporter Assay System (Promega) and a VictorLight 1420 luminescence counter (PerkinElmer). Normalized luciferase activity was calculated from the *Renilla/*firefly signal ratio. Repression of *Renilla* reporter gene by a given miRNA was determined by comparing the relative luciferase activity between from cells infected with an RCAS expressing a given miRNA and the RCAS-*SC* infected cells using the student's t-test ($p < 0.05$). The assay was independently repeated to confirm the results.

Results

Characteristics of the small RNA libraries

To investigate the miRNome of SAMs and the effect of PRRSV infection on miRNA expression small RNA deep sequencing libraries were generated from PRRSV-infected SAMs *in vitro*. The total number reads obtained for each library ranged from 704,925 to 1,107, 968 (Table 4.2). The total number of high quality reads (Phred ≥20) ranged from 499,848 to 790,003 (Table 4.2). The number of high quality reads representing known

porcine miRNAs ranged from 30,216 to 173,166 (Table 4.3), while the number of reads matching homologous miRNAs in other species ranged from 8,703 to 40,656 (Table 4.3). The total number of known porcine miRNAs identified in each library ranged from 104 to 124 (Table 4.3) and the number of homologous miRNAs per library ranged from 187 to 262 (Table 4.3). These results indicate that a diverse group of miRNAs is present in SAMs. The top 50 most frequently sequenced miRNAs in each library is shown in figures 4.2-4.8. The miRNA representing the highest number of reads in all libraries was *ssc-miR-21*.

Differentially expressed miRNAs in PRRSV infected SAMs

In order to determine what effect if any, PRRSV infection has on the porcine alveolar macrophage miRNome, pairwise comparisons were performed between time-matched mock and VR-2332 infected cells. Overall, the expression of 40 miRNAs was significantly ($p<0.05$) altered in PRRSV infected SAMs at one or more time points compared to mock-infected controls (Table 4.4). The expression of 19 miRNAs was significantly altered in PRRSV-infected SAMs compared to mock-infected cells at 12hpi. Of the 19 differentially expressed miRNAs at 12hpi in PRRSV infected SAMs, the miRNAs displaying the highest log fold changes were miR-98* (~6.7) and miR-27c (~ -6.3). At 24hpi 15 miRNAs were found to be differentially expressed between PRRSV infected and mock infected SAMs. At 24hpi the miRNAs with the largest log fold changes in expression were *miR-380-3p* (~7.1) and *miR-147* (~ -6.3). Twelve miRNAs displayed altered expression patterns in PRRSV infected SAMs at 48hpi. The most differentially expressed miRNA at 12hpi in PRRSV infected SAMs was *miR-3555* which had ~7 log fold

increase in PRRSV infected SAMs compared to mock infected macrophages (Table 4.4). The next most altered miRNA was *miR-500* which had a log fold change of ~-6.8 in PRRSV infected SAMs. Of the differentially expressed miRNAs 6 (*miR-30a-3p, miR-132, miR-27b*, miR-29b, miR-146a* and *miR-9-2*) were altered at more than one time point in PRRSV infected macrophages (Table 4.4).

Target prediction analysis and validation of differentially expressed miRNAs

Target prediction and subsequent validation of selected putative targets via a luciferase assay suggest that cellular miRNAs that are differentially expressed in PRRSV infected pathways likely regulate numerous cellular pathways including immune and intracellular trafficking pathways (Tables 4.5-4.7 and Figures 4.8-4.10). Of the 10 potential *miR-24* regulated genes selected for binding site validation, the *miR-24* binding sites of 6 genes (*IRG6, IL1A, IL1B, IL13, GBP1*, and *ICAM1*) significantly reduced *Renilla* luciferase expression in DF1 cells infected with RCAS-*ssc-miR-24* compared to cells infected with RCAS-*SC* (Figure 4.9). The 3′UTR of *IRG6* has three potential *miR-24* binding sites (Table 4.5). When 2 of these binding sites were inserted into the 3′UTR of *Renilla* luciferase, its expressed was knocked-down ~50%, when all 3 sites were included *Renilla* expression was further decreased (Figure 4.9). For *ssc-miR-147* 16 potential regulated genes were selected for validation using the luciferase assay. The *miR-147* binding sites for 11 of these genes (*Snapin, IFNGR2, STAT6, CSF2, CCR5, IL12RB, IL12A, NIT1, SMAP1L, PLA2G6,* and *TPSN*) were successful in significantly reducing *Renilla* luciferase expression (Figure 4.11). The 3′UTR of *Snapin* was predicted to contain 2 *miR-147* binding sites (Table 4.6). When both sites were included in

the *Renilla* luciferase construct, there was a greater repression of expression than when only a single site was included (Figure 4.11). Seven of the predicted *ssc-miR-146a* regulated genes (*C1QTNF3, CCNK, CD47, MAFB, HZ3, PSMD5,* and *EDRF1*) out of the 9 selected for validation were able to significantly reduce *Renilla* luciferase expression (Figure 4.11). Both *C1QTNF3* and *MAFB* contain two putative *miR-146a* binding sites within their 3′UTRs (Table 4.7).

Discussion

It has been well established that cellular miRNAs are important regulators of animal immunity and viral pathogenesis. The present study was undertaken to determine the changes in cellular miRNA expression in porcine alveolar macrophages in response to PRRSV infection *in vitro*. To this end, small RNA profiles of PRRSV infected SAMs at 12hpi, 24hpi, and 48hpi were generated using Illumina deep sequencing. Approximately 120 known porcine miRNAs and ~200 homologous miRNAs were found to be expressed in SAMs. This suggests that miRNAs are likely important regulators in porcine macrophages. A total of 40 cellular miRNAs were differentially expressed in PRRSV infected macrophages, six of which (*miR-30a-3p*, *miR-132*, *miR-27b**, *miR-29b*, *miR-146a* and *miR-9-2*) were altered at more than one time point (Table 4.4). To determine what functions these differentially miRNAs undertake, *in silico* target prediction analysis and subsequent *in vitro* validation was carried out (Figures 4.9-4.12).

MiRNAs have been shown to play several important physiological roles in mammalian macrophages. When murine macrophages are stimulated with LPS the

expression of both *miR-223* and *miR-210* is altered, which in turn affects the production of pro-inflammatory cytokines (Chen et al. 2012; Qi et al. 2012). In LPS-stimulated RAW264.7 cells, a murine macrophage cell line, *miR-34a* expression is repressed (Jiang et al. 2012). This repression of *miR-34a* expression results in increased expression of its target gene Notch1, which ultimately results in increased expression of the pro-inflammatory cytokines TNFα and IL6. An increase in *miR-92a* expression is linked to increased migration of infiltrating macrophages in breast cancer tumors (Nilsson et al. 2012). A difference in expression of miRNAs is involved in the determination of macrophage phenotype determination (Graff et al. 2012). For example, the expression of *miR-27a*, *miR-29b*, *miR-125a*, *miR-146a*, *miR-155* and *miR-222* is needed for macrophages to develop into an M1 or an M2b phenotype. Dicer null murine myeloid progentior cells are unable to differentiate into macrophages and undergo abnormal cell growth (Alemedehy et al. 2012). Together these studies demonstrate the miRNAs are needed for the proper development and function of mammalian macrophages.

The expression of the miRNA *miR-24* was significantly down-regulated in PRRSV infected SAMs at 24hpi (Table 4.4). Target prediction analysis suggests that *miR-24* is involved in the regulation of several immune-associated genes (Table 4.5, Figure 4.12). Porcine inflammatory response protein 6 (IRG6; also known as RSAD2 or viperin) contains three potential *miR-24* binding sites in its 3′UTR (Table 4.5). When cloned into the 3′UTR of *Renilla* luciferase they were able to significantly reduce *Renilla* expression in DF1 cells over-expressing *miR-24* (Figure 4.9). IRG6 is known to function as an anti-viral protein and

is induced upon viral infections or LPS simulation in many different cell types (reviewed by Mattijssen and Pruijn 2012). Typically IRG6 levels are low in resting cells and are induced upon immune stimulation (Mattijssen and Pruijn 2012). As *miR-24* was found to be significantly down-regulated in PRRSV infected SAMs compared to mock-infected cells it would be expected that IRG6 levels should be induced in PRRSV infected cells. It is possible that one function of *miR-24* is to maintain reduced levels of IRG6 in healthy cells and then upon viral infection, as in the case of the present study of PRRSV, *miR-24* expression is down-regulated resulting in increased IRG6 expression and induction of an anti-viral response. Two related cytokines interleukin one alpha (IL1A) and interleukin one beta (IL1B) have potential miR-24 binding sites in their 3′UTRs (Table 4.5). Treatment of LPS-stimulated RAW-264.7 cells with melatonin results in increased expression of both IL1A and IL1B (Ban et al. 2011) indicating a role for these cytokines in the macrophage inflammatory response. IL1A and IL1B are pro-inflammatory cytokines that are often co-induced and function in the activation of the NFκB signaling pathway (Tamura et al. 2012). NFκB activation is induced upon PRRSV infection and is a key component of PRRSV pathogenesis (Lee and Kleiboeker 2005). The results of the present study add to the already known complex regulation of NFκB expression during PRRSV infections by suggesting that this activation, in part, may be due to decreased expression of *miR-24* in PRRSV infected cells and thus results in increased expression of IL1A and IL1B. However this needs to be further experimentally validated.

The miRNA *miR-147* had a log fold difference of ~-6.3 in PRRSV infected SAMs compared to mock infected SAMs at 24hpi (Table 4.4). Among the potential porcine genes predicted to contain *miR-147* binding sites was *Snapin* (Table 4.6). Snapin contains two potential *miR-147* binding sites within its 3′UTR and the results of the luciferase validation assay suggest that these sites are functional (Figure 4.11). In the previous chapter it was demonstrated that Snapin, a critical part of the SNARE membrane fusion complex, is associated with the PRRSV lifecycle via interactions with the major envelope proteins GP5 and M. SiRNA-mediated knock-down of Snapin expression resulted in decreased viral replication, suggesting a role for the GP5/M/Snapin interaction in the intracellular transport mechanisms of PRRSV. A decrease in *miR-147* expression in PRRSV infected macrophages should result in a reciprocal increase in Snapin. This potential increase in Snapin expression may help better facilitate PPRSV virion budding. Other potential *miR-147* regulated genes include *CSF2* (Table 4.6 and Figure 4.11). Colony stimulating factor 2 (granulocyte-macrophage) or CSF2 is a cytokine that controls the production, differentiation, and function of granulocytes and macrophages (Kaushansky et al. 1986). CSF2 was recently shown to function in the antiviral response to influenza A infections (Sever-Chroneos et al. 2011). STAT5 induced expression of CSF2 results in increased production of monocytic chemoattractant protein 1 (CCL2) by monocytic cells, which functions in the recruitment of monocytic cells, including macrophages to the sites of injury or infection (Tanimoto et al. 2008). Therefore, if *CSF2* is a *bona fide miR-147* target in vivo then a decrease in *miR-147* expression in PRRSV infected macrophages may act in the anti-viral response by increasing

CSF2 production. However, this may also result in the increased migration of macrophages to sites of PRRSV infection thus increasing host susceptibility.

The miRNA *miR-146a* is one of the better characterized vertebrate miRNAs and is known to play various roles in the immune system (reviewed by Labbaye and Testa 2012). The expression of *miR-146a* is induced in monocytes and other immune cells when these cells are exposed to pathogens. This up-regulation in expression is thought to be dependent upon NFκB activation. *MiR-146a* has previously been shown to regulate a diverse group of genes including the immune response modulators TRAF6, IRAK1, IRAK2, IL-8 and RANTES (reviewed by Lbbaye and Testa 2012). In the present study *miR-146a* was up-regulated at 12hpi and more dramatically at 24hpi in PRRSV infected SAMs (Table 4.4). Binding site prediction and validation identified additional genes regulated by miR-146a, including *C1QTNF3* and *MAFB* (Table 4.7 and Figure 4.11). C1q and tumor necrosis factor related protein 3 (C1QTNF3) are predicted to contain two *miR-146a* binding sites in its 3′UTR. C1QTNF3 is a recently identified cytokine that involved in the anti-inflammatory response of monocytic cells (Kopp et al. 2010). As *miR-146a* expression is significantly higher in PRRSV infected SAMs compared to mock infected cells, C1QTNF3 expression would therefore be expected to be lower in PRRSV infected cells. This potential decrease of C1QTNF3 may serve to aid in the immune response to PRRSV infection. MAFB, v-maf musculoaponeurotic fibrosarcoma oncogene homolog B (avian), was also predicted to contain two potential miR-146a binding sites within its 3′UTR (Table 4.7) and the luciferase assay data suggest that these sites are functional (Figure 4.11). MAFB is a transcription

factor that, among other roles, functions in macrophage differentiation (Kelly et al. 2000). MAFB was recently shown to be involved in the response of murine macrophages stimulated with either TLR agonists or subjected to *Salmonella* infection (McDermott et al. 2011). This suggests that MAFB-mediated gene regulation is involved in the response of macrophages to pathogenic infections. Based on the roles of *miR-146a* in the regulation of immune responsive genes and that it is up-regulated at both 12hpi and 24hpi in PRRSV-infected SAMS, it is likely that miR-146a mediated gene regulation is an important aspect of the host response to a PRRSV infection.

Generation of miRNA profiles of PRRSV infected alveolar macrophages has identified 40 cellular miRNAs whose expression is significantly altered within the first 48 hours of PRRSV infection *in vitro*. This suggests that miRNAs are likely important mediators of PRRSV pathogenesis and host defense to infection. Target gene identification for selected miRNAs including, *miR-24*, *miR-147*, and *miR-146a*, suggests that these miRNAs are involved in regulating immune signaling pathways, cytokine and transcription factor production, and intracellular trafficking. Overall, the present study has revealed that a large and diverse group of miRNAs are expressed in swine alveolar macrophages and that the expression of a subset of these miRNAs is altered in PRRSV infected macrophages. Initial analysis into the functional roles of these miRNAs suggests that these miRNAs are involved in the regulation of the interplay between PRRSV and its intracellular environment.

A.

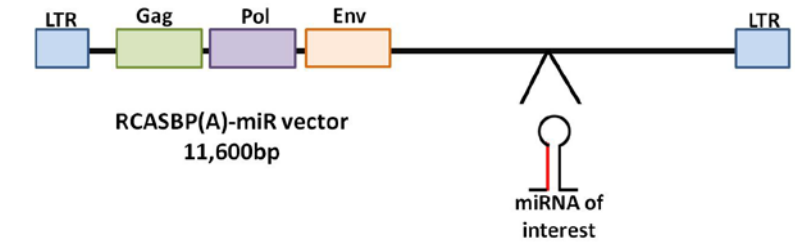

B.

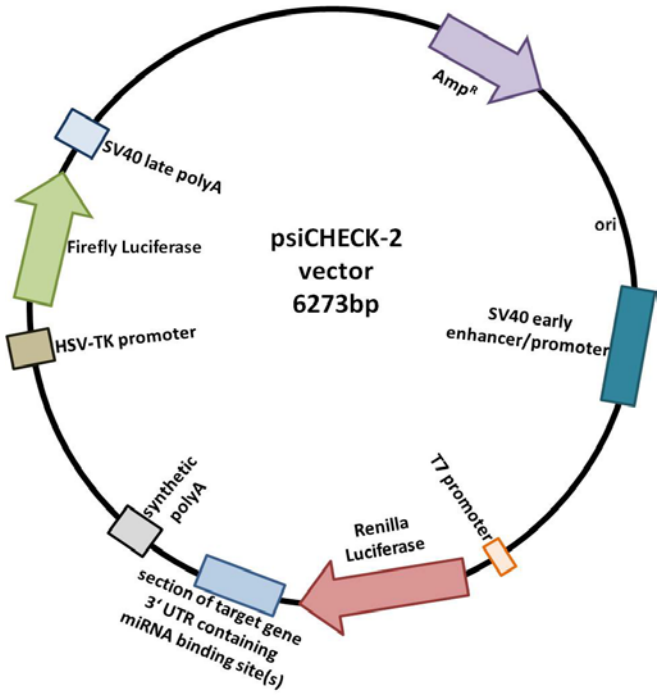

Figure 4.1. Diagrams of RCAS-miRNA and psiCHECK-2-miRNA target gene constructs.

A. Diagram of RCAS-miRNA vector used to over express a miRNA of interest. The hairpin precursor of a miRNA of interest (red line) is inserted into the RCASBP(A) vector via gateway cloning.

B. Diagram of the psiCHECK-2 vector containing miRNA binding sites. An approximate 500bp region of the 3'UTR of a pontential miRNA regulated gene containing miRNA bind site(s) is inserted into the 3'UTR of Renilla Luciferase in the psiCHECK-2 vector

A.

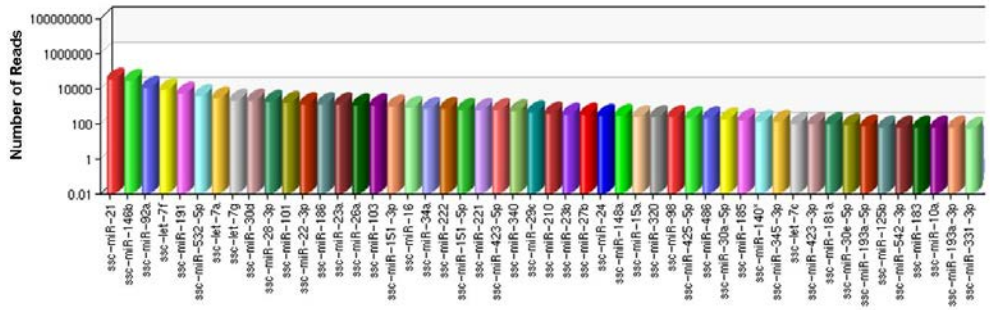

B.

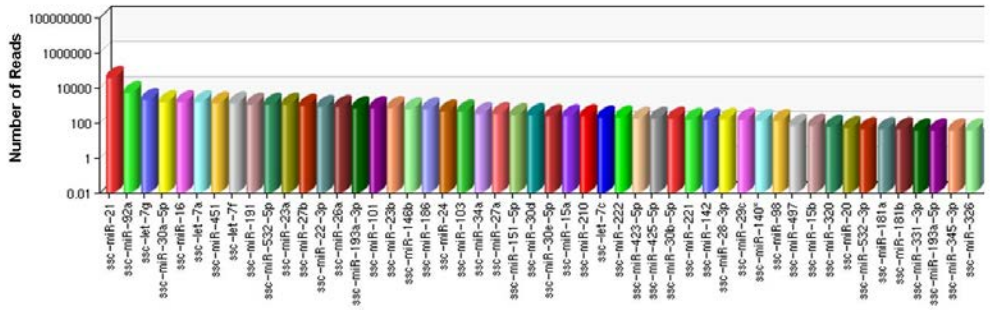

C.

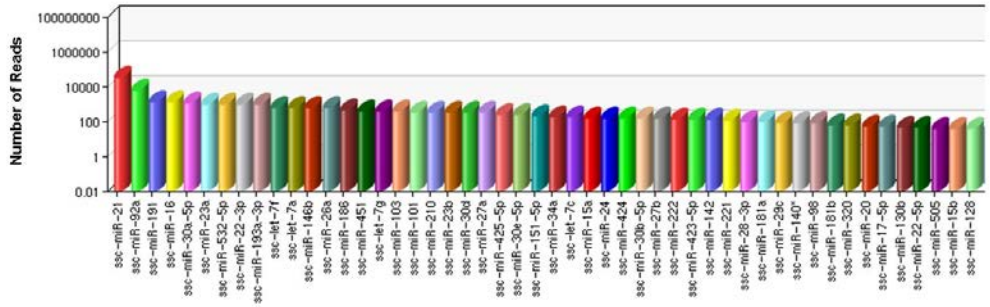

Figure 4.2. Most frequently sequenced porcine miRNAs at 0hpi in swine alveolar macrophages.

A. The 50 most frequently sequenced known porcine miRNAs in pig#1.
B. The 50 most frequently sequenced known porcine miRNAs in pig#2.
C. The 50 most frequently sequenced known porcine miRNAs in pig#3.
Number of reads representing each miRNA was determined using the DSAP small RNA sequence analysis pipeline (http://dsap.life.nthu.edu.tw/)

A.

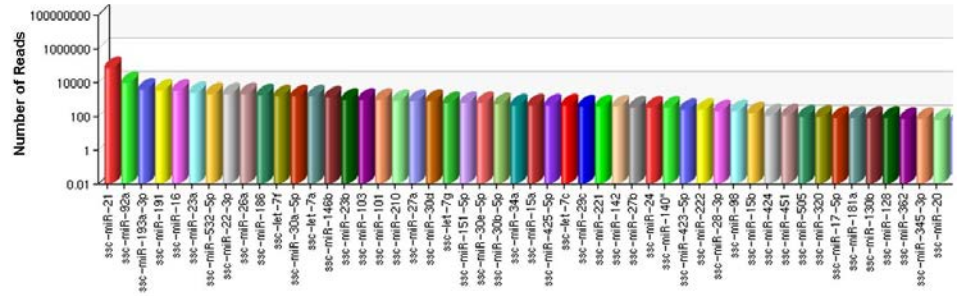

B.

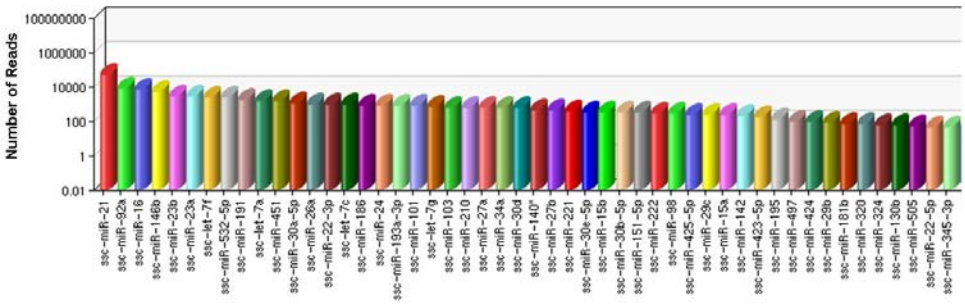

C.

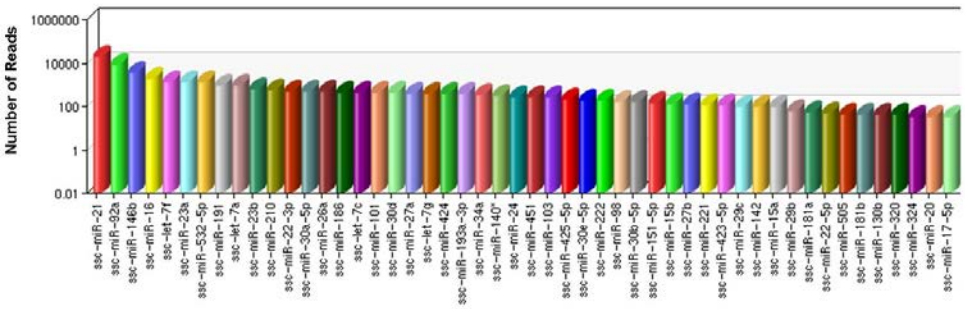

Figure 4.3. Most frequently sequenced porcine miRNAs at 12phi in mock infected swine alveolar macrophages.

A. The 50 most frequently sequenced known porcine miRNAs in pig#1.
B. The 50 most frequently sequenced known porcine miRNAs in pig#2.
C. The 50 most frequently sequenced known porcine miRNAs in pig#3.
Number of reads representing each miRNA was determined using the DSAP small RNA sequence analysis pipeline (http://dsap.life.nthu.edu.tw/)

A.

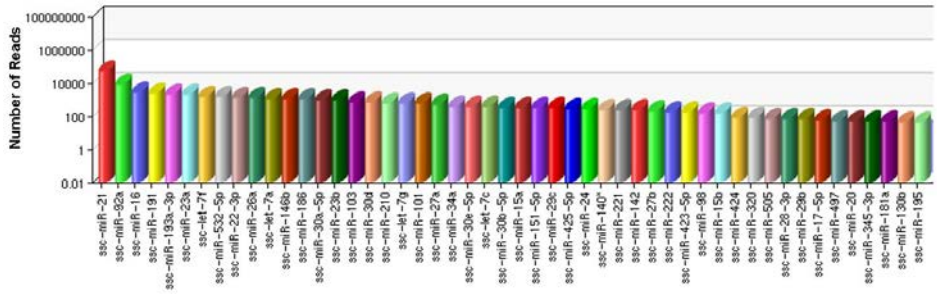

B.

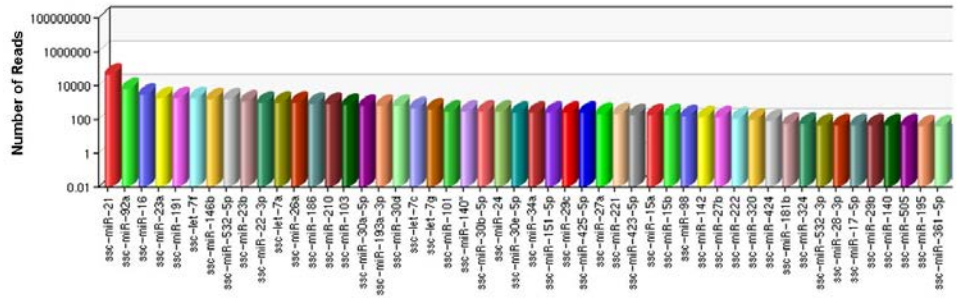

C.

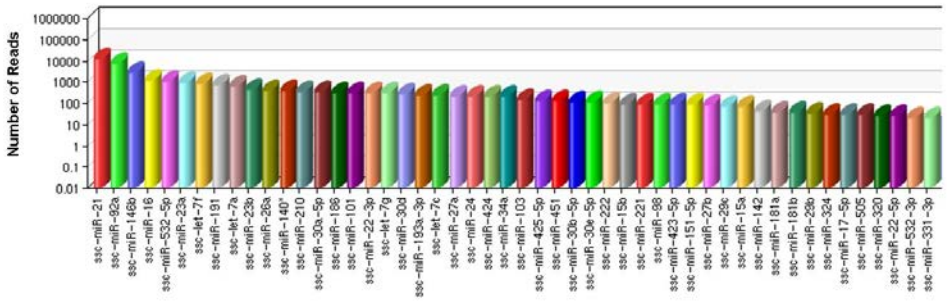

Figure 4.4. Most frequently sequenced porcine miRNAs at 12phi in PRRSV infected swine alveolar macrophages.

A. The 50 most frequently sequenced known porcine miRNAs in pig#1.
B. The 50 most frequently sequenced known porcine miRNAs in pig#2.
C. The 50 most frequently sequenced known porcine miRNAs in pig#3.
Number of reads representing each miRNA was determined using the DSAP small RNA sequence analysis pipeline (http://dsap.life.nthu.edu.tw/)

A.

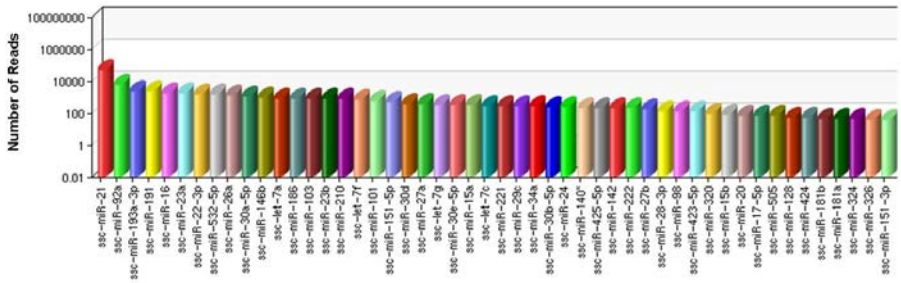

B.

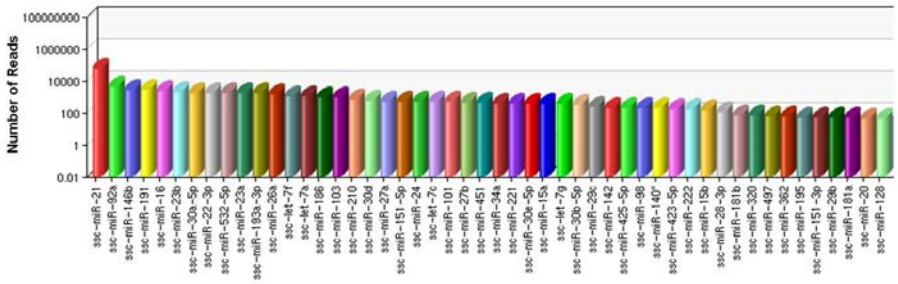

C.

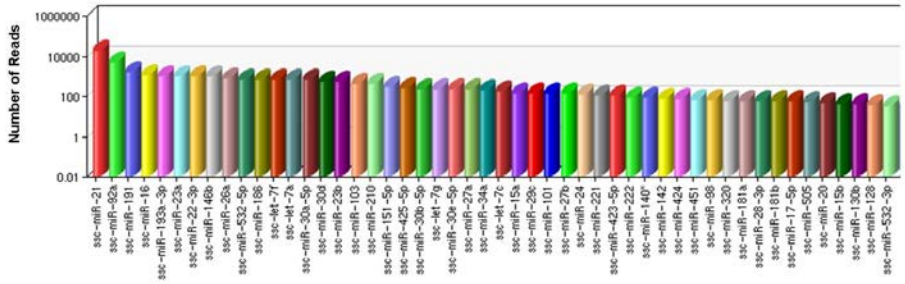

Figure 4.5. Most frequently sequenced porcine miRNAs at 24phi in mock infected swine alveolar macrophages.

A. The 50 most frequently sequenced known porcine miRNAs in pig#1.
B. The 50 most frequently sequenced known porcine miRNAs in pig#2.
C. The 50 most frequently sequenced known porcine miRNAs in pig#3.
Number of reads representing each miRNA was determined using the DSAP small RNA sequence analysis pipeline (http://dsap.life.nthu.edu.tw/)

A.

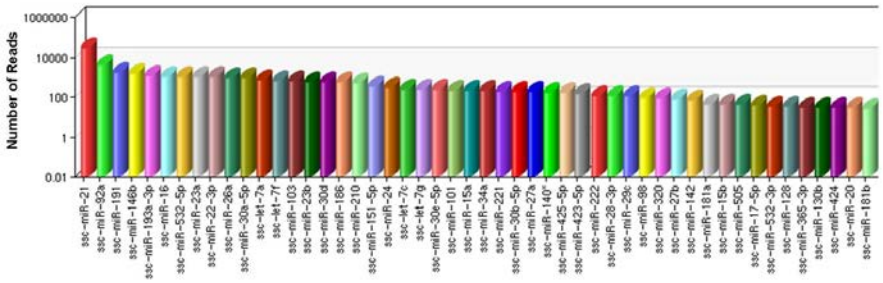

B.

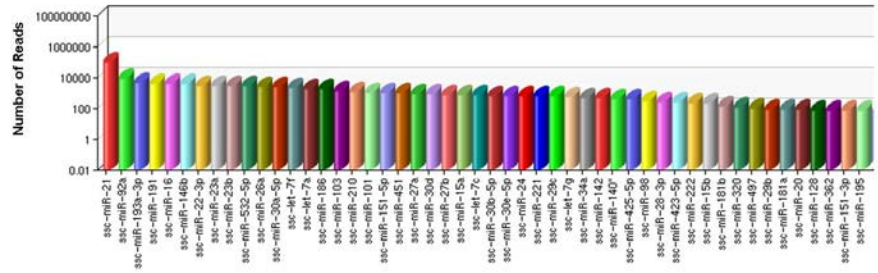

C.

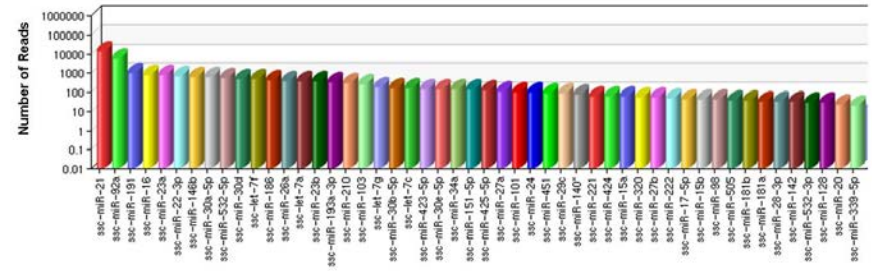

Figure 4.6. Most frequently sequenced porcine miRNAs at 24phi in PRRSV infected swine alveolar macrophages.

A. The 50 most frequently sequenced known porcine miRNAs in pig#1.
B. The 50 most frequently sequenced known porcine miRNAs in pig#2.
C. The 50 most frequently sequenced known porcine miRNAs in pig#3.
Number of reads representing each miRNA was determined using the DSAP small RNA sequence analysis pipeline (http://dsap.life.nthu.edu.tw/)

A.

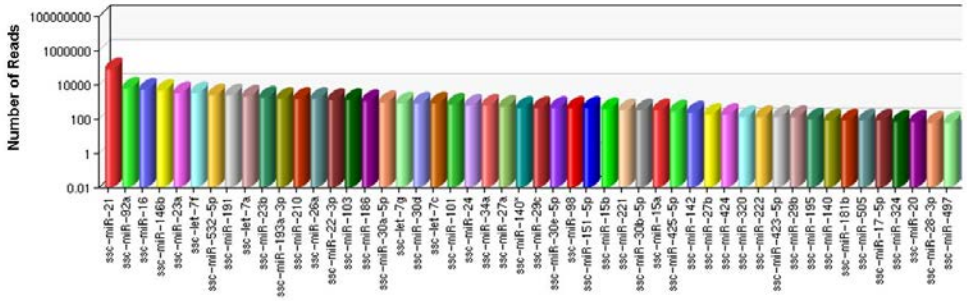

B.

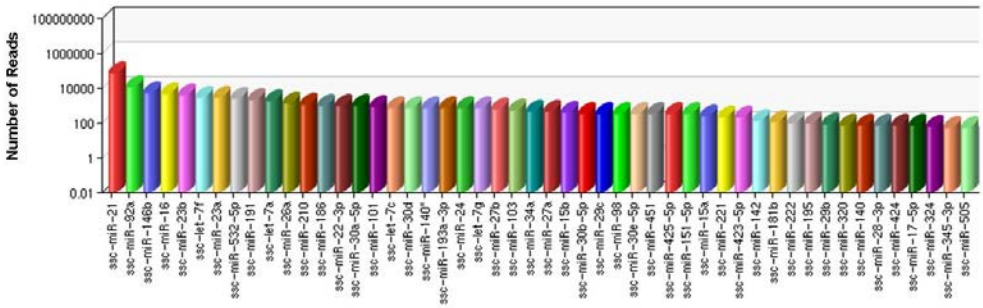

C.

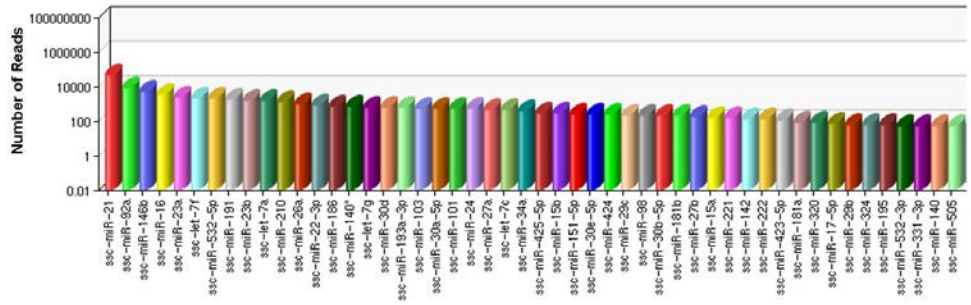

Figure 4.7. Most frequently sequenced porcine miRNAs at 48phi in mock infected swine alveolar macrophages.

A. The 50 most frequently sequenced known porcine miRNAs in pig#1.
B. The 50 most frequently sequenced known porcine miRNAs in pig#2.
C. The 50 most frequently sequenced known porcine miRNAs in pig#3.
Number of reads representing each miRNA was determined using the DSAP small RNA sequence analysis pipeline (http://dsap.life.nthu.edu.tw/)

A.

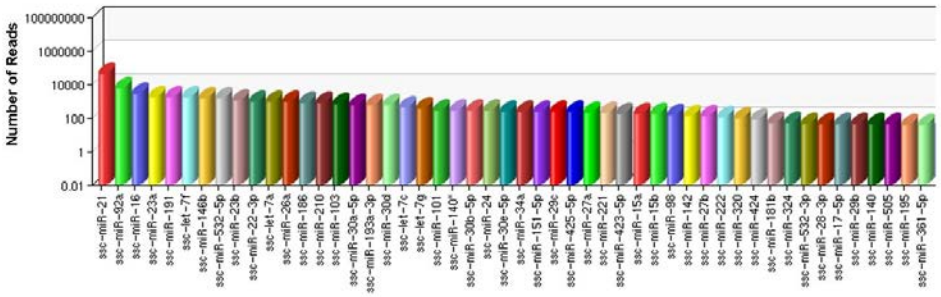

B.

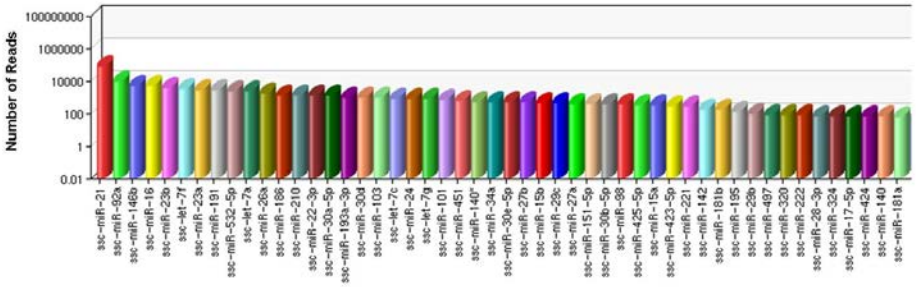

C.

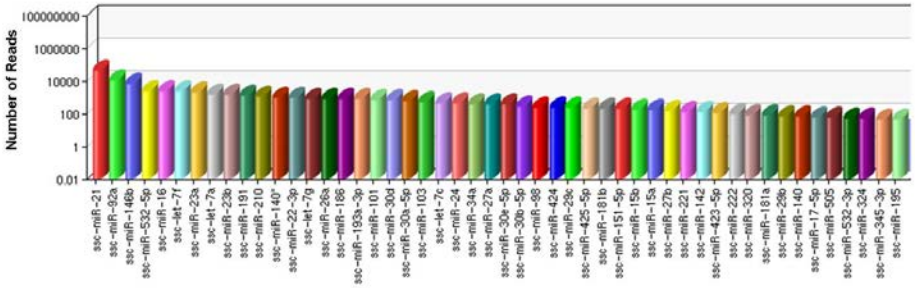

Figure 4.8. Most frequently sequenced porcine miRNAs at 48phi in PRRSV infected swine alveolar macrophages.

A. The 50 most frequently sequenced known porcine miRNAs in pig#1.
B. The 50 most frequently sequenced known porcine miRNAs in pig#2.
C. The 50 most frequently sequenced known porcine miRNAs in pig#3.
Number of reads representing each miRNA was determined using the DSAP small RNA sequence analysis pipeline (http://dsap.life.nthu.edu.tw/)

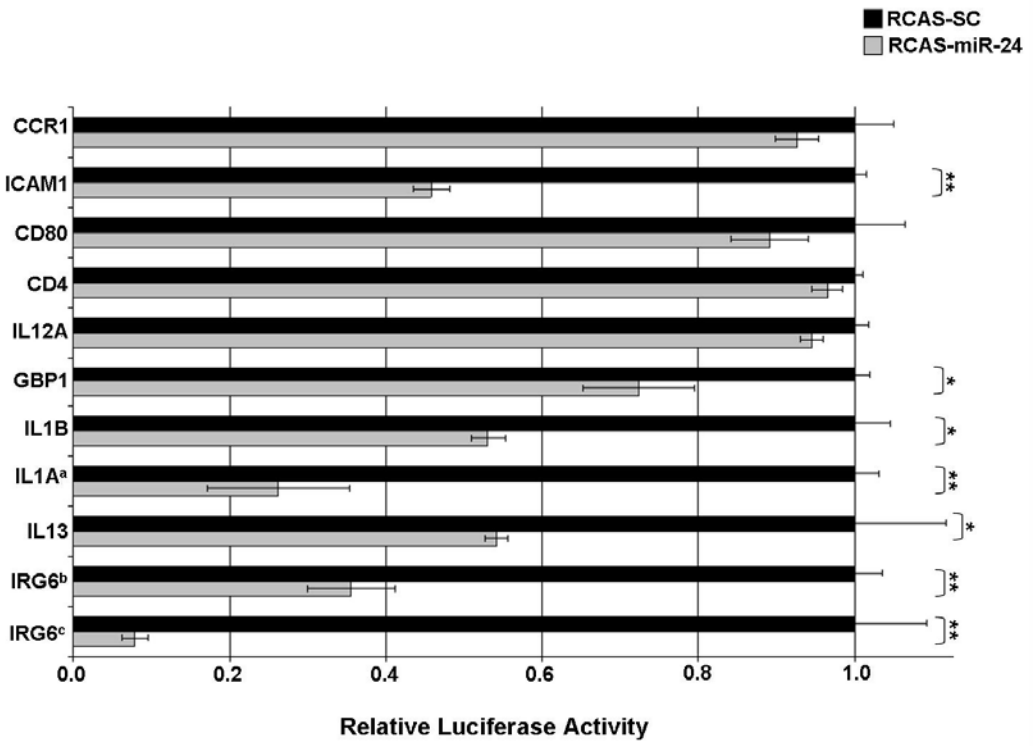

Figure 4.9. Validation of predicted *ssc-miR-24* target genes.
Luciferase assays for *miR-24* and a scrambled control sequence (SC) for target gene validation are shown. DF1 cells infected with either an RCAS-*miR-24* expressing virus or an RCAS-*SC* expressing virus were transfected with predicted target 3' UTR luciferase constructs. Relative *Renilla* luciferase activity is shown. *: $p<0.05$, **: $p<0.01$. [a]This construct contains two *miR-24* binding sites. [b]This construct contains two *miR-24* binding sites. [c]This construct contains three *miR-24* binding sites.

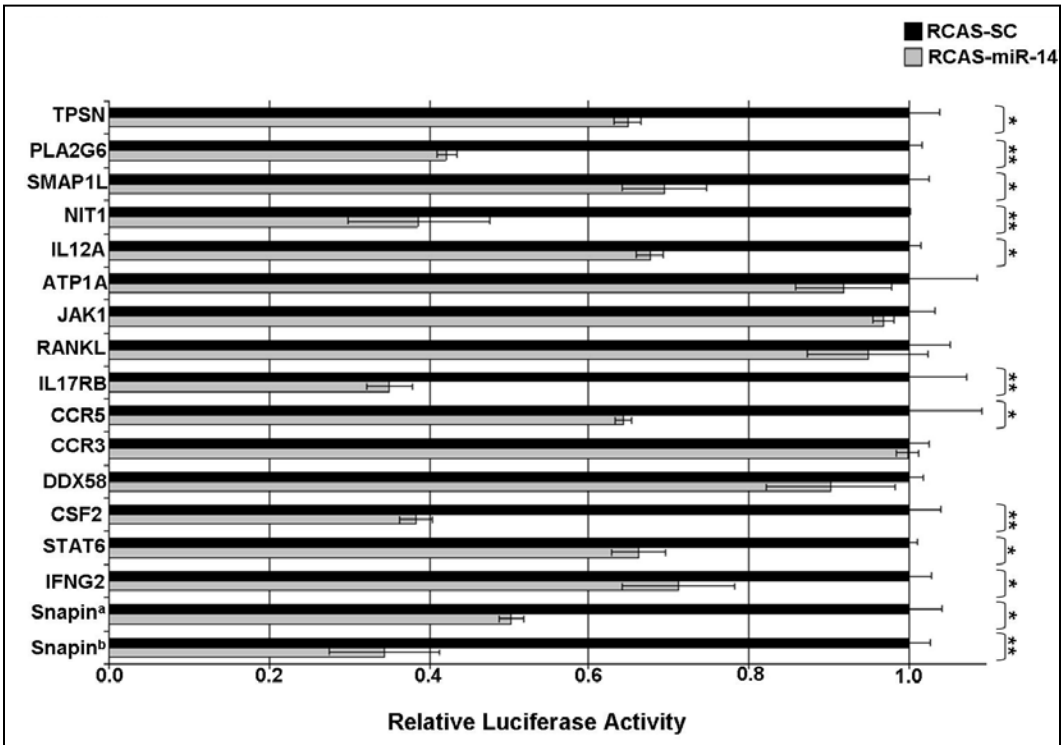

Figure 4.10. Validation of predicted *ssc-miR-147* target genes.
Luciferase assays for *miR-147* and a scrambled control sequence (SC) for target gene validation are shown. DF1 cells infected with either an RCAS-*miR-147* expressing virus or an RCAS-*SC* expressing virus were transfected with predicted target 3' UTR luciferase constructs. Relative *Renilla* luciferase activity is shown. *: $p<0.05$, **: $p<0.01$. [a]This construct contains one *miR-147* binding site. [b]This construct contains two *miR-147* binding sites.

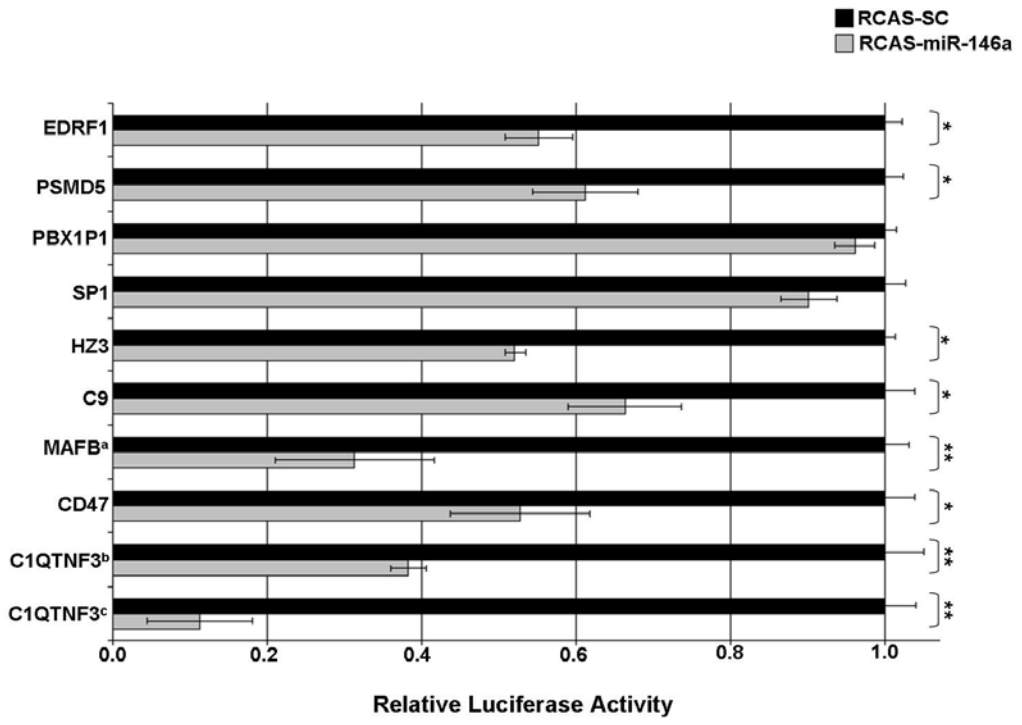

Figure 4.11. Validation of predicted *ssc-miR-146a* target genes.
Luciferase assays for *miR-146a* and a scrambled control sequence (SC) for target gene validation are shown. DF1 cells infected with either an RCAS-*miR-146a* expressing virus or an RCAS-*SC* expressing virus were transfected with predicted target 3' UTR luciferase constructs. Relative *Renilla* luciferase activity is shown. *: $p<0.05$, **: $p<0.01$. [a]This construct contains two *miR-146a* binding sites. [b]This construct contains one *miR-146a* binding site. [c]This construct contains two *miR-146a* binding sites.

Figure 4.12. Pathway analysis of potential miR-147, miR-146a, and miR-24 regulated genes.
The KEGG pathway database (http://www.genome.jp/kegg/pathway.html) was utilized to identify pathways associated with potential *miR-147*, *miR-146a* and *miR-24* regulated genes chosen for experimental validation. Example pathways include cell adhesion molecules and cytokine-cytokine receptor interaction. A: Cell Adhesion Molecules: multiple cell adhesion molecules involved in immune signaling pathways are potentially regulated by *miR-147*, *miR-146a*, and *miR-24*. B: Cytokine-Cytokine Receptor Interaction: multiple genes involved in the regulation of cytokine signaling are likely regulated by *miR-147*, *miR-146a* and *miR-24*. Red stars denote *miR-147*, *miR-146a* and/or *miR-24* targeted genes.

A.

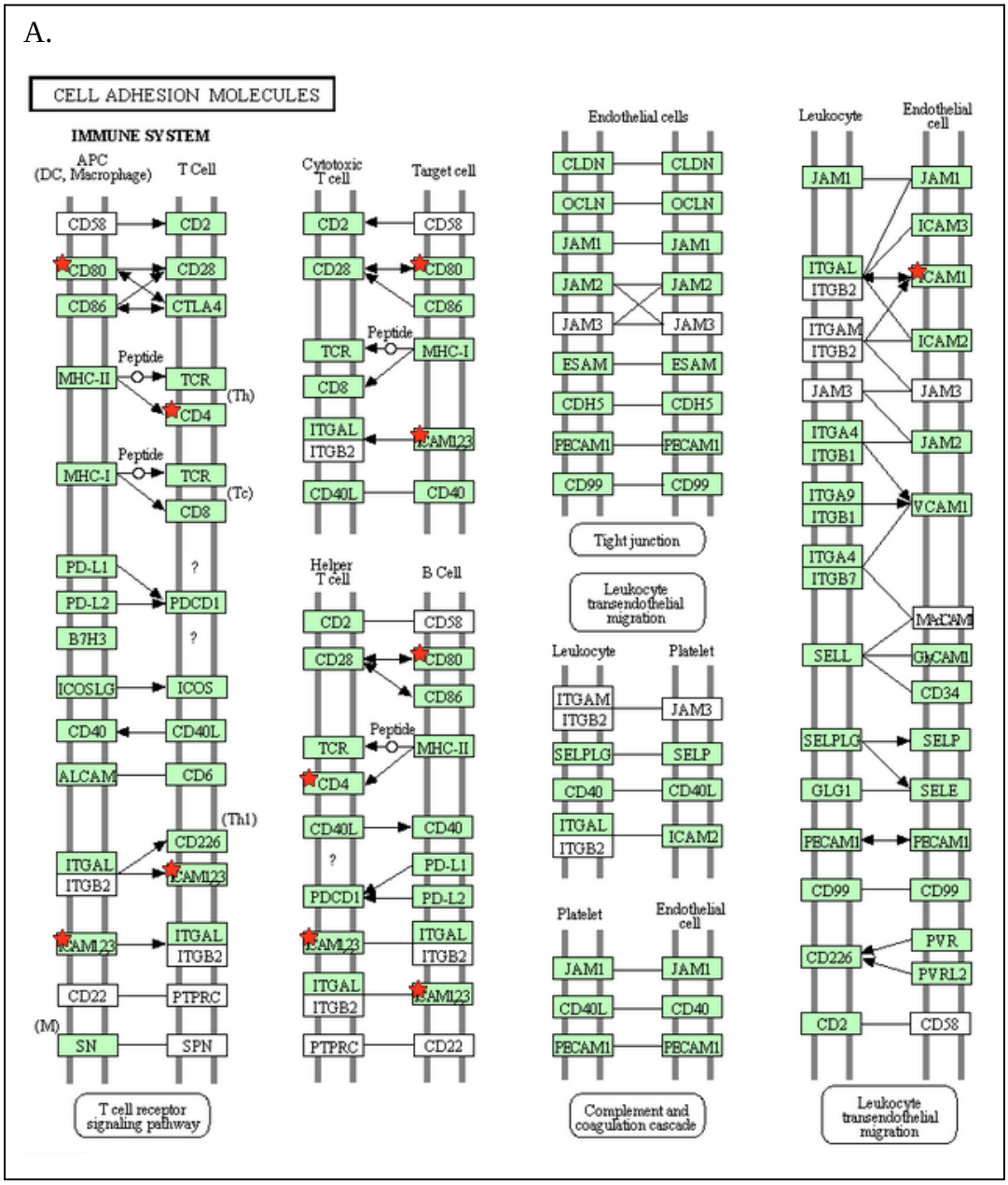
CELL ADHESION MOLECULES
IMMUNE SYSTEM
APC (DC, Macrophage)
T Cell
CD58
CD2
CD80
CD28
CD86
CTLA4
Peptide
MHC-II
TCR
(Th)
CD4
Peptide
MHC-I
TCR
(Tc)
CD8
PD-L1
PD-L2
PDCD1
B7H3
ICOSLG
ICOS
CD40
CD40L
ALCAM
CD6
(Th1)
CD226
ITGAL
ITGB2
ITGAM123
ITGAL
ITGB2
CD22
PTPRC
(M)
SN
SPN
T cell receptor signaling pathway
Cytotoxic T cell
Target cell
CD2
CD58
CD28
CD80
CD86
Peptide
TCR
MHC-I
CD8
ITGAL
ITGB2
ITGAM123
CD40L
CD40
Helper T cell
B Cell
CD2
CD58
CD28
CD80
CD86
Peptide
TCR
MHC-II
CD4
CD40L
CD40
?
PD-L1
PDCD1
PD-L2
ITGAM123
ITGAL
ITGB2
ITGAL
ITGB2
ITGAM123
PTPRC
CD22
Endothelial cells
CLDN
CLDN
OCLN
OCLN
JAM1
JAM1
JAM2
JAM2
JAM3
JAM3
ESAM
ESAM
CDH5
CDH5
PECAM1
PECAM1
CD99
CD99
Tight junction
Leukocyte transendothelial migration
Leukocyte
Platelet
ITGAM
ITGB2
JAM3
SELPLG
SELP
CD40
CD40L
ITGAL
ITGB2
ICAM2
Platelet
Endothelial cell
JAM1
JAM1
CD40L
CD40
PECAM1
PECAM1
Complement and coagulation cascade
Leukocyte
Endothelial cell
JAM1
JAM1
ICAM3
ITGAL
ITGB2
ITGAM123
CAM1
ICAM2
ITGAM
ITGB2
JAM3
JAM3
ITGA4
ITGB1
JAM2
ITGA9
ITGB1
VCAM1
ITGA4
ITGB7
MAdCAM1
SELL
GlyCAM1
CD34
SELPLG
SELP
GLG1
SELE
PECAM1
PECAM1
CD99
CD99
PVR
CD226
PVRL2
CD2
CD58
Leukocyte transendothelial migration

B.

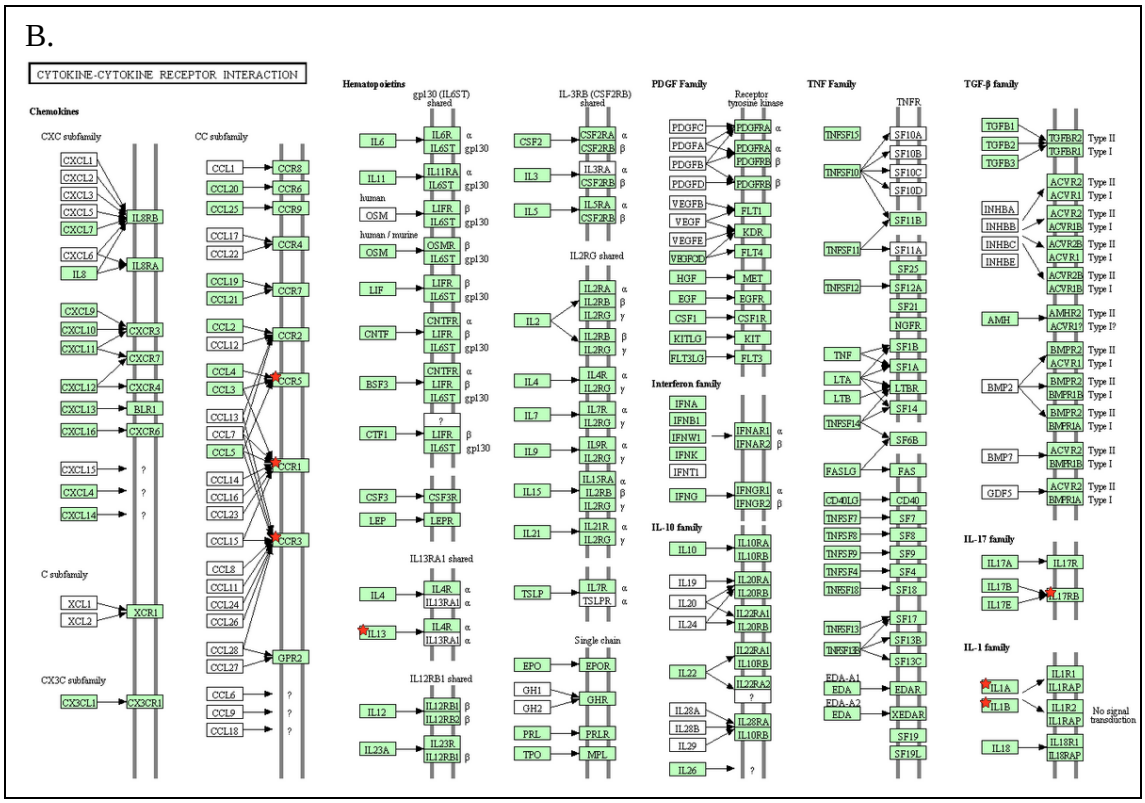
CYTOKINE-CYTOKINE RECEPTOR INTERACTION
Chemokines
CXC subfamily
CC subfamily
C subfamily
CX3C subfamily
Hematopoietins
IL-3RB (CSF2RB) shared
IL2RG shared
IL13RA1 shared
IL12RB1 shared
Single chain
PDGF Family
Receptor tyrosine kinase
Interferon family
IL-10 family
TNF Family
TNFR
TGF-β family
IL-17 family
IL-1 family
No signal transduction

Table 4.1. Primers used in this study

miRNA hairpin primers for RCAS cloning	
ssc-miR-147 forward primer	GTAGTGGAAACACTTCTGCACAAACTAGATTCTGGATACCAGTGTGCGGAAATGCTTCTGCAGC
ssc-miR-147 reverse primer	CCGGGCTGCAGAAGCATTTCCGCACACTGGTATCCAGAATCTAGTTTGTGCAGAAGTGTTTCCACTACCATG
ssc-miR-24 forward primer	GTGCCGTGCCTACTGAGCTGAAACACAGTTGATTTGTGCAGACTGGCTCAGTTCAGCAGGAACAGAGC
ssc-miR-24 reverse primer	CCGGGCTCTGTTCCTGCTGAACTGAGCCAGTCTGCACAAATCAACTGTGTTTCAGCTCAGTAGGCACGGCACCATG
ssc-miR-146a forward primer	CGCTGAGAACTGAATTCCATGGGTTGTGTCATTGTCAGACCTGTGAAGTTTAGTTCTTCTTG
ssc-miR-146a reverse primer	CCGGCAAGAAGAACTAAACTTCACAGGTCTGACAATGACACAACCCATGGAATTCAGTTCTCAGCGCATG
scrambled control forward primer	CGCCAGTTCGCACTACTAATATGCTAGTGAAGCAGCAGATGGTAGCATATTAGTAGTGCGAACTGTTG
scrambled control reverse primer	CCGGCAACAGTTCGCACTACTAATATGCTACCATCTGCTGCTTCACTAGCATATTAGTAGTGCGAACTGGCGCATG
porcine primers for target region cloning	
GBP1-F	CCCTCGAGATGACTGGCAGCTGGGTGATAA
GBP1-R	GGGCGGCCGCCGTCTTCCCATTTACCTAG
IRG6-1F	CCCTCGAGAGTTTAGAAATAGTCCACA
IRG6-1R	GGGCGGCCGCAGTGATTCAGAGTTAAGTG

Table 4.1 continued

CD4-F	CCCTCGAGTCTCAGATCAAGAGACTCC
CD4-R	GGGCGGCCGCTGTGTGATCTTGGGCTAGT
CD80-F	CCCTCGAGACTCAGAAGAAGAGACAAG
CD80-R	GGGCGGCCGCGTCCTGTGGAGCTCCTGCG
ICAM1-F	CCCTCGAGCAGCCATGAAACTTAGCAC
ICAM1-R	GGGCGGCCGCAATACTGCACGTGTCTGTG
CCR1-F	CCCTCGAGTTGCTCCCACTGACAGAGCC
CCR1-R	GGGCGGCCGCAATATGAAGTTCAAGCTTA
DDX58-F	CCCTCGAGCAGTGTATACCCATAGCCA
DDX58-R	GGGCGGCCGCGGCAAGATGTCAATAAACTG
CCR3-F	CCCTCGAGGCCATCTACCTGAGCAAAT
CCR3-R	GGGCGGCCGCTGTCAATAACTGGCTGAAG
CCR5-F	CCCTCGAGATCGAGTCAGCTCCGTTTACACA
CCR5-R	GGGCGGCCGCACTGATCATGGGCGTGTCTT
IL17RB-F	CCCTCGAGCACATACCACCTCATGAAGG
IL17RB-R	GGGCGGCCGCGTAGCAACTTTATTGGCATAA
RANKL-F	CCCTCGAGTCTGGATCCAGACCAAGACG
RANKL-R	GGGCGGCCGCGCTTTAATTCTTGGAATTCA
JAK1-F	CCCTCGAGAGCTGTGGGATACTTTGCTGCA
JAK1-R	GGGCGGCCGCGCTAGCCAGCATCAACGAA
IFNGR2-F	CCCTCGAGTGTCACTGCTGAGGTTCTG
IFNGR2-R	GGGCGGCCGCAGCCAGGAATCTGCACGTGA
STAT6-F	CCCTCGAGATCTACTGTACACGATCTGA
STAT6-R	GGGCGGCCGCCCATGGGCATAGAACTATGG
ATP1A1-F	CCCTCGAGCTACTCGCTCCTCATCTTC
ATP1A1-R	GGGCGGCCGCTAGCCATCTTTATTTGTA
IL12A-147F	CCCTCGAGCCTGGAAGAACTGGATTT
IL12A-147R	GGGCGGCCGCACATGTTCTGTGAGGACATT
CSF2-F	CCCTCGAGAAGCACTATGAGCAGCACTG
CSF2-R	GGGCGGCCGCCCATTACAGCCTTGGCCAG
NIT1-F	CCCTCGAGGGCTGACCTAGTCCTCTTAC
NIT1-R	GGGCGGCCGCCCTCTGGAGCTTACATACTG
SMAP1L-F	CCCTCGAGCTGTCAGACTCAGAAAGGTA
SMAP1L-R	GGGCGGCCGCTTAGGCTGTGGATAGATTAA
PLA2G6-F	CCCTCGAGTGGATGAGGTCAATGACAC
PLA2G6-R	GGGCGGCCGCTGAGCCAGTCATCCTTGGTG
TPSN-F	CCCTCGAGAAGCTGGCTTCGTCTCTCAT
TPSN-R	GGGCGGCCGCCTCACAGTTAATGAACTGTG
SNAPIN-1F	CCCTCGAGCCACAGAACAGCACAAATAC
SNAPIN-1R	GGGCGGCCGCCATATACCAGAGTAAACTG
SNAPIN-2R	GGGCGGCCGCATGAGGCTTGAAGATGGTAG

Table 4.1 continued

SNAPIN-2F	CCCTCGAGTACATACTCATCAGGCCCAC
HZF3-F	CCCTCGAGGCAGATGAGGAATGTATTGG
HZF3_R	GGGCGGCCGCCCTAACTTATAGCATGATT
SP1-F	CCCTCGAGTGGAAGTAACTCAAGTGGTC
SP1-R	GGGCGGCCGCAGCTCTCTGACAAGATACCA
PBXIP1-F	CCCTCGAGGCGATTCTGATTCTGAAGCCAA
PBXIP1-R	GGGCGGCCGCAATGCAGAGTTCCAGCCCA
C1QTNF3-1F	CCCTCGAGCTCTGCCTTGAGATAAGTGT
C1QTNF3-2R	GGGCGGCCGCGCAGCCCTAATTCATTCTCTC
C1QTNF3-1R	GGGCGGCCGCGCACAGCTTCTCTGTGAATAT
C1QTNF3-2F	CCCTCGAGGCTGAGCCACAACAGGAACTC
CCNK-F	CCCTCGAGATGAGATAACGCGCCGCCTT
CCNK-R	GGGCGGCCGCAGCTTGACTGGCTCCGCATG
CD47-F	CCCTCGAGGTGAAGTGATGGACTCTGAT
CD47-R	GGGCGGCCGCCAGGAGCAGCAGACACATTA
PSMD5-F	CCCTCGAGCTAGAGTCTAGACCATTTA
PSMD5-R	GGGCGGCCGCGCGATGAGAATTCACAAAC
MAFB-F	CCCTCGAGGCTTAGAGAACGTGGCAGCA
MAFB-R	GGGCGGCCGCCAACACAGTTGAATCCGTAA
EDRF1-F	CCCTCGAGAAGTATGTTAAGCTATGTGG
EDRF1-R	GGGCGGCCGCGAGAGTACCTGTTCTTGATC
IRG6-2F	CCCTCGAGTTACTGGACTGGCATGAGCTGTT
IRG6-2R	GGGCGGCCGCCGCATGGTGGCTTAACAGAATCT
IRG6-3F	CCCTCGAGGTCTGGATGTATGATAAAGT
IRG6-3R	GGGCGGCCGCTACGGTTTCCCTCAGCTCTA
IL1A-F	CCCTCGAGCCACAATAGCAGCTGGAATGAGA
IL1A-R	GGGCGGCCGCTCAACCTGGAAAACACTGTCTGC
IL1B-F	CCCTCGAGTCCCTAAGGAAAGCCATACCCA
IL1B-R	GGGCGGCCGCCACACTCACCCCAAAGAAATTGA
IL13-F	CCCTCGAGAGCAAGTTCCTGGCAAGCACAT
IL13-R	GGGCGGCCGCTCAAGCCGATGCCTCCTCA
IL12A-24F	CCCTCGAGTGATACTCTGATCAAGTGTA
IL12A-24R	GGGCGGCCGCCAAGGTATATTTCAAATCC

Table 4.2. Read characteristics of small RNA libraries generated from mock or PRRSV VR-2332 infected SAMs

Pig#1 0hpi	959,032	674,411
Pig#2 0hpi	784,659	559,218
Pig#3 0hpi	837,944	604,270
Pig#1 12hpi-U	1,107,968	790,003
Pig#1 12hpi-I	835,635	598,284
Pig#2 12hpi-U	877,405	624,764
Pig#2 12hpi-I	925,267	662,195
Pig#3 12hpi-U	975,776	699,594
Pig#3 12hpi-I	704,925	499,848
Pig#1 24hpi-U	941,306	669,665
Pig#1 24hpi-I	763,441	545,828
Pig#2 24hpi-U	773,521	554,208
Pig#2 24hpi-I	1,009,128	717,815
Pig#3 24hpi-U	723,461	516,278
Pig#3 24hpi-I	873,303	622,818
Pig#1 48hpi-U	971,660	687,708
Pig#1 48hpi-I	837,838	592,634
Pig#2 48hpi-U	936,687	653,247
Pig#2 48hpi-I	880,547	625,246
Pig#3 48hpi-U	907,033	647,948
Pig#3 48hpi-I	927,701	658,526
Total	18,554,237	13,204,508

*Library names are given as the pig#, stage on infection and state of infection: U=mock-infected and I= PRRSV VR-2332 infected at an M.O.I. of 10

**Phred score≥20 over the entire read

Table 4.3. The number of known porcine and homologus miRNAs identified in small RNA libraries generated from mock or PRRSV VR-2332 infected SAMs

Library	# of known porcine miRNAs	# reads representing porcine miRNAs	# of known homologous miRNAs	# reads representing homologous miRNAs
Pig#1 0hpi	124	120700	212	19069
Pig#2 0hpi	115	70198	235	17932
Pig#3 0hpi	120	56718	219	14553
Pig#1 12hpi-U	123	124102	255	33364
Pig#1 12hpi-I	122	91554	231	26065
Pig#2 12hpi-U	116	111530	247	35226
Pig#2 12hpi-I	112	77920	227	20595
Pig#3 12hpi-U	112	50845	203	19044
Pig#3 12hpi-I	104	33714	187	12847
Pig#1 24hpi-U	116	92024	238	21238
Pig#1 24hpi-I	112	51803	212	14970
Pig#2 24hpi-U	117	101348	236	25735
Pig#2 24hpi-I	124	173166	262	40656
Pig#3 24hpi-U	108	43253	205	12191
Pig#3 24hpi-I	105	30216	187	8703
Pig#1 48hpi-U	117	140903	240	40198
Pig#1 48hpi-I	112	77920	227	20595
Pig#2 48hpi-U	112	125832	230	33923
Pig#2 48hpi-I	119	143550	260	36843
Pig#3 48hpi-U	119	89174	230	26631
Pig#3 48hpi-I	113	92986	217	27917
Total		1,899,456		508,295

Table 4.4. Significant differentially expressed miRNAs at 12hpi, 24hpi, and 48hpi in PRRSV infected SAMs

12hpi			24hpi			48hpi		
miRNA	Log FC*	p-value	miRNA	Log FC*	p-value	miRNA	Log FC*	p-value
miR-451	-2.3053	1.38E-10	miR-29b*	-4.2215	2.95E-10	miR-30b-3p	2.6724	3.24E-05
miR-212	2.7793	6.73E-05	miR-30a-3p	3.1645	2.66E-09	miR-222*	6.5960	0.000792
miR-30a-3p	1.8506	0.000247	miR-9-2	3.2710	5.85E-09	miR-362-3p	-2.3064	0.001638
miR-132	1.2390	0.000969	miR-29b-2*	2.3750	7.00E-06	miR-9-2	-1.9932	0.003833
miR-27b*	-1.0012	0.002566	miR-27a	-0.6524	0.012779	let-7e	-1.0534	0.00428
miR-193a	1.3993	0.005037	miR-380-3p	7.1000	0.013954	miR-2904	-6.0559	0.011713
miR-144	-6.0776	0.009675	miR-7*	-6.0323	0.024055	miR-27b*	-0.5884	0.034349
miR-98*	6.7175	0.010022	miR-146a	6.0397	0.024055	miR-3555	7.0555	0.037248
miR-450b-5p	-1.1018	0.012519	miR-1306	-1.2961	0.030115	miR-219-5p	-2.6122	0.042565
miR-146a	0.7948	0.013856	miR-132*	1.6283	0.03028	miR-30d*	-2.7058	0.044275
miR-130b*	3.1070	0.017761	miR-24	-2.8016	0.031308	miR-365-5p	-2.0743	0.045497
miR-99a	-1.6808	0.021217	miR-147	-6.3432	0.037235	miR-500	-6.8198	0.049273
miR-362	-0.7871	0.023627	miR-18	-0.9048	0.040609			
miR-374a	-1.7926	0.026362	miR-132	0.6813	0.042978			
miR-181c*	1.1261	0.029184	miR-331-5p	0.8473	0.044026			
miR-29b*	1.2232	0.03123						
miR-192	1.3390	0.037039						
miR-223*	-0.6014	0.038478						
miR-27c	-6.3416	0.043774						

Table 4.5. Computationally predicted porcine *miR-24* target sites.

Symbol /GI	*miRNA* : mRNA (3´UTR) interaction	Score/ Energy (kcal/mol)	Binding site

IL1A/ 1987	3' gACAAGGACGACUU-GACUCGGu 5'
	  || |:|| |||| |||||||
	5' aTGCTTCT--TGAAGCTGAGCCt 3'
	
	3' gaCAAGGA-CGACU------UGACUCGGu 5'
	  || || ||||| :|||||||
	5' taGTCACTCGCTGAGCATGTGCTGAGCCt 3'
		165/-23.1
		
		154/-22.8
			1493-1513
			
			931-959

IL1B/ 47522925	3' gacaAGGA---CG----ACUUGACUCGGU 5' |||| || | ||||||||| 5' cccaTCCTCAGGCCCCATCCACTGAGCCA 3'	153/-21	1061-1089
IL13/ 189176150	3' gacAAGGA--CGA--CUUGACUCGGu 5' ||||| ||| || :|||||| 5' gatTTCCTTAGCTTAGACTTGAGCCt 3'	151/-18.9	581-606

IRG6/	3' gaCAAGGACG-ACUU----GACUCGGu 5'
	  | | |||: |||| |||||:|
	5' ggGGTGCTGTGTGAATCTCCTGAGTCt 3'
	
	3' gACAAGGACGACUUGACUCGGU 5'
	  || || | :|||||||:|:||
	5' aTG-TCAT-TTGAACTGGGTCA 3'
	
	3' GACAA---GGAC----GACUU--GACUCGGU 5'
	  ||| | :||| | || |||||:||
	5' CTGATGAGTCTGAAGCCCAAATCCTGAGTCA 3'
		142/-18.1
		
		140/-22.2
		
		135/-17.6
			1737-1763
			
			2058-2077
			
			2683-2713

GBP1/ 166202345	3' GACAAGGACGACUUGACUCGGu 5' ||| |||| |||||||: 5' CTG----TGCTTCACTGAGCTt 3'	144/-17.8	2956-2973
IL12A/ 47522811	3' gACAAGGACGACUU--------GACUCGGu 5' |||| ||: ||| :|||||| 5' gTGTT--TGTAGAAACAAACACTTGAGCCt 3'	136/-20.1	1248-1275
CD4/ 47641126	3' gacaaGGACGACUUGACUCGGU 5' ||||| ||||||:: 5' ccaccCCTGCCTCCCTGAGCTG 3'	138/-18.6	2652-2673
CD80/ 55742787	3' GACAAGGACG--ACUU----GACUCGGu 5' || | | |: |||: ||||||| 5' CTCTCACAGTAGTGAGAATTCTGAGCCc 3'	146/-19.7	1606-1636
ICAM1/ 55742637	3' GACAAGGACGACUUGACUCGGU 5' |||| | | | |||||||| 5' CTGTAGCCACAGCACTGAGCCA 3'	167/-21.7	1855-1876
CCR1/ 44890871	3' gacAAGGACGAC---UUGACUCGgu 5' |||: |:|| ::|||||| 5' ggcTTCTAGTTGTACGGCTGAGCgt 3'	139/-16.8	2398-2422

Table 4.6. Computationally predicted porcine *miR-147* target sites.

Symbol /GI	*miRNA* : mRNA (3´UTR) interaction	Score/ Energy (kcal/mol)	Binding site
SNAPIN/ 194036138	3' CGUCUUCGUAAAGGUGUGUG 5' || ||:|| |||:|||||: 5' GCTGAGGC--TTCTACACAT 3'	153/-19.8	649-666
	3' CGUCUUCGUA----AAGGUGUGUG 5' |||:||		|:||||:| 5' GGAGAGGCTTCCTCTGCTACACGC 3'	131/-19.3	733-756
IFNGR2/ 162287024	3' cgucuUCGUA--AAGGUGUGUG 5' ||||| |||:|||:|| 5' tgtttAGCATGATTCTACATAC 3'	140/-17.6	1513-1534
STAT6/ 194037565	3' cgUCUUCGUAAAGGUGUGUG 5' :|::||| ||||:||| 5' agGGGGGCA---CCACGCAC 3'	140/-21.2	4367-4383
CSF2/ 47523043	3' cGUCUU--CGU-AAAGGUGUGUg 5' ||||: || ||||||||| 5' cCAGAGTCCCACCTTCCACACAg 3'	157/-19.7	487-510
DDX58/ 47523231	3' cgucUUCGUAAAGGUGUGUG 5' |||| |:||||||| 5' tctaAAGC---TTCACACAC 3'	142/-16.2	3450-3466
CCR3/ 44890873	3' CGUCUUCGUAAAGGUGUGUG 5' |::||:|:|| ||:|::||| 5' GTGGAGGTATATCTATGCAC 3'	133/-18.9	1588-1607
CCR5/ 44890879	3' cgucuucguaAAGGUGUGUG 5' |||||||:|| 5' cttgcctcccTTCCACATAC 3'	149/16.1	1326-1345
IL17RB/ 194041250	3' CGUCUUCGUAAAGGUGUGUG 5' ||||:		||||:|:|: 5' GCAGGTGAAAATCCATATAT 3'	133/-16.7	1696-1715
	3' cgUCUUCGUAAAGGUGUGUG 5' :||||	|:||:|||| 5' aaGGAAGGA--TTCATACAC 3'	131/-16.9	1869-1886
RANKL/ 194040708	3' cGUCUUCGUAAA--GGUGUGUg 5' ::|||| :||| ::||||| 5' aTGGAAGGGTTTTCTTACACAg 3'	133/-18.7	1140-1161
JAK1/ 6635249	3' CGUCUU-CGUA---AAGGUGUGUG 5' || ||| ||||	||||::|| 5' GCTGAATGCATATATACCACGTAC 3'	137/-18.4	4585-4608
ATP1A1/ 47523569	3' cgUCUUCGUA--AAGGUGUGUG 5' |:||||| |||||:|| 5' cgtGGAGCATCACGCCACATAC 3'	144/-22.1	3116-3137
IL12A/ 47522811	3' cgUCUUCGUA---AAGGUGUGUg 5' ||:||	|||||||| 5' tgtGAGGC-TCCCATCCACACAa 3'	148/-19	1053-1074
NIT1/ 194036899	3' cGUCUU--CGU-AAAGGUGUGUg 5' ||||: || ||||||||| 5' cCAGAGTCCCACCTTCCACACAg 3'	157/-19.6	2044-2066
SMAP1L/ 183223972	3' cGUCUUCGUAAAGGUGUGUG 5' || |:|	|||||||| 5' tCAAAGG---TCCCACACAC 3'	153/-16.6	2385-2401
PLA2G6/ 194037216	3' cGUCUUCG---UAAAGGUGUGUG 5' ||| ||| :| ||||||||| 5' cCAGCAGCTCTGTGTCCACACAC 3'	168/-23.3	2475-2497
TPSN/ 194040292	3' cGUCUUCGUAAAGGUGUGUg 5' || |: || ||||||| 5' cCACAGCCACAGCCACACAg 3'	151/-17.1	1652-1671

Table 4.7. Computationally predicted porcine *miR-146a* target sites.

Symbol /GI	*miRNA* : mRNA (3´UTR) interaction	Score/ Energy (kcal/mol)	Binding site

C1QTNF3/19 4719516	3' uuGGGUACCUUAAGUCAAGAGU 5'
	  |||| || ||||||||||
	5' ttCCCA--AAAATCAGTTCTCA 3'
	
	3' uuGGGUACC-----UUAAGUCAAGAGU 5'
	  |:||||| |:|| :|||||:|
	5' tcCTCATGGATACTAGTTGGGTTCTTA 3'
		169/-21.7
		
		141/-21.2
			2325-2344
			
			2015-2041

CD47/ 47522789	3' uUGGGU--ACCUUAAGUCAAGAGu 5' :|||| || :|| |||||||: 5' tGCCCAATTGAGATCCAGTTCTTt 3	155/-18.9	1257-1280

MAFB/ 194033944	3' UUGGGUACCUUAAGUCAAGAGU 5'
	  || |:| ||:||||||||
	5' AAAGCGTATTTTTTAGTTCTCA 3'
	
	3' uuGGGUACCUUAAGUCAAGAGU 5'
	  |||:| ||:||||:|||
	5' ctCCCGT----TTTAGTTTTCA 3
		159/-17.8
		
		147/-18.9
			2607-2628
			
			2015-2032

C9/ 86604372	3' uuGGGUACCUUAAGUCAAGAGu 5' ||:|||| | ||||:|: 5' ctCCTATGGTTTCCAGTTTTTt 3'	140/-20.4	1960-1981
HZ3/ 194043551	3' UUGGGUAC-CUUAAGUCAAGAGU 5' ||||| || ||| |||||||| 5' AACCC-TGTGAA---AGTTCTCA 3'	167/-20.8	3433-3451
SP1/ 194037363	3' uUGGGUACC-UUAAGUCAAGAGu 5' ||| :||| || |||||||: 5' tACCAGTGGCAAGGCAGTTCTTt 3'	153/-20.8	3804-3826
PBXIP1/ 194036092	3' uuGGGUACCUUAAGUCAAGAGu 5' ||| | :: |||||||: 5' ccCCCTTTTGGCCCAGTTCTTc 3'	136/-18	2299-2320
PSMD5/ 194033944	3' UUGGGUACCUUAAGUCAAGAGU 5' :| ||| || ||||||||| 5' GAACCA--GA---CAGTTCTCA 3'	156/-17.2	1443-1459
EDRF1/ 194041642	3' UUGGGUACCUUAAGUCAAGAGu 5' :| ||| |::| |||||||| 5' GAGCCA--GGGTGCAGTTCTCt 3'	162/-22.6	1866-1885

References

Alemdehy MF, van Boxtel NG, de Looper HW, van den Berge IJ, Sanders MA, Cupedo T, Touw IP, Erkeland SJ.Dicer1 deletion in myeloid-committed progenitors causes neutrophil dysplasia and blocks macrophage/dendritic cell development in mice. Blood. 2012 119(20):4723-30.

Ban JY, Kim BS, Kim SC, Kim DH, Chung JH.Microarray Analysis of Gene Expression Profiles in Response to Treatment with Melatonin in Lipopolysaccharide Activated RAW 264.7 Cells.Korean J Physiol Pharmacol. 2011 15(1):23-9.

Behm-Ansmant I., Rehwinkel J. & Izaurralde E. (2006) MicroRNAs silence gene expression by repressing protein expression and/or by promoting mRNA decay. Cold Spring Harbor symposia on quantiative biology 71, 523-530.

Bignami F, Pilotti E, Bertoncelli L, Ronzi P, Gulli M, Marmiroli N, Magnani G, Pinti M, Lopalco L, Mussini C, Ruotolo R, Galli M, Cossarizza A, Casoli C.Stable changes in CD4+ T lymphocyte miRNA expression after exposure to HIV-1. Blood. 2012 119(26):6259-67.

Boldin MP, Taganov KD, Rao DS, Yang L, Zhao JL, Kalwani M, Garcia-Flores Y, Luong M, Devrekanli A, Xu J, Sun G, Tay J, Linsley PS, Baltimore D.miR-146a is a significant brake on autoimmunity, myeloproliferation, and cancer in mice. J Exp Med. 2011 208(6):1189-201.

Brennecke J., Stark A., Russell R.B. & Cohen S.M. (2005) Principles of microRNA-target recognition. PloS Biology 3, e85.

Buchan JR, Parker R.Eukaryotic stress granules: the ins and outs of translation.Mol Cell. 2009 36(6):932-41.

Cai X., Hagedorn C.H. & Cullen B.R. (2004) Human microRNAs are processed from capped, polyadenylated transcripts that can also function as mRNAs. RNA 10,1957-1966.

Cichocki F, Felices M, McCullar V, Presnell SR, Al-Attar A, Lutz CT, Miller JS.Cutting edge: microRNA-181 promotes human NK cell development by regulating Notch signaling.J Immunol. 2011 187(12):6171-5.

Chen Q, Wang H, Liu Y, Song Y, Lai L, Han Q, Cao X, Wang Q.Inducible MicroRNA-223 Down-Regulation Promotes TLR-Triggered IL-6 and IL-1β Production in Macrophages by Targeting STAT3. PLoS One. 2012 7(8):e42971.

Didiano D. & Hobert O. (2006) Perfect seed pairing is not a generally reliable predictor for miRNA-target interactions. Nature structural and molecular biology 13, 849-851.

Graff JW, Dickson AM, Clay G, McCaffrey AP, Wilson ME.Identifying functional microRNAs in macrophages with polarized phenotypes. J Biol Chem. 2012 287(26):21816-25.

Hammond S.M., Boettcher S., Caudy A.A., Kobayashi R. & Hannon G.J. (2001) Argonaute2, a link between genetic and biochemical analyses of RNAi. Science 293, 1146-1150.

Houzet L, Yeung ML, de Lame V, Desai D, Smith SM, Jeang KT.MicroRNA profile changes in human immunodeficiency virus type 1 (HIV-1) seropositive individuals. Retrovirology. 2008 5:118.

Huang J, Wang F, Argyris E, Chen K, Liang Z, Tian H, Huang W, Squires K, Verlinghieri G, Zhang H.Cellular microRNAs contribute to HIV-1 latency in resting primary CD4+ T lymphocytes. Nat Med. 2007 13(10):1241-7.

Imig J, Motsch N, Zhu JY, Barth S, Okoniewski M, Reineke T, Tinguely M, Faggioni A, Trivedi P, Meister G, Renner C, Grässer FA.microRNA profiling in Epstein-Barr virus-associated B-cell lymphoma. Nucleic Acids Res. 2011 39(5):1880-93.

Jiang P, Liu R, Zheng Y, Liu X, Chang L, Xiong S, Chu Y.MiR-34a inhibits lipopolysaccharide-induced inflammatory response through targeting Notch1 in murine macrophages. Exp Cell Res. 2012 318(10):1175-84.

Kaushansky K, O'Hara PJ, Berkner K, Segal GM, Hagen FS, Adamson JW.Genomic cloning, characterization, and multilineage growth-promoting activity of human granulocyte-macrophage colony-stimulating factor. Proc Natl Acad Sci U S A. 1986 83(10):3101-5.

Kelly LM, Englmeier U, Lafon I, Sieweke MH, Graf T.MafB is an inducer of monocytic differentiation. EMBO J. 2000 19(9):1987-97.

Ketting R.F., Fischer S.E., Bernstein E., Sijen T., Hannon G.J. & Plasterk R.H. (2001) Dicer functions in RNA interference and in synthesis of small RNA involved in developmental timing in C. elegans. Genes & Development 15, 2654-2659.

Labbaye C, Testa U.The emerging role of MIR-146A in the control of hematopoiesis, immune function and cancer. J Hematol Oncol. 2012 5:13.

Lee R.C., Feinbaum R.L. & Ambros V. (1993) The C. elegans heterochronic gene lin-4 encodes small RNAs with antisense complementarity to lin-14. Cell 75, 843-845.

Lee Y., Ahn C., Han J., Choi H., Kim J., Yim J., Lee J., Provost P., Rådmark O., Kim S. & Kim V.N. (2003) The nuclear RNase III Drosha initiates microRNA processing. Nature. 425, 415-419.

Lee SM, Kleiboeker SB.Porcine arterivirus activates the NF-kappaB pathway through IkappaB degradation. Virology. 2005 342(1):47-59.

Lewis B.P., Shih I.H., Jones-Rhoades M.W., Bartel D.P. & Burge CB. (2003) Prediction of mammalian microRNA targets. Cell 115:787-798.

Li QJ, Chau J, Ebert PJ, Sylvester G, Min H, Liu G, Braich R, Manoharan M, Soutschek J, Skare P, Klein LO, Davis MM, Chen CZ.miR-181a is an intrinsic modulator of T cell sensitivity and selection.Cell. 2007 129(1):147-61.

Mattijssen S, Pruijn GJ. Viperin, a key player in the antiviral response.Microbes Infect. 2012 14(5):419-26.

McDermott JE, Archuleta M, Thrall BD, Adkins JN, Waters KM.Controlling the response: predictive modeling of a highly central, pathogen-targeted core response module in macrophage activation.PLoS One. 2011 6(2):e14673.

Nilsson S, Möller C, Jirström K, Lee A, Busch S, Lamb R, Landberg G.Downregulation of miR-92a is associated with aggressive breast cancer features and increased tumour macrophage infiltration. PLoS One. 2012 7(4):e36051.

Otsuka M, Jing Q, Georgel P, New L, Chen J, Mols J, Kang YJ, Jiang Z, Du X, Cook R, Das SC, Pattnaik AK, Beutler B, Han J.Hypersusceptibility to vesicular stomatitis virus infection in Dicer1-deficient mice is due to impaired miR24 and miR93 expression. Immunity. 2007 27(1):123-34.

Pedersen IM, Cheng G, Wieland S, Volinia S, Croce CM, Chisari FV, David M.Interferon modulation of cellular microRNAs as an antiviral mechanism. Nature. 2007 449(7164):919-22.

Petrocca F, Lieberman J.Micromanagers of immune cell fate and function. Adv Immunol. 2009 102:227-44.

Qi J, Qiao Y, Wang P, Li S, Zhao W, Gao C.microRNA-210 negatively regulates LPS-induced production of proinflammatory cytokines by targeting NF-κB1 in murine macrophages.FEBS Lett. 2012 586(8):1201-7.

Rusca N, Dehò L, Montagner S, Zielinski CE, Sica A, Sallusto F, Monticelli S.miR-146a and NF-κB1 Regulate Mast Cell Survival and T Lymphocyte Differentiation. Mol Cell Biol. 2012 32(21):4432-44.

Sever-Chroneos Z, Murthy A, Davis J, Florence JM, Kurdowska A, Krupa A, Tichelaar JW, White MR, Hartshorn KL, Kobzik L, Whitsett JA, Chroneos ZC. GM-CSF modulates pulmonary resistance to influenza A infection. Antiviral Res. 2011 92(2):319-28.
Soifer H.S., Sano M., Sakurai K., Chomchan P., Saetrom P., Sherman M.A., Collingwood M.A., Behlke M.A. & Rossi J.J. (2008) A role for the Dicer helicase domain in the processing of thermodynamically unstable hairpin RNAs. Nucleic Acids Research 36, 6511-6522.

Stik G, Dambrine G, Pfeffer S, Rasschaert D.The oncomiR-21 overexpressed during Marek's disease lymphomagenesis is transactivated by the viral oncoprotein Meq.
J Virol. 2012. [Epub ahead of print]

Tamura R, Chen Y, Shinozaki M, Arao K, Wang L, Tang W, Hirano S, Ogura H, Mitsui T, Taketani S, Ando M, Kataoka T.Eudesmane-type sesquiterpene lactones inhibit multiple steps in the NF-κB signaling pathway induced by inflammatory cytokines.Bioorg Med Chem Lett. 2012 22(1):207-11.

Tanimoto A, Murata Y, Wang KY, Tsutsui M, Kohno K, Sasaguri Y.Monocyte chemoattractant protein-1 expression is enhanced by granulocyte-macrophage colony-stimulating factor via Jak2-Stat5 signaling and inhibited by atorvastatin in human monocytic U937 cells.J Biol Chem. 2008 22;283(8):4643-51.

Tay Y, Zhang J, Thomson AM, Lim B, Rigoutsos I.MicroRNAs to Nanog, Oct4 and Sox2 coding regions modulate embryonic stem cell differentiation. Nature. 2008 455(7216):1124-8.

Tili E, Croce CM, Michaille JJ.miR-155: on the crosstalk between inflammation and cancer.Int Rev Immunol. 2009 28(5):264-84.

Triboulet R, Mari B, Lin YL, Chable-Bessia C, Bennasser Y, Lebrigand K, Cardinaud B, Maurin T, Barbry P, Baillat V, Reynes J, Corbeau P, Jeang KT, Benkirane M.Suppression of microRNA-silencing pathway by HIV-1 during virus replication. Science. 2007 315(5818):1579-82.

Verschueren K., Remacle J.E., Collart C., Kraft H., Baker B.S., Tylzanowski P., Nelles L., Wuytens G., Su M.T., Bodmer R., Smith J.C. & Huylebroeck D. (1999) SIP1, a novel zinc finger/homeodomain repressor, interacts with Smad proteins and binds to 5'-CACCT sequences in candidate target genes. Journal of Biological Chemistry 274, 20489-20498.

Watanabe Y., Tomita M. & Kanai A. (2007) Computational methods for microRNA target prediction. Methods in enzymology 427, 65-86.

Winter J., Jung S., Keller S., Gregory R.I. & Diederichs S. (2009) Many roads to maturity: microRNA biogenesis pathways and their regulation. Nature Cell Biology 11, 228-234.

Yang J, Yuan YA.A structural perspective of the protein-RNA interactions involved in virus-induced RNA silencing and its suppression. Biochim Biophys Acta. 2009 -1789(9-10):642-52.

Yi R., Qin Y., Macara I.G. & Cullen B.R. (2003) Exportin-5 mediates the nuclear export of pre-microRNAs and short hairpin RNAs. Genes & Development 17, 3011-3016.

Ying S.Y. & Lin S.L. (2009) Intron-mediated RNA interference and microRNA biogenesis. Methods in Molecular Biology 487, 387-413.

Zheng Q, Zhou L, Mi QS.MicroRNA miR-150 is involved in Vα14 invariant NKT cell development and function. J Immunol. 2012 188(5):2118-26

Chapter Five: Conclusions and Future Directions

It has been more than one hundred years since the initial discovery of viruses. During this time thousands of viruses have been and continue to be discovered. Viruses are diverse, exhibiting broad host ranges, pathogenicities, etc. However, a shared feature of all viruses is the complexity of their relationships with their cellular hosts. Viruses must utilize various components of the host cell for completion of their life cycle, while at the same time trying to evade detection. On the flip side the host cell tries to minimize the damage done by the invading virus, often by inducing cell death.

All viruses, at some stage of their infection cycles, must interact with cellular transport machinery. First, in order to enter a cell, a virus has to bind to the proper receptor(s) on the cell surface. Upon entry via one of several different mechanisms, the viral genome must be carried to the appropriate site of genome replication and virus progeny production. Nascent virus particles then must exit the cell. Knowledge of how a virus interacts with its cellular host is critical in understanding viral pathogenesis and in developing more efficient prevention strategies.

To develop a better understanding of interaction between PRRSV with its intracellular environment we performed a yeast two-hybrid screening to identify cellular interacting partners of its two major envelope proteins GP5 and M. We determined that both GP5 and M interact with snapin, a member of the SNARE membrane fusion complex. SNARE proteins are found in most eukaryotic cells and serve to position vesicles at target membranes and mediate fusion (Parpura and Mohideen 2008). Snapin is an accessory SNARE protein that

localizes to multiple cellular membranes and mediates both SNAP-23, a ubiquitous SNARE core protein, and SNAP-25, a neuron-specific SNARE core protein, vesicle trafficking (Buxton et al. 2003). To elucidate the functional role of the GP5/M/snapin interaction a snapin-specific siRNA was used to knock-down snapin expression in PRRSV infected cells. This siRNA-mediated knock-down of snapin resulted in decreased PRRSV replication as indicated by the reduction of both PRRSV N expression and reduced PRRSV titers in cells transfected with snapin-specific siRNA compared to cells transfected with a negative control. Future studies into the temporal and spatial specifics of GP5/M/snapin interaction should aid in determine the exact stage in which this interaction is essential. It will also be interesting to determine if the GP5/M/snapin interaction is a shared feature of arteriviruses and/or nidoviruses, in general, or if this is a unique feature of PRRSV. If the snapin interaction itself is not shared among other arteriviruses it is possible that they may still rely on the SNARE complex via interactions with other SNARE-associated proteins. As reviewed in chapter one numerous viruses have been shown to manipulation the SNARE membrane fusion machinery for virus trafficking.

To further characterize the interaction between PRRSV and its cellular host we profiled changes in cellular miRNA expression of the course of an *in vitro* PRRSV infection in swine alveolar macrophages. Most viruses induce changes in the cellular miRNome upon infection (reviewed by Liber and Haas 2011). The changes are the results of either the virus manipulation or response of the host cell. It is well known that viruses usurp many host regulatory mechanisms for their own benefit. Therefore, it is not surprising that viruses have developed multiple ways of utilizing their hosts' small RNA regulatory system. For example,

the liver specific miRNA, *miR-122a* is a vital part of the hepatitis C virus replication (Jopling 2012). In addition some DNA viruses, in particular herpesviruses, encode their miRNAs, including orthologs to cellular miRNAs (Cullen 2011). From aspect of the host many cellular miRNAs have been shown to function in modulating the immune response. As miRNAs function as fine tuners of gene expression rather than robust regulators they are ideal for modulating the immune response. MiRNA-mediated regulation can be used to prevent a too robust response, while still allowing for sufficient immune gene expression. Also a single miRNA has the potential to regulate hundreds of genes allowing for a simple yet effective way to modulate related genes. We determined that expression of ~40 cellular miRNAs is altered within the first 48 hours of PRRSV infection in SAMs *in vitro*. Analysis of the potential genes and pathways regulated by these differentially expressed miRNAs suggests that they are involved in regulating multiple cellular pathways including the immune related and intracellular trafficking pathways.

Interestingly we found that one of the differentially expressed *miR-147*, which was significantly down regulated in PRRSV infected cells at 24hpi, likely regulates snapin expression. A decrease in *miR-147* expression in PRRSV infected macrophages should result in a reciprocal increase in Snapin. The next steps into understanding the involvement of miRNA-mediated gene regulation during PRRSV infections will include determining the changes of the differentially expressed miRNAs identified in this study over the course of *in vivo* PRRSV infections. As miRNA research has grown exponentially in the last few years, there are a few commercially available options for elucidating miRNA functions. These

include synthetic mimics and inhibitors that can be used to over-express or reduce miRNA binding ability, respectively. Future studies in which miRNAs are experimentally altered using these mimics and inhibitors should clarify the functional roles they play in PRRSV infections in SAMs. It will be particularly interesting to determine if *miR-147* over-expression in PRRSV infected SAMs alters virus production and/or intracellular transport.

References

Buxton P, Zhang XM, Walsh B, Sriratana A, Schenberg I, Manickam E, Rowe T. Identification and characterization of Snapin as a ubiquitously expressed SNARE-binding protein that interacts with SNAP23 in non-neuronal cells. Biochem J. 2003 375(Pt 2):433-40.

Cullen BR. Herpesvirus microRNAs: phenotypes and functions. Curr Opin Virol. 2011 1(3):211-5.

Jopling C. Liver-specific microRNA-122: Biogenesis and function. RNA Biol. 2012 9(2):137-42

Lieber D, Haas J. Viruses and microRNAs: a toolbox for systematic analysis. Wiley Interdiscip Rev RNA. 2011 2(6):787-801.

Parpura V, Mohideen U.Molecular form follows function: (un)snaring the SNAREs. Trends Neurosci. 2008 31(9):435-43.